ELECTROCHEMICAL CHARACTERIZATION AND SYNTHESIS OF POLYMER SYSTEMS

by

Li-chien Hsu

Chem. Eng., Taipei Institute of Technology (Taiwan), 1971

M.Sc., University of Bradford (U.K.), 1975

A THESIS SUBMITTED IN PARTIAL FULFILLMENT

OF THE REQUIREMENTS FOR THE DEGREE OF

DOCTOR OF PHILOSOPHY

in the Department

of

Chemistry

SIMON FRASER UNIVERSITY

December 1980

APPROVAL

Name: Li-chien Hsu

Degree Doctor of Philosophy

Title of Thesis: Electrochemical Synthesis and Characterization of Polymer Systems

Examining Committee:

Chairman: D. Sutton

Dr. B.L. Funt
Senior Supervisor

Dr. Y.L. Chow

Dr. E.J. Wells

Dr. M.J. Gresser

Dr. W.M. Pasika
External Examiner
Professor
Department of Chemistry
Laurentian University
Ontario

Date Approved:

PARTIAL COPYRIGHT LICENSE

I hereby grant to Simon Fraser University the right to lend my thesis, project or extended essay (the title of which is shown below) to users of the Simon Fraser University Library, and to make partial or single copies only for such users or in response to a request from the library of any other university, or other educational institution, on its own behalf or for one of its users. I further agree that permission for multiple copying of this work for scholarly purposes may be granted by me or the Dean of Graduate Studies. It is understood that copying or publication of this work for financial gain shall not be allowed without my written permission.

Title of Thesis/Project/Extended Essay

"Electrochemical Characterization and Synthisis of Polymer Systems"

Author: _____
(signature)

Li-Chien Hsu
(name)

December 18, 1980
(date)

ABSTRACT

This thesis consists of three parts: (1) kinetic studies of aqueous redox polymerization, (2) electrochemically - initiated graft copolymerization, and (3) electrochemical behavior and characterization of polymers.

Elementary reactions relevant to the initiation of a polymerization in aquequs media were investigated utilizing a rotating ring disk electrode (RRDE). The kinetics of radical formation in redox initiator systems, their rate constants, and the competitive reactions which occur on addition of monomer to the systems were studies. The rate constant for the reaction $Cu^{+}/S_2O_8^{=}$ was 6.3×10^3 M^{-1} sec^{-1} and the Arrhenius temperature dependence of the rate was

$$k = 3.37 \times 10^6 \exp(-3625/RT)$$

where $R = 1.987$ cal $°K^{-1}$ $mole^{-1}$

The relative reactivities of the series of monomers - acrylic acid, acrylamide, methacrylic acid, and acrylonitrile - towards $SO_4^{-\cdot}$ were determined and are indicative of the relative ease of the initiation step in the respective polymerizations. Parallel studies for $Fe^{+2}/S_2O_8^{=}$, $Fe(C_2O_4)_3^{-4}/S_2O_8^{=}$, and Fe^{+2}/H_2O_2 were also conducted and the rate constants determined.

Transfer of electrons to appropriate functional groups incorporated into a macromolecular structure was also studied. Poly(vinylbenzophenone-co-styrene) (PVBP/ST) was prepared and utilized for an electrochemically initiated graft copolymerization. Benzophenone moieties on the backbone polymer served as electroactive centers and grafting sites upon electrochemical activation . Electrolysis of the backbone polymers was performed in N, N'-

dimethylformamide with tetraethylammonium perchlorate as a supporting electrolyte or in tetrahydrofuran with sodium tetraphenylboride. The resulting macroradical anions initiated graft copolymerization of acrylonitrile and methyl methacrylate. The graft copolymers were characterized. Under appropriate conditions, a high grafting efficiency could be obtained by this electrolytic method.

Electrochemical studies of poly(vinylbenzophenone) and benzophenone at solid electrodes revealed that, despite the higher regularity and lower flexibility of the macromolecular structures compared with the random association of small molecule systems, the electrochemical behavior of the two systems (the reduction potentials, the shape of the current-potential curves, the reversibility) were closely similar. The only major difference was in the magnitude of the limiting current, a reflection of the much reduced rate of diffusion of the polymeric molecules. Detailed studies of the effects of chain length and of the spacing between electroactive centers in the polymer system further indicated that the electrochemical behavior of benzophenone groups attached to a polymer chain was not influenced by the macromolecular environment or by the neighboring group interaction. Even when 1000 electrons were added sequentially to a single polymeric molecule, each electron transfer was independent and occurred at the same energy.

Quantitative determination of the diffusion coefficients of a series of relatively monodisperse PVBP-ST were made through the measurements of limiting current at a rotating disk electrode and yielded $b = 0.529$, $K_T = 1.25 \times 10^4$ cm^2/sec from the relation $D = K_T M^{-b}$. The effects of polymer concentration and temperature on the diffusion coefficient were determined. The

deduced Mark-Houwink coefficient, "a", of PVBP-ST in N,N'-dimethylformamide at 25°C was 0.587, in comparison with the value, 0.583, determined from direct measurement via viscometry and gel permeation chromatography. The agreement led to the precise determination of molecular weights and diffusion coefficients of polymers by voltammetric methods.

TO MY PARENTS

ACKNOWLEDGEMENTS

The author would like to express his most sincere gratitude to Dr. B. L. Funt for his continued guidance, advice, and encouragement throughout the course of this work.

Thanks are also due to Drs. A. Glasel, J. F. Skinner, Mr. J. Landa for their helpful comments and stimulating discussions, and to Mr. P. H. Hoang and Dr. J.-P. Martenot for assistance in some of the experiments. I am also indebted to Dr. A. J. Bard of the University of Texas at Austin for providing a copy of the RRDE digital simulation programme.

The friendship and help of various members of the Department of Chemistry, and the technical assistance of the personnel of the Electronics, Machine, and Glassblowing Shops, are acknowledged with appreciation.

I am grateful to Mr. K. Takahashi for the convenience and encouragement provided during the preparation of this thesis.

I should also like to thank Mrs. J. Morton, who endured the typing of the manuscript.

TABLE OF CONTENTS

LIST OF TABLES

LIST OF FIGURES

LIST OF FIGURES PAGE

LIST OF FIGURES

LIST OF FIGURES

LIST OF FIGURES PAGE

GENERAL INTRODUCTION

Electrolysis is characterized by the occurrence of oxidation at the anode and reduction at the cathode of an electrolytic cell. For each electron transferred through the solution, a corresponding chemical reaction occurs at the electrode. Numerous substances are capable of undergoing electron transfer reactions at electrodes. This has led to the use of electrolysis as a method for the synthesis and the degradation of many organic compounds.

The electrochemical formation of polymers, although exploited much later, has been an area in which considerable progress has been made in recent years. Experimental variables, such as electrode potential, current, and time, which govern the type and amount of initiating species generated at the electrodes, have been utilized to control the mechanism and the rate of initiation of a reaction. Under appropriate conditions, current reversal serves to terminate the propagation reaction. Polymers with very specific molecular weight distributions and/or molecular weights can be prepared by this method of controlled synthesis. Several recent reviews (1 - 4) have shown the diversity of electrode reactions which can result in polymerization reactions.

Electrochemical techniques provide new method of polymerization with a fine control of the initiation and termination reaction. They also offer possibilities for fundamental studies of the rate of elementary polymerization steps. Addition polymerization reactions frequently involve electron transfers in such steps as initiation, chain transfer, and termi-

nation reactions. The use of fast, transient electrochemical methods to monitor continuously and, sometimes, simultaneously the concentrations of one or more components of a reaction mixture and to identify short-lived intermediates have proven to be useful in studies of homogeneous kinetics and should be equally applicable to polymerization reactions. Kinetic studies of fast reactions are otherwise possible only for photo-polymerizable monomers by the use of stop-flow techniques(5).

Voltammetric or polarographic measurements permit the detection of electroactive groups in solution. The groups may be isolated or bonded to a more complicated molecular framework. Studies of electrode processes involved in transfer of electrons to functional groups incorporated into macromolecular structures can be made through a comparison of their electrochemical behavior with that of low molecular weight molecules having an identical electroactive functionality. An understanding of the electron transfer processes to polymers at electrodes is of importance. Quantitative evaluations of substituent effects and the correlation of structural parameters with electrochemical data may be used to characterize polymers of analogous structures and to support structure-elucidation studies. Some practical applications such as the formation of polymer modified electrodes require greater understanding of the electrochemical behavior of polymers than currently exists. This particular example is one of a newly developed area of active research (6,7). The mechanism of electron transfer and its dependence on the segmental mobilities and the

structure of polymers require further experimental and theoretical elaboration. Furthermore, polymers with suitably placed electroactive groups may be reduced (or oxidized) and these reduced groups may undergo chemical reactions similar to those of the corresponding monomeric forms, e.g. radical anions (or cations). Electrochemical methods can, thus provide a means for polymer modification.

This thesis is concerned with the electrochemical characterization and synthesis of polymer systems and is divided into three sections. The first deals with the use of the rotating ring disk electrode to study the kinetics of redox initiation in aqueous polymerizations; the second section describes a method of electrochemically initiating a graft copolymerization; and the third section reports the electrochemical behavior and characterization of electro-active polymers.

CHAPTER I

KINETIC STUDIES OF ELECTROCHEMICALLY - INDUCED REDOX INITIATION IN AQUEOUS POLYMERIZATION

1.1 INTRODUCTION

The primary process in many electrochemically initiated polymerizations is the formation of a chemically active species by electron transfer. The electron transfer process may result in the direct addition of an electron to the monomer at the electrode, or in a rapid transfer from a transient species to the monomer. Alternatively, a "catalytic" species may be generated at the electrode, and this product can react with a second substance in the bulk of the solution.

A number of elementary reactions of considerable relevance to polymerization kinetics may be studied advantageously at the electrode. If, for example, the species $A^{\bullet -}$ capable of initiating a polymerization is stable and electrochemically reversible:

$$A \underset{-e}{\overset{+e}{\rightleftharpoons}} A^{\bullet -} \qquad [1]$$

$$A^{\bullet -} + M \longrightarrow {}^{\bullet}AM^{-} \qquad [2]$$

the decay of the active species, $A^{\bullet -}$, may be followed amperometrically in the absence and presence of monomers. A comparison of the total decay rates should yield the rate constant for the initiation step in the polymerization. The method provides an "in situ" detection of the concentration of an active species.

Dropping mercury polarography (8 - 10) and rotating disk voltammetry (11, 12) have been used to study the kinetics of electrochemically generated persistent ions with monomers. The investigation of less stable species and their reactions with monomers require a method that is applicable to a short time scale. Recently, Funt et al (13) employed a rotating ring disk electrode (RRDE) to study the interaction of a series of radical cations with monomers. Radical cations were generated at a central disk electrode and flowed to a collecting ring which was controlled potentiostatically to reduce the unreacted radical cations. In this application the RRDE is analogous to the flow system employed in kinetic studies of fast reactions. The disk electrode may be considered as an upstream generator, the ring as a downstream detector. The flux of one reactant is controlled by the rotation speed, and the other reactant by the disk potential or current, so that the reaction zone can be placed between the disk and the ring electrodes. Rate constants for irreversible reactions up to 10^8 $M^{-1}sec^{-1}$ can be measured (14, 15). Thus electrochemical techniques provide an opportunity for the study of transient species whose persistence or stability can vary from days to milliseconds. Reactions occurring during this period can be investigated quantitatively and pertinent rate constants of competitive reactions can be obtained.

The use of electrochemical methods for studying polymerization kinetics is not limited to the initiation by ionic species. Free radicals produced in a secondary reaction dependent on an initial reaction at an electrode may also be studied. An example of this type of reaction would be the secondary reaction of ferrous ion and hydrogen peroxide following

the electro-reduction of ferric ion to ferrous ion in the presence of hydrogen peroxide. Numerous redox pairs of this type have been used to initiate polymerizations under very mild reaction conditions. These redox systems are, however, remarkably complex in their detailed overall chemistry. The elementary steps of electrochemical reduction, radical formation and initiation of a polymerization are intertwined. The metal ions may act as initiators as well as terminators of polymerization (16, 17). It is desirable to study and quantify the individual processes separately.

1.1.1. Redox Initiation in Free Radical Polymerization

A very effective method of generating free radicals under mild conditions is through a one-electron transfer reaction, the most effective of which is the redox reaction. This particular method has found wide application for initiating polymerization reactions, especially in aqueous emulsion systems.

The kinetics and mechanisms of redox reactions have received considerable attention, with the Fenton reagent, Fe (II)/H_2O_2, being most thoroughly investigated (18 -20). It is generally accepted that the reaction proceeds through the two one-electron transfer steps given in Eqs. [3] and [4].

$$Fe^{2+} + H_2O_2 \longrightarrow Fe^{3+} + HO^- + HO\bullet \qquad [3]$$

$$Fe^{2+} + HO\bullet \longrightarrow Fe^{3+} + HO^- \qquad [4]$$

If monomer is present, reaction [4] will compete with reaction [5] for HO•.

$$HO\bullet + CH_2{=}CHX \longrightarrow HOCH_2\dot{C}HX \qquad [5]$$

At relatively high peroxide concentrations, the following reactions may need to be considered.

$$HO\cdot + H_2O_2 \longrightarrow HO_2\cdot + H_2O \qquad [6]$$

$$HO_2\cdot + Fe^{2+} \longrightarrow HO_2^- + Fe^{3+} \qquad [7]$$

$$H_2O_2 + HO_2\cdot \longrightarrow O_2 + H_2O + HO\cdot \qquad [8]$$

Ferrous ions can promote the decomposition of a number of other types of compounds, including alkyl and acyl peroxides, disulfides, peroxydisulfate and elementary halogens. Ag (I), Ce (III), V^{+5}, Ti^{+3}, $Co(NH_4)_6^{+3}$, $Fe_2(CN)_6^{=}$ and many other reductant ions have been used to replace Fe^{+2} in analogous reactions (21 - 24).

The kinetics of redox reactions is normally deduced from the concentrations of metal ions or their complexes, which are measured by spectroscopic techniques. For fast reactions, stop-flow techniques were employed in conjunction with spectroscopic methods (25).

Using a dropping mercury electrode, Kolthoff et al (26) found that hydrogen peroxide increased the limiting current in the polarographic reduction of ferric ion. Upon addition of acrylonitrile the limiting current, however, decreased. A qualitative interpretation was given to account for the observed change in currents.

Haberland and Landsberg (27) have reported a study of Fe^{+2}/H_2O_2 reaction using a gold rotating disk electrode, while Opekar and Beran (28) have studied this reaction on palladium, glassy carbon, and gold rotating disk electrodes. Bard and Prater (29) have used a platinum rotating ring disk electrode for a limited study of the kinetics of this reaction. They suggested a method for determining rate constants based on a computer simulation of the appropriate hydrodynamic and reaction parameters.

1.1.2. Rotating Disk Electrodes (RDE)

It was shown by V. G. Levich (30) that a disk-shaped electrode has an important set of properties: high accuracy in the measurement of diffusional fluxes, uniform accessibility of the surface and stationary conditions. These properties have made the RDE a unique tool for investigating the kinetics of electrochemical reactions at solid electrodes and for the measurement of diffusion coefficients of dissolved species. Application of the RDE became considerably more extensive after the development of the rotating ring disk electrode (RRDE). The addition of a ring electrode to the rotating disk electrode permits a virtually simultaneous detection of species generated at the disk and provides a revealing technique in areas such as electro-analysis (31), reaction intermediate identification (32), kinetics and mechanisms of chemical and electrochemical reactions (14), transient phenomena (33), and many others. A recent article gave a thorough review of this experimental technique (34).

The rotating disk electrode method was developed as a result of the application of concepts of physico-chemical hydrodynamics to the requirement of electro-chemical experiments. The rotating disk geometry permits precisely defined mass transport to be set, and a quantitative treatment of hydrodynamic and diffusion behavior to be made. The quantitative theory was developed by Levich and Ivanov (35). In recent years, a series of calculations concerning practical applications of the RRDE were made by Albery, Bruckenstein and others (36, 37). The full theoretical treatments of RDE and RRDE are not within the scope of this work and can be found in several reviews (14, 38-40). However, a qualitative description of fundamental concepts is presented.

1.1.2.1. Hydrodynamic Diffusion Layer at Rotating Disk Electrodes

Rotating a disk electrode causes liquid to flow from the bulk of the solution toward the center of the disk and thence outward toward its edges. The surface velocity increases with increasing distance from the center, and does so in such a way that the current density is the same at every point. This current density may be conveniently described by invoking a Nernst diffusion layer treatment. According to Fick's first law

$$\left(\frac{dN}{dt}\right)_{x=o} = DA\left(\frac{\partial C}{\partial x}\right)_{x=o} \qquad [9]$$

where $(dN/dt)_{x=o}$ is the number of moles of the electroactive substance that reaches the electrode surface in each second, D is the diffusion coefficient of the electroactive substance, A is the area of the electrode in cm^2, and $(\partial C/\partial x)_{x=o}$ is the concentration gradient at the electrode surface; x represents the distance from the electrode surface. One may define a parameter δ by the equation

$$\delta = \frac{C^b - C^e}{(\partial C/\partial x)_{x=o}} \qquad [10]$$

where C^b and C^e denote the concentrations of the electroactive species in the bulk of the solution and at the electrode surface respectively.

Nernst visualized δ as the thickness of a quiet layer of solution in contact with the electrode. Within this layer, it was postulated that diffusion alone controlled the transfer of substances to the electrode. Outside the layer diffusion was negligible and the concentration of electroactive substances was maintained at the value of bulk concentration by

convective transfer.

In a stirred solution, however, motion has been detected at values of x that are much smaller than δ (41). Hydrodynamic treatment of the convective diffusion leads to the concept of a thin diffusion boundary layer that has no exactly defined thickness. It is simply a depth which is conveniently defined as the region within which the maximum change in concentration occurs. It can be shown that this diffusion boundary layer thickness is proportional to the physical properties of the solution (flow velocity, viscosity) as well as the diffusion coefficient. In principle, each electroactive species has its own value of δ . The concentration profile near the surface of an electrode at a potential corresponding to the limiting current plateau is schematically presented in Fig.1.

1.1.2.2. Levich Equation

According to Levich (38), the value of δ for a rotating disk electrode of virtually infinite area is given by

$$\delta = kD^{1/3}\nu^{-1/6}\omega^{1/2} \qquad [11]$$

where ν is the kinematic viscosity of the solution, given by

$$\nu = \eta/d \qquad [12]$$

and ω is the angular velocity of the disk in radians/sec, given by

$$\omega = 2\pi N \qquad [13]$$

in which N is the number of revolution per second. Gregory and Riddiford(42) gave the following expression for the quantity k in Eq. [11].

$$k = 1.6125 + 0.5704\ (D/\nu)^{0.36} \qquad [14]$$

With the usual values of D andν the second term in Eq.[14] can be neglected.

FIGURE 1: CONCENTRATION PROFILE CLOSE TO THE SURFACE OF A ROTATING DISK ELECTRODE

(a) Actual profile

(b) Hypothetical profile showing distance corresponding to Value δ defined by Eq. [10]

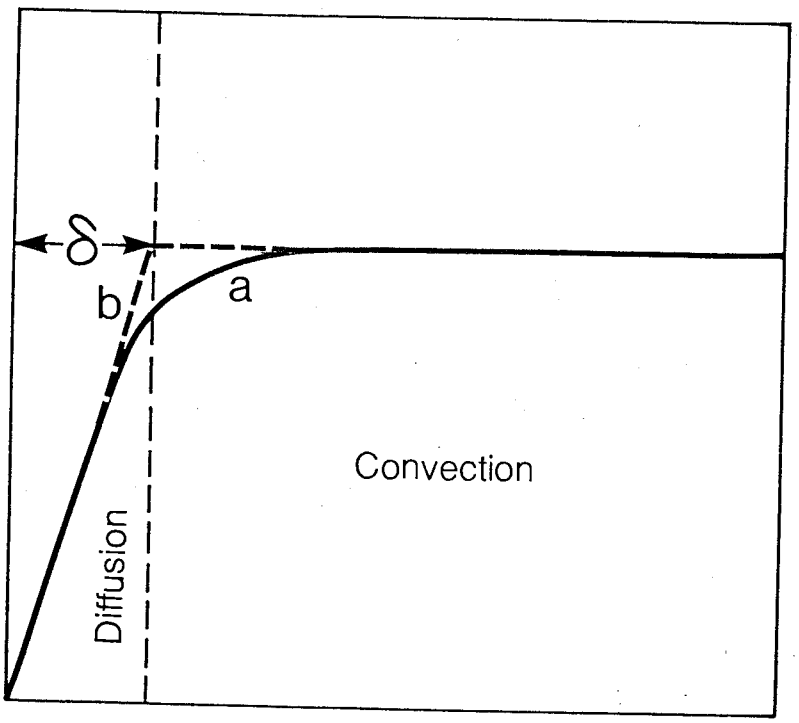
δ
b
a
Convection
Diffusion

Combining Eqs. [9], [10], [11], and [14] with a description of the current

$$i = nF\ (dN/dt)_{x=o} \qquad [15]$$

and setting $C^e = 0$ to obtain an expression for the limiting current equation, one obtains

$$i_L = 0.6201\ nFAC D^{2/3}\ \nu^{-1/6}\ \omega^{1/2} \qquad [16]$$

It can be seen from Eq.[11] that δ contains no term involving electrode geometry, i.e., the thickness is not a function of the geometry of the electrode but is constant over the entire surface. This type of reaction surface is termed uniformly accessible by Levich (38). Of considerable importance to electrochemistry is the fact that, on this uniformly accessible surface, the rate of electrochemical reaction is everywhere the same. However, the possibility of non-uniform current densities, due to an ohmic potential drop at currents $< i_L$, has been pointed out by Newman (43, 44) recently.

The behavior of a RDE assumes that laminar flow exists near the surface. Such a condition can be maintained apparently up to Reynold numbers between 10^4 and 10^5 (45). The value of N_{Re} for a RDE is given by

$$N_{Re} = \frac{r^2\ \omega}{\nu} \qquad [17]$$

where r is the disk radius in cm and is the total radius of working plus non-working area.

1.1.3. Comparison of Common Types of Electrode System

Some common types of electrode system and their characteristics with respect to time are listed in Table 1.

TABLE I

COMMON TYPES OF ELECTRODE SYSTEM

ELECTRODE	WELL DEFINED TRANSPORT	CALCULABLE TRANSPORT	TIME CHARACTERISTICS
Stationary	short time only	short time only	transient
Rotating wire	yes	no	steady state
Vibrating wire	yes	no	cyclic
Mercury drop	yes	no	cyclic
Rotating disk	yes	yes	steady state

The current at an electrode is determined by one or more of the following factors: transport of species to and from the electrode; kinetics of the electrode process; kinetics of homogeneous chemical reaction. In order to obtain a reproducible current it is necessary that the transport of the electroactive species from the bulk of the solution to the electrode and vice versa should be well defined and controlled. In addition, in order to separate the effect of different factors, the transport of the system must be described by a theoretical model.

Although the exact equations can be written for currents at a plane stationary electrode, the electrode only has defined characteristics for a short time. Thereafter, the thickness of the diffusion layer becomes too large and the transport depends on such factors as random fluctuations, local eddies, and vibrations. Consequently, no true steady state can be set up; the electrode potential and the current tend to vary with time.

Rotating and vibrating wire electrodes have well defined diffusion layers. However, the hydrodynamic complexities defy theoretical analysis. Therefore, these electrodes can only be used in a semi-empirical fashion.

The dropping mercury electrode has been the most widely used system. During the life-time of each drop it is similar to a stationary electrode with a diffusion layer spreading out from the electrode surface. Before this layer becomes too large, the drop falls off. The current and potential vary with time during the life-time of each drop; the system is therefore a cyclic one.

In the rotating disk electrode, a known pattern of hydrodynamic flow is imposed on the solution giving well defined and calculable transport. A steady state is quickly reached, and currents and potentials that do not vary with time may be observed.

1.1.4 Rotating Ring Disk Electrode (RRDE)

The RRDE developed by Frumkin (46) consists of two separate electroactive surfaces, an inner disk and, separated from it by an insulated band, an outer electrode. In practice the electrode is so connected as to provide two independent voltammetric circuits, one to the disk and one to the ring. The electrode geometry and flow patterns are schematically illustrated in Fig. 2.

The electrode can be divided into three zones of interest in the following fashion

Zone I	$r < r_1$	disk, active surface
Zone II	$r_1 < r < r_2$	insulating spacer
Zone III	$r_2 < r < r_3$	ring, active surface

FIGURE 2: ROTATING RING DISK ELECTRODE (RRDE) AND FLOW PATTERNS

r_1 : radius of disk electrode

r_2 : inner radius of ring electrode

r_3 : outer radius of ring electrode

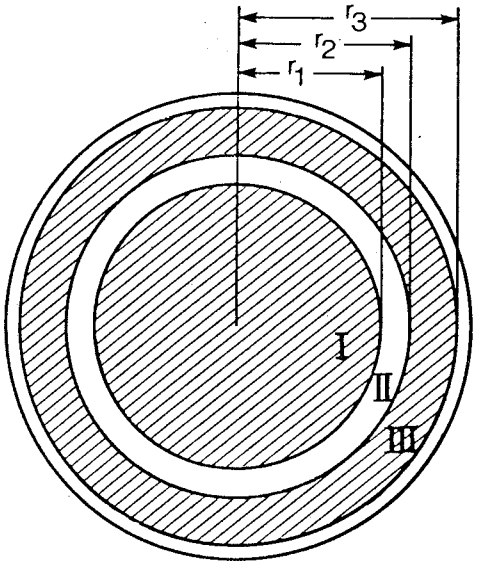
r3
r2
r1
I
II
III

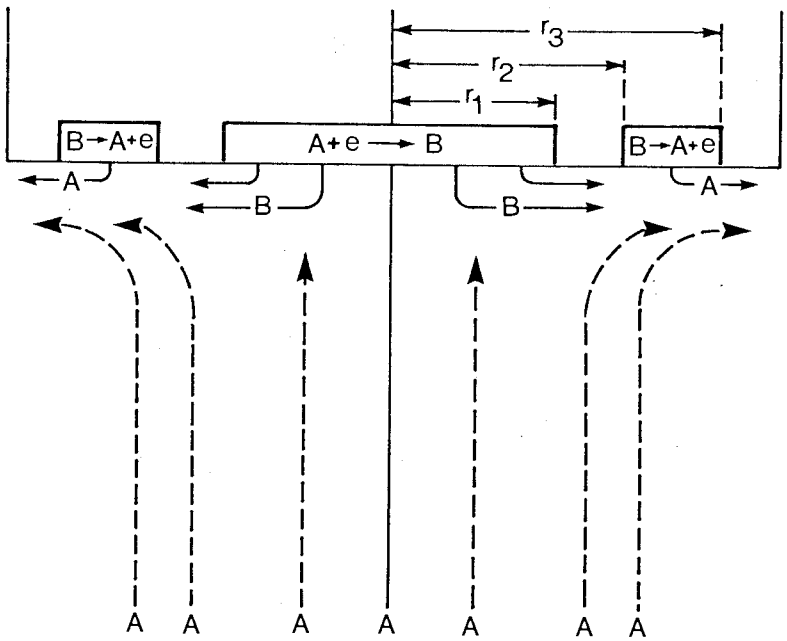
r3
r2
r1
B→A+e
A+e → B
B→A+e
A
B
B
A
A
A
A
A
A
A
A

In Zone I, an electrochemical reaction can be caused by the application of the potential E_1. If the reaction is designated as

$$A + ne \longrightarrow B \qquad [18]$$

then the product B is formed uniformly over the inner disk surface. The product will then be swept outward from Zone I, through Zone II, to Zone III. The potential applied to Zone III is such that all B reaching the ring is transformed to A by the reaction

$$B \longrightarrow A + ne \qquad [19]$$

If B is a stable species, then the ratio of the current at the ring electrode to the current at the disk electrode is a function of the geometry of the electrode. This ratio is called the collection efficiency, N, and is given by the expression

$$N = i_r/i_d \qquad [20]$$

where i_r and i_d are the currents at the ring and the disk electrodes respectively.

The quantitative treatment of the transport of species from the disk electrode to the ring is a rather cumbersome function of r_1, r_2 and r_3. The approximate calculation of N, introduced by Levich and Ivanov (35), was modified by Bruckenstein and Feldman (47). Most recently Albery and Bruckenstein (36, 37) have refined the calculation of N for RRDE with thin rings and thin insulating gaps. The final results for the N_o are:

$$N_o = \frac{i_r}{i_d} = 1-F\left(\frac{\alpha}{\beta}\right) + \beta^{2/3}\,[1-F(\alpha)] - (1+\alpha+\beta)^{2/3}\,\{1-F[\alpha/\beta(1+\alpha+\beta)]\} \qquad [21]$$

where α and β are determined by the geometry of the electrode

$$\alpha = \left(\frac{r_2}{r_1}\right)^3 - 1 \qquad [22]$$

$$\beta = \left(\frac{r_3}{r_1}\right)^3 - \left(\frac{r_2}{r_1}\right)^3 \qquad [23]$$

The function $F(\theta)$ for a given argument θ is

$$F(\theta) = \frac{\sqrt{3}}{4\pi} \ln\left[\frac{(1+\theta^{1/3})}{1+\theta}\right]^3 + \frac{3}{2\pi} \tan^{-1}\left(\frac{2\theta^{1/3} - 1}{3^{1/2}}\right) + 1/4 \qquad [24]$$

Values of N and $F(\theta)$ have been tabulated and showed good agreement with experimental results.

If species B undergoes a chemical reaction which depletes its concentration as it passes from the disk to the ring, then the observed collection efficiency, N_k - the kinetic collection efficiency, will be smaller than that in the absence of this chemical reaction. In this case, the collection efficiency is a function, not only of the electrode geometry, but also of the rate constant of the reaction, the rotation rate, ω , and other solution parameters.

It should be noted that the algebraic sum of i_r and i_d is collected at the counter electrode. Changes in the ring current, due to intervening chemical reaction will be accompanied by corresponding changes in the counter electrode current.

Albery and Bruckenstein (37) have given a mathematical analysis of steady- state kinetic collection efficiencies for the first order EC mechanism (where EC denotes an electron transfer followed by a chemical

reaction).

$$B \xrightarrow{k_1} X \qquad [25]$$

Their solution to the problem was stated as

$$N_0/N_k = 1 + 1.28\ (\nu/D)^{1/3}\ (k/\omega) \qquad [26]$$

where N_k is the collection efficiency for a given rotation rate ω (rad/sec), ν is the kinematic viscosity (cm^2/sec), D is the diffusion coefficient (cm^2/sec), and k is the rate constant (sec^{-1}).

Albery et al (14) have also presented an approximate treatment of the second-order EC mechanism

$$B + C \xrightarrow{k_2} Y + Z \qquad [27]$$

where C,Y, and Z are electro-inactive species. But the second-order treatment is limited only to certain regions of rotation rate and rate constant.

Recently, numerical methods have been applied to the calculation of concentration profiles around a ring disk electrode. Feldberg's digital simulation technique (48) has been adapted by Bard and Prater (49, 50) to the RRDE for determining rate constants based on a computer simulation of the appropriate hydrodynamic, diffusion, and solution reaction parameters. Bard and co-workers have analysed the kinetics of a variety of reactions including first and second order (49, 50), catalytic, isomerization and dimerization (51 -54). A more detailed account of this technique is given in the Experimental Section.

1.2 EXPERIMENTAL

1.2.1 Apparatus

The potentiostat used in RRDE experiments was similar to that described by Bruckenstein (55) and provided an independent control of both electrodes. It permitted simultaneous measurements of ring and disk currents. A Hewlett-Packard 3300A function generator was used to sweep the disk voltage; the currents were recorded on a Hewlett-Packard T0464A X-Y/Y' recorder. Two digital voltmeters, a Hewlett-Packard Model 3472 and a Data Precision Model 134, were used to measure the potentials of the disk and ring electrodes. The speed of rotation was controlled to within 1% by a Carter motor tachometer assembly with an electronic feedback circuit.

The electrochemical cell contained separate reference and counter compartments, the former being connected to the cell by a Luggin capillary, the latter being separated from the cell by a fritted disk. The cell is schematically illustrated in Fig. 3.

The ring and disk electrodes were constructed of bright platinum with the dimensions r_1 = 0.30 cm, r_2 = 0.33 cm, and r_3 = 0.43 cm, where r_1, r_2 and r_3 are the outer radii of the disk, the insulating spacer and the ring, respectively. Electrical contact was established by sets of three silver-graphalloy brushes per electrode. A platinum wire spiral served as the counter electrode. A saturated calomel electrode (SCE) was used as the reference electrode, in contact with the test solution through a Luggin capillary positioned 1mm below the RRDE surface. The RRDE was preconditioned immediately before each run by spinning it in 6M HCl, followed by saturated $FeSO_4$ in 2M H_2SO_4, and then three changes of distilled water. This procedure provided a consistent electrode surface as judged by the reproducibility of repeated experiments.

FIGURE 3: RRDE ELECTROCHEMICAL CELL

A. Ring-Disk Electrode

B. Counter Electrode

C. Reference Electrode

D. Luggin Capillary

E. Fritted Disk

F. Bearing Assembly

G. Brushes

H. Speed Control Pulley

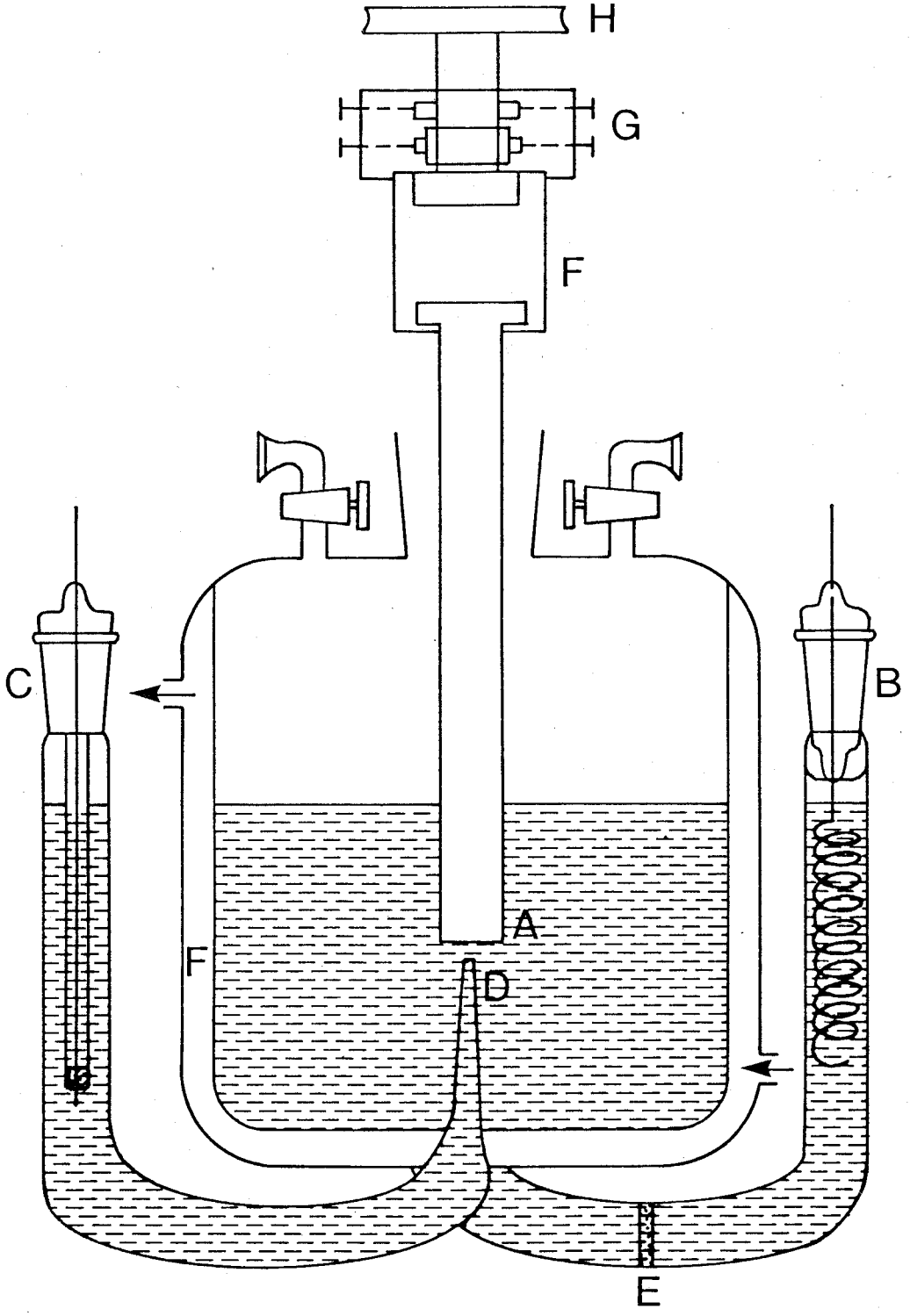
H
G
F
C
B
A
F
D
E

For the measurements on the Cu (II) solutions, the ring was potentiostated at 0.5 volts,(vs SCE) while the disk was swept from 0.5 to -0.25 volts. For the Fe (III) solutions, the ring was held at 1.00 volt while the disk was swept from 0.7 to 0.0 volts. The disk voltage was swept at approximately 10 mv/sec, the collection efficiency being essentially independent of the sweep rate over the range 5 to 50 mv/sec for the test solution.

1.2.2 Materials

Acrylic acid, methacrylic acid and acrylonitrile were distilled on a spinning band column prior to use. Acrylamide was recrystallized from chloroform and washed with benzene, then dried under vacuum at room temperature for 24 hours.

Water was doubly distilled, then purified by percolation through an ion exchange demineralizer. Inorganic salts were analytical grades and were not purified further. The 3% H_2O_2 was vigorously flushed with nitrogen and titrated against $KMnO_4$ before each run.

The test solutions were deaerated and thermostated within 0.1°C for electrical measurements.

1.2.3. Digital Simulation

The digital simulation technique for the catalytic reaction was developed by Bard and Prater (50). The author is indebted to them for supplying a copy of the computer program. For simplicity and consistency, the same notation has been adapted to describe the method and the modification made to accommodate the reaction mechanism.

Briefly, the solution below the electrode is divided into a number of "boxes" in both the r and z directions (Fig. 4). J refers to the boxes in the vertical direction and K to the box in the radial direction. FA (J, K) is the fractional concentration of A in the (J, K) box. The disk and ring currents depend on the concentrations of the electroactive species in the volume elements immediately below the electrode surfaces. The simulation takes into account changes in concentrations resulting from convective flow due to concentration gradients and from the reaction occurring in the solution just below the electrode.

For the redox couple of $Cu(I)/S_2O_8^{=}$, the relevant reactions are (56):

$$Cu^{+2} + e \longrightarrow Cu^{+} \qquad \text{at the disk} \qquad [28]$$

$$Cu^{+} + S_2O_8^{=} \xrightarrow{k_1} Cu^{+2} + SO_4^{\cdot -} + SO_4^{=} \qquad \text{in solution} \qquad [29]$$

$$Cu^{+} + SO_4^{\cdot -} \xrightarrow{k_2} Cu^{+2} + SO_4^{=} \qquad \text{in solution} \qquad [30]$$

$$Cu^{+} \longrightarrow Cu^{+2} + e \qquad \text{at the ring} \qquad [31]$$

where the following rate equations can be written for Eqs. [29] and [30]

$$\frac{-d\,[Cu^{+}]}{dt} = k_1\,[Cu^{+}]\,[S_2O_8^{=}] + k_2\,[Cu^{+}]\,[SO_4^{\cdot -}] \qquad [32]$$

$$= \frac{d\,[Cu^{+2}]}{dt}$$

FIGURE 4: DIGITAL SIMULATION MODEL OF RRDE

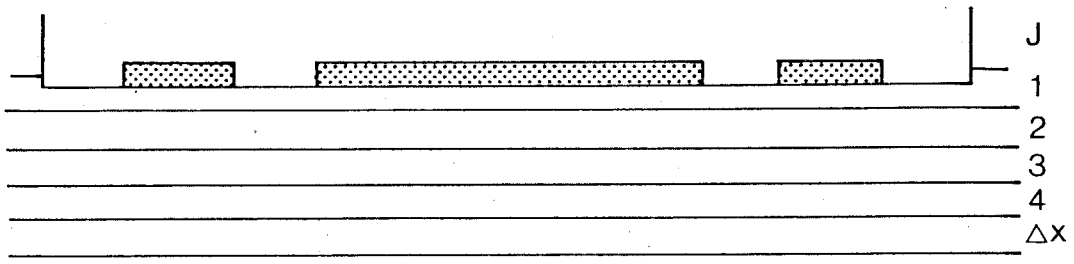
J
1
2
3
4
Δx

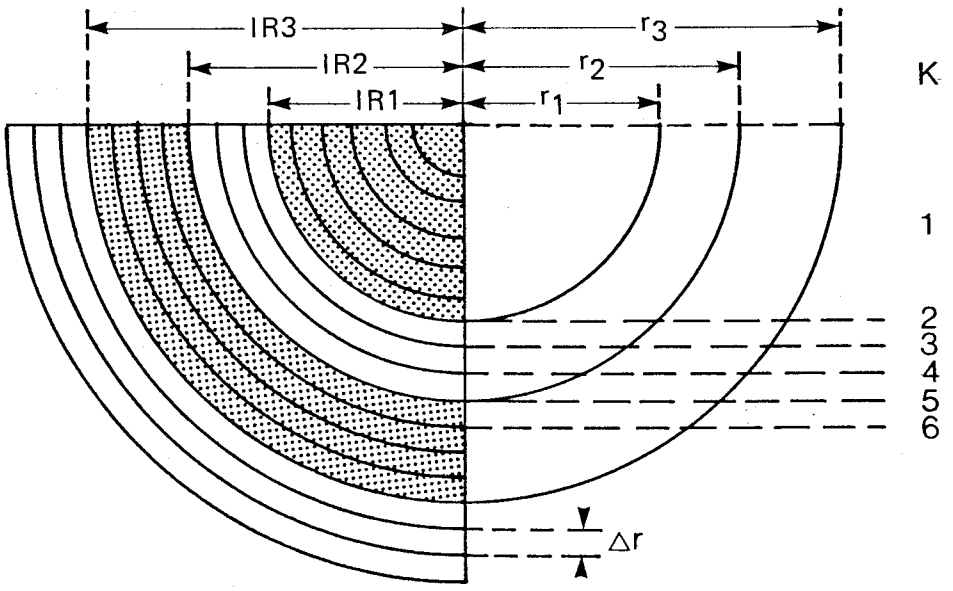
IR3
IR2
IR1
r3
r2
r1
K
1
2
3
4
5
6
Δr

$$\frac{-d\,[S_2O_8^{=}]}{dt} = k_1\,[Cu^{+}]\,[S_2O_8^{=}] \qquad [33]$$

$$\frac{-d\,[SO_4^{-}]}{dt} = k_2\,[Cu^{+}]\,[SO_4^{-}] - k_1\,[Cu^{+}]\,[S_2O_8^{=}] \qquad [34]$$

If a steady-state approximation can be applied to $[SO_4^{-}]$, Eq.[34] can be equated to zero and Eq. [32] rewritten as :

$$\frac{-d\,[Cu^{+}]}{dt} = 2k_1\,[Cu^{+}]\,[S_2O_8^{=}] = \frac{d\,[Cu^{+2}]}{dt} \qquad [35]$$

Eq. [35] is considered to be correct as the reaction [30] is much faster than reaction [29]. For the $Fe(II)/H_2O_2$ system, the ratio of the rates, k_2/k_1, is greater than 10^6 (56). Furthermore, the rate constant for the $Ce(III)/SO_4^{-}$ reaction is 1.43×10^8 $mole^{-1}$ sec^{-1} (57). This is far in excess of the rate constant reported for the reaction of a metal ion with a peroxide. In Eqs. [28-35], Cu^{+2} and Cu^{+} may be replaced by Fe^{+3} and Fe^{+2}, and $S_2O_8^{=}$ may be replaced by H_2O_2 or other peroxides respectively.

Defining $[Cu^{+2}] = C_A$, $[Cu^{+}] = C_B$, $[S_2O_8^{=}] = C_C$ and combining Eqs.[33] and [35] the rate is

$$\frac{-\Delta C_C}{\Delta t} = \frac{-\Delta C_B}{2\Delta t} = \frac{\Delta C_A}{2\Delta t} = k_1 C_B C_C \qquad [36]$$

or $$-\Delta F_C = \frac{1}{2}\Delta F_B = \frac{1}{2}\Delta F_A = k_1 F_B F_C\,\Delta t\,C_A^{o} = DEL \qquad [37]$$

when F_C and F_B represent fractional concentrations normalized with respect to the bulk concentration of Cu(II), C_A^o

$$F_C = C_C/C_A^o \qquad F_B = C_B/C_A^o$$

The effects of the solution reactions [29] and [30] on the concentrations within a given volume element are taken into account by replacing F_A, F_B and F_C with

$$F_A = F_A + 2\,\Delta F_A \qquad [38]$$

$$F_B = F_B - 2\,\Delta F_B \qquad [39]$$

$$F_C = F_C - \Delta F_C \qquad [40]$$

or in the FORTRAN form:

$$\text{DEL} = \text{XKTC} * F_B * F_C \qquad [41]$$

$$F_A\,(J, K) = F_A\,(J, K) + 2.*\text{DEL} \qquad [42]$$

$$F_B\,(J, K) = F_B\,(J, K) - 2.*\text{DEL} \qquad [43]$$

$$F_C\,(J, K) = F_C\,(J, K) - \text{DEL} \qquad [44]$$

where XKTC is the dimensionless parameter, $k_1 C_A^o \omega^{-1} \nu^{1/3} D_A^{-1/3} (0.51)^{-2/3}$, ν is the kinematic viscosity of the solvent, ω is the rotation speed and D is the diffusion coefficient of Cu^{2+}. The final result of the simulation is the series of working curves shown in Fig. 5 for two different values of the bulk molarity ratio, $m = [S_2O_8^{=}] / [Cu^{+2}]$, where N_k, the collection

efficiency, is the ratio of the ring current to the disk current at a given ω. Working curves have also been calculated for different values of m, but these have not been included in Fig. 5.

FIGURE 5: SIMULATED COLLECTION EFFICIENCY VS m(XKTC)

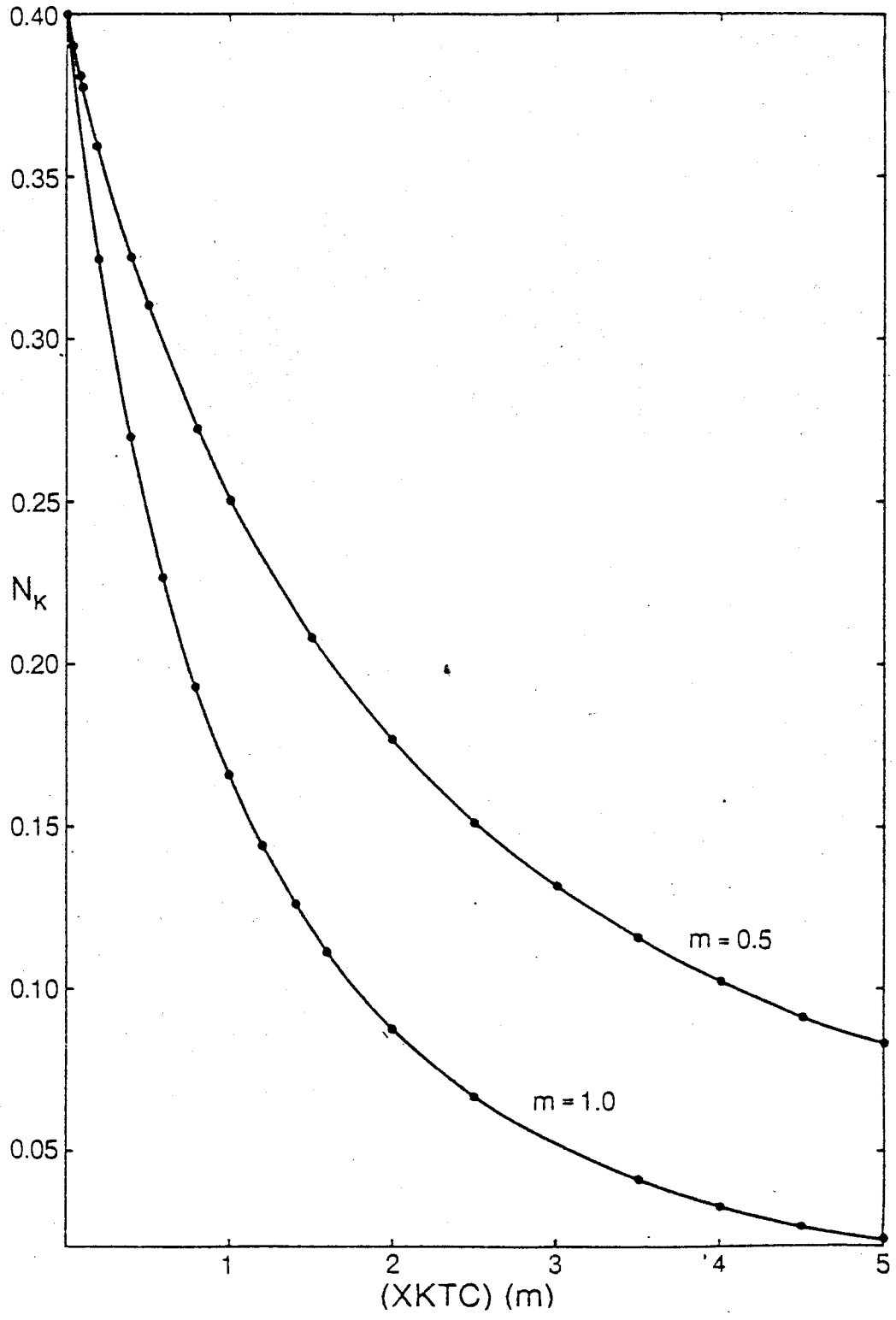
0.40
0.35
0.30
0.25
N_K
0.20
0.15
0.10
0.05
1
2
3
4
5
(XKTC) (m)
m = 0.5
m = 1.0

1.3. RESULTS AND DISCUSSION

1.3.1. Introduction

The work described in this section involved the application of the rotating ring disk electrode to the study of a free radical competitive reaction subsequent to the reduction of a metal ion in the presence and absence of monomer. In essence, a metal ion reduced at the disk electrode is collected at the ring electrode. The ratio of the ring to disk current is termed collection efficiency and is a constant defined by the geometry of the electrode. If a intervening chemical reaction occurs in the transit time between the disk and the ring, the collection efficiency will be altered. The variation of collection efficiency with rotation rate, and thus, the transit time, provides a steady state method to determine the rate constant of the reaction. In the presence of monomers, the currents and the collection efficiency may be employed to probe the kinetic parameters of the competing reactions.

In this work the rates of formation of radicals were determined for $Cu(I)/S_2O_8^{=}$, $Fe(II)/H_2O_2$, and $Fe(II)/S_2O_8^{=}$ including cases where ferrous ions were complexed. The efficiency of capturing of $SO_4^{\bullet -}$ by several water soluble monomers was also investigated.

1.3.2. Redox Reaction of Cu(I) with Peroxydisulfate Ion

At a RRDE the disk current (i_d) is determined by the electrode reaction,

$$Cu^{+2} + e \longrightarrow Cu^{+} \qquad [45]$$

and the ring current (i_r) is determined by

$$Cu^{+} \longrightarrow Cu^{+2} + e \qquad [46]$$

In the presence of peroxydisulfate ions, $S_2O_8^{=}$, Cu(I) formed at the disk electrode reacts with $S_2O_8^{=}$ and $SO_4^{-\bullet}$ (reactions [29] and [30]) regenerating Cu(II) which is again reduced at the disk electrode. The reaction pattern is, therefore, an electrocatalytic type. When monomers are present in the system, reactions[30] and [47] are competitive for $SO_4^{-\bullet}$ and the amount of Cu(I) reaching the ring electrode will depend upon the concentration of monomers and the relative rates of reactions [30] and [47].

$$SO_4^{-\bullet} + M \longrightarrow \bullet MSO_4^{-\bullet} \qquad [47]$$

The behavior of the Cu(II) system in the absence of any secondary reactions is shown in Fig. 6a. The disk voltage is swept negatively from +0.6 V and the first limiting current corresponds to the one-electrode transfer reducing Cu(II) to Cu(I). The ring potential is maintained at 0.5 V vs SCE and the observed i_r is therefore due to the oxidation of cuprous to cupric ion. The second reduction wave on the i_d corresponds to the reduction of Cu(I) to Cu(0) and the corresponding i_r drops to zero as there is no further flow of Cu(I) to the ring. The ratio i_r/i_d (N_o, the collection efficiency) is 0.399,which is in a close agreement with the value expected for the particular geometry of the electrode. When $S_2O_8^{=}$ is added to the above solution, i_r and i_d are changed as shown in Fig. 6b. The i_d for the first reduction step increases significantly, reflecting the homogeneous solution reaction [39] and [30]. These reactions rapidly regenerate Cu(II) ion for repeated reduction at the disk resulting in the catalytic contribution to the i_d. The i_r is reduced correspondingly as a result of these reactions.

A blank test performed on solutions of $S_2O_8^{=}$ in the absence of Cu(II) ion is shown as part of the data in Fig. 7 and indicates quite

FIGURE 6: RRDE VOLTAMMOGRAMS FOR ONE- AND TWO- ELECTRON TRANSFER IN 5 mM Cu(II) AND 0.5 M KCl AT 25°C

------- Disk Current;

——— Ring Current;

(a) 5 mM Cu(II)/0.5 M KCl/ω = 131 rad/sec

(b) 5 mM Cu(II)/5 mM $K_2S_2O_8$/0.5 M KCl/ω = 259 rad/sec

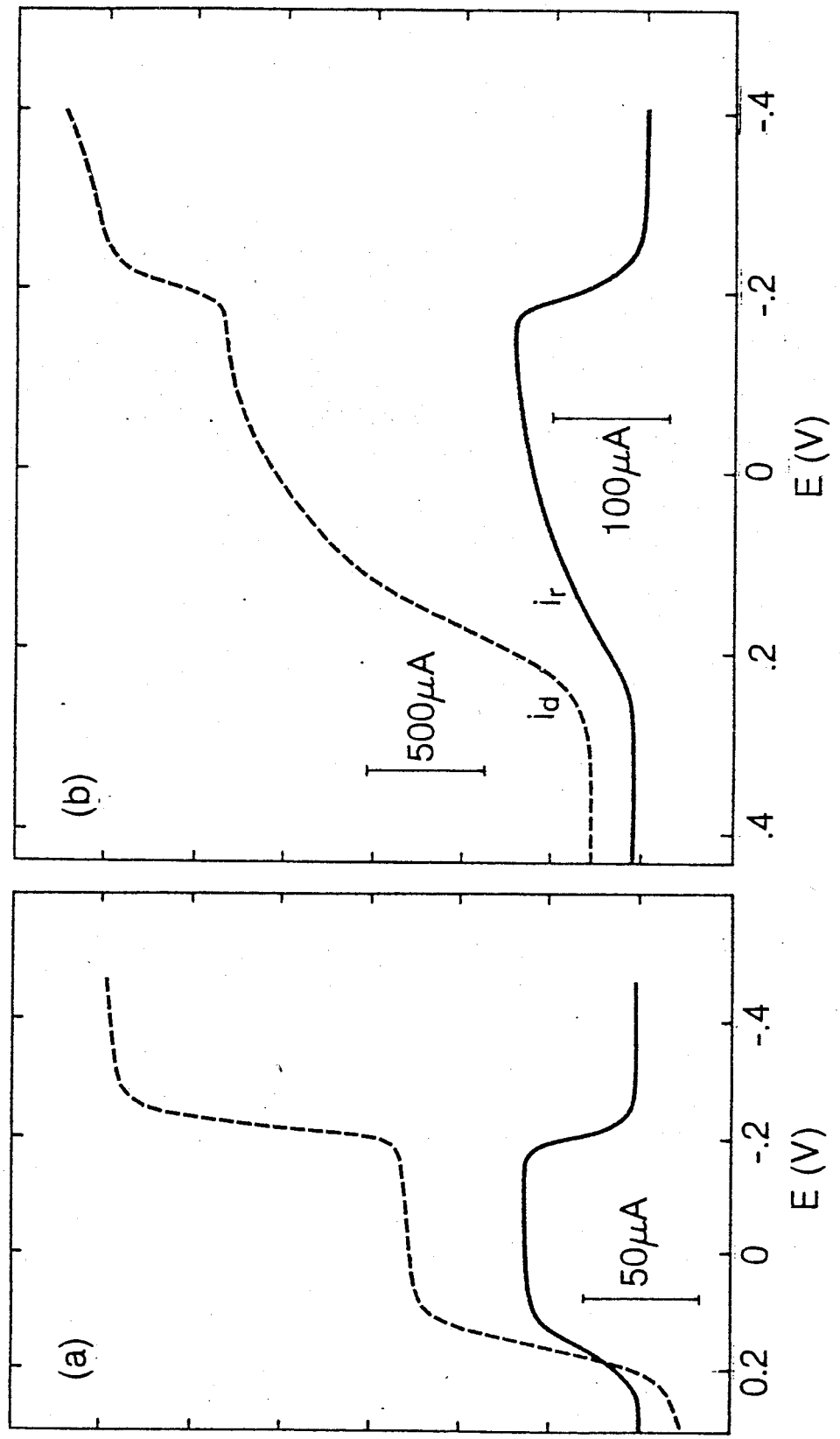
(a)
50μA
0.2
0
-.2
-.4
E (V)
(b)
500μA
i_d
i_r
100μA
.4
.2
0
-.2
-.4
E (V)

FIGURE 7: LIMITING DISK CURRENT FOR ONE- AND TWO-ELECTRON REDUCTION WITH AND WITHOUT $K_2S_2O_8$

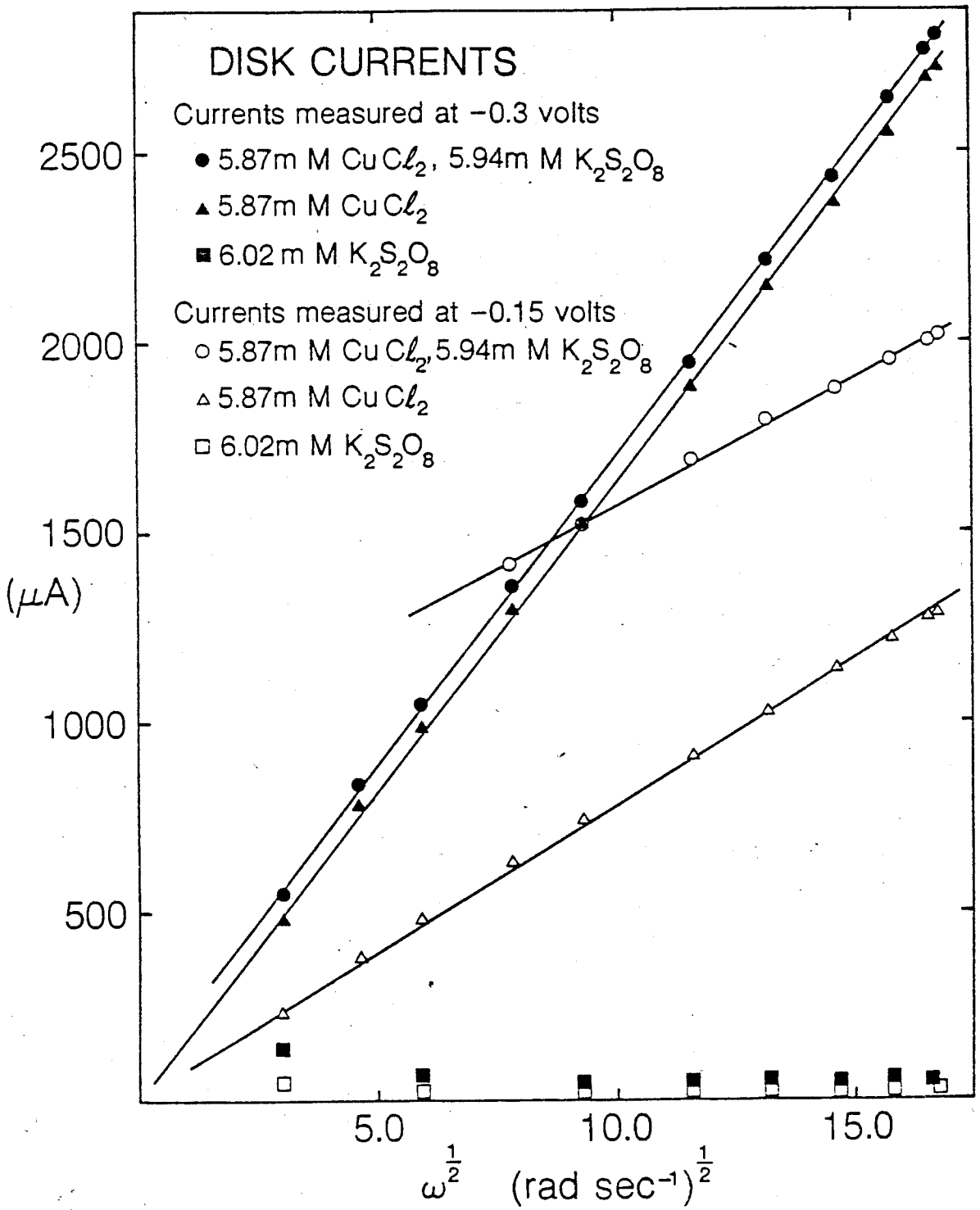
DISK CURRENTS
Currents measured at −0.3 volts
● 5.87m M Cu Cℓ2, 5.94m M K2S2O8
▲ 5.87m M Cu Cℓ2
■ 6.02 m M K2S2O8
Currents measured at −0.15 volts
○ 5.87m M Cu Cℓ2, 5.94m M K2S2O8
△ 5.87m M Cu Cℓ2
□ 6.02m M K2S2O8
2500
2000
1500
1000
500
(μA)
5.0
10.0
15.0
ω^1/2 (rad sec⁻¹)^1/2

conclusively that this ion is not involved in any direct electron transfer reactions at the electrode in this range of potentials. The currents measured at the potential corresponding to the 2 electron transfer, -0.3 V, are identical in the presence and absence of $S_2O_8^{=}$. This confirms the view that this ion is not directly involved with the electrode.

The effect of $S_2O_8^{=}$ concentration can be seen from Fig. 8. Without $S_2O_8^{=}$ both i_d and i_r are linearly dependent on ω and pass through the origin as predicted by the Levich equation. At $S_2O_8^{=}$ = 50 mM, i_r was reduced essentially to zero while i_d increased by a factor of 5. It is obvious that at concentrations as high as 50 mM the rate of the homogeneous reaction is too great for quantitative determination of the rate constant by these techniques. However, the great sensitivity of this system to variation in $S_2O_8^{=}$ concentration makes it an ideal choice for quantitative measurements in a convenient region of interest lying below this value.

The kinetic collection efficiency, N_k, obtained from the systems containing 1 mM $S_2O_8^{=}$/1 mM Cu(II), 1 mM $S_2O_8^{=}$/2 mM Cu(II), 2 mM $S_2O_8^{=}$/ 2 mM Cu(II) and 5 mM $S_2O_8^{=}$/5 mM Cu(II) at various speed of rotation along with the XKTC values calculated from the working curves shown in Fig. 5 are compiled in Table 2. The product

$$\omega\,(XKTC) = k_1 C_A^{o}\, \nu^{1/3}\, D_A^{1/3}\, (0.51)^{2/3}$$

should be a constant. The data in Table 2 show some variability in this parameter,

FIGURE 8: EFFECT OF CONCENTRATION OF $K_2S_2O_8$ ON CATALYTIC CURRENTS IN SOLUTION OF 5 mM Cu(II)

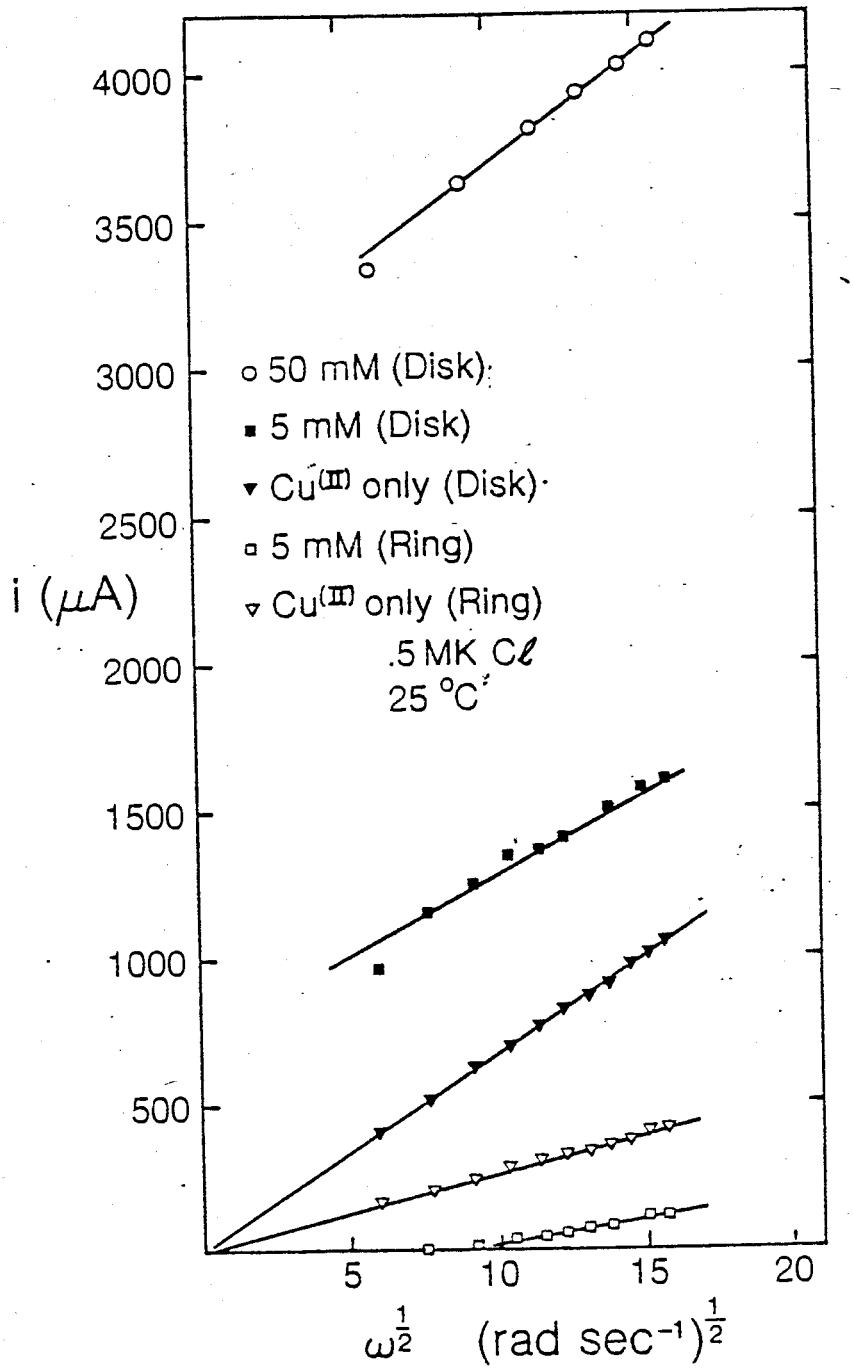
4000
3500
3000
2500
2000
1500
1000
500
i (μA)
50 mM (Disk)
5 mM (Disk)
Cu(II) only (Disk)
5 mM (Ring)
Cu(II) only (Ring)
.5 MK Cℓ
25 °C
5
10
15
20
ω^½ (rad sec⁻¹)^½

TABLE 2

RRDE DATA FOR Cu(II) PEROXYDISULFATE SYSTEM

(rad/sec)	Disk Current i_d (μA)	Ring Current i_r (μA)	N_K	XKTC	ω(XKTC)
1 mM $S_2O_8^{=}$/1 mM Cu(II)					
60.7	149	16.7	0.112	1.59	96.6
85.9	166	23.0	0.139	1.26	107.8
110.0	178	30.5	0.171	0.95	104.5
132.0	189	35.6	0.188	0.81	106.9
155.0	203	42.6	0.210	0.69	106.9
178.0	213	45.5	0.214	0.67	119.3
199.0	223	51.6	0.231	0.57	113.4
216.8	231	55.7	0.241	0.52	112.7
236.7	239	59.5	0.249	0.48	113.6
				average	109.1
				k_1 (average) = 6.36×10^3	
1 mM $S_2O_8^{=}$ /2 mM Cu(II)					
62.8	294	37.3	0.137	3.15	197.9
90.1	324	51.1	0.158	2.35	211.6
114.2	354	65.4	0.185	1.85	211.2
138.2	385	78.1	0.203	1.56	215.6
161.3	402	85.1	0.212	1.45	233.8
184.3	422	95.7	0.227	1.25	230.0
225.2	460	112.7	0.245	1.06	238.7
				average	219.8
				k_1 (average) = 6.41×10^3	

(rad/sec)	Disk Current i_d (μA)	Ring Current i_r (μA)	N_K	XKTC	ω(XKTC)
2 mM $S_2O_8^{=}$/2 mM Cu(II)					
61.8	370	18	0.049	3.09	190.9
86.9	398	29	0.073	2.33	202.5
113.1	422	41	0.097	1.83	207.5
137.2	444	49.5	0.112	1.60	219.5
160.2	463	58.2	0.126	1.41	225.9
183.3	476	67.7	0.142	1.22	223.6
205.3	492	74.6	0.152	1.12	229.6
227.2	507	83.2	0.164	1.00	227.2
247.1	518	87.5	0.169	0.96	237.2
				average	218.2
				k_1 (average) = 6.36 x 10^3	
5 mM $S_2O_8^{=}$/5 mM Cu(II)					
35.6	964	-		-	-
60.2	1153	-		-	-
108.8	1341	30	0.022	4.98	541.9
131.4	1361	44	0.032	4.10	539.0
151.8	1411	58	0.041	3.50	531.4
172.3	1480	76	0.051	3.04	523.7
191.1	1530	98	0.064	2.57	491.2
226.2	1570	107	0.068	2.46	556.4
243.5	1620	130	0.080	2.17	528.3
				average	530.3
				k_1 (average) = 6.19 x 10^3	

Conditions: Temperature = 25°C
Supporting Electrolyte: 0.5 M KCl
D_A = 6.8 x 10^{-6} cm^2/sec
ν^A = 8.91 x 10^{-3} cm^2/sec
XKTC calculated using simulated curves in Fig. 5

particularly at higher values of rotation speed, ω. However, the drift does not produce any significant change in the rate constant k_1, whose average value is constant for data obtained over a range of concentrations.

The effect of temperature on the rate constant for the reaction $Cu(I)/S_2O_8^{=}$ was studied. Table 3 shows the k_1 value measured at several different temperatures.

TABLE 3

EFFECT OF TEMPERATURE ON RATE CONSTANT OF $Cu(I)/S_2O_8^{=}$ REACTION

TEMP. °C	k_1 (M^{-1} sec^{-1})
35	8.16×10^3
25	6.36×10^3
15	5.29×10^3
10	4.73×10^3

A plot of the empirical rate constant, k_1, vs 1/T shown in Fig. 9 was linear and yielded

$$k_1 = 3.37 \times 10^6 \exp(-3625/RT)$$

where $R = 1.987$ cal $°K^{-1}$ $mole^{-1}$

The value of the rate constant for the reaction $Cu(I)/S_2O_8^{=}$ at 25°C, 6.3×10^3 $M^{-1}sec^{-1}$, differs from the value 1.4×10^3 $M^{-1}sec^{-1}$ obtained

FIGURE 9: DEPENDENCE OF RATE CONSTANT ON TEMPERATURE FOR $Cu(I)/K_2S_2O_8$

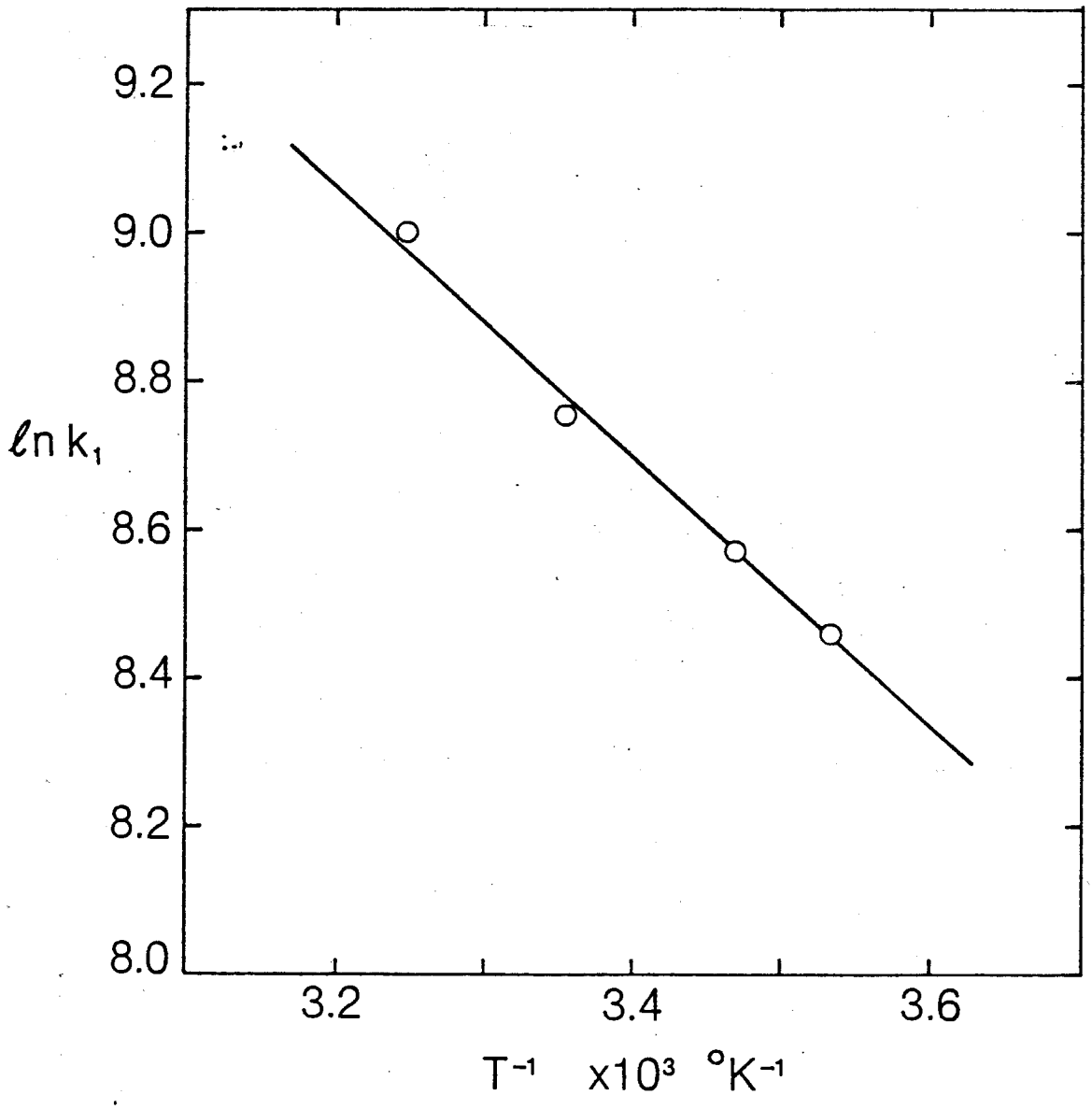
9.2
9.0
8.8
8.6
8.4
8.2
8.0
ℓn k1
3.2
3.4
3.6
T-1 x10³ °K-1

by Kolthoff (58) using a polarographic technique based upon the dropping mercury electrode. Reasons for the discrepancy are not apparent. Information in the leterature on the rate constant for the reaction of Cu(I) and peroxide is limited. Anber (25) reported a value of K_1 = 850 M^{-1} sec^{-1} for the reaction of bis(bipyridyl) copper(I) complex ion with H_2O_2 at 25°C.

The literature data available on second-order rate constants determined by the digital simulation techniques with the RRDE are relatively scarce. Although Bard and Prater (50) obtained good results in the comparison of the Fe(II)/H_2O_2 system, the comparison is somewhat clouded by the stoichiometry they employed in their working curves where the value for $m = C_C^\circ/C_A^\circ = 1$ was chosen rather than the proper value m = 0.5 (59). Their rate constant is therefore approximately twice as great as reported.

1.3.3. Comparative Study of Fe(II)/H_2O_2 Reaction

For comparative purposes experiments were carried out with the Fe(II)/H_2O_2 system where good literature values for the rate constant were available. Fig. 10 shows current-potential sweeps for the disk and the ring for the 2.0 M HCl solvent, for the solvent with H_2O_2, and for an Fe(III)/H_2O_2 solution. Fig. 10A gives the dependence of the currents on $\omega^{1/2}$ in the presence and absence of H_2O_2. The detailed results for the system containing 6.48 mM Fe(III) and 6.40 mM H_2O_2 in 2.0 M HCl are shown in Table 4 while the results for runs at other concentrations are shown in a condensed form in Table 5.

FIGURE 10: CURRENT POTENTIAL SWEEPS IN 2.0M HCl at 25°C

A and B for ring and disk, respectively,
solvent only, ω = 143 rad/sec;
C and D for ring and disk, respectively,
6.40 mM H_2O_2, ω = 87 rad/sec;
E and F for ring and disk, respectively,
for 6.40 mM $FeCl_3$/6.40 mM H_2O_2, ω = 87 rad/sec

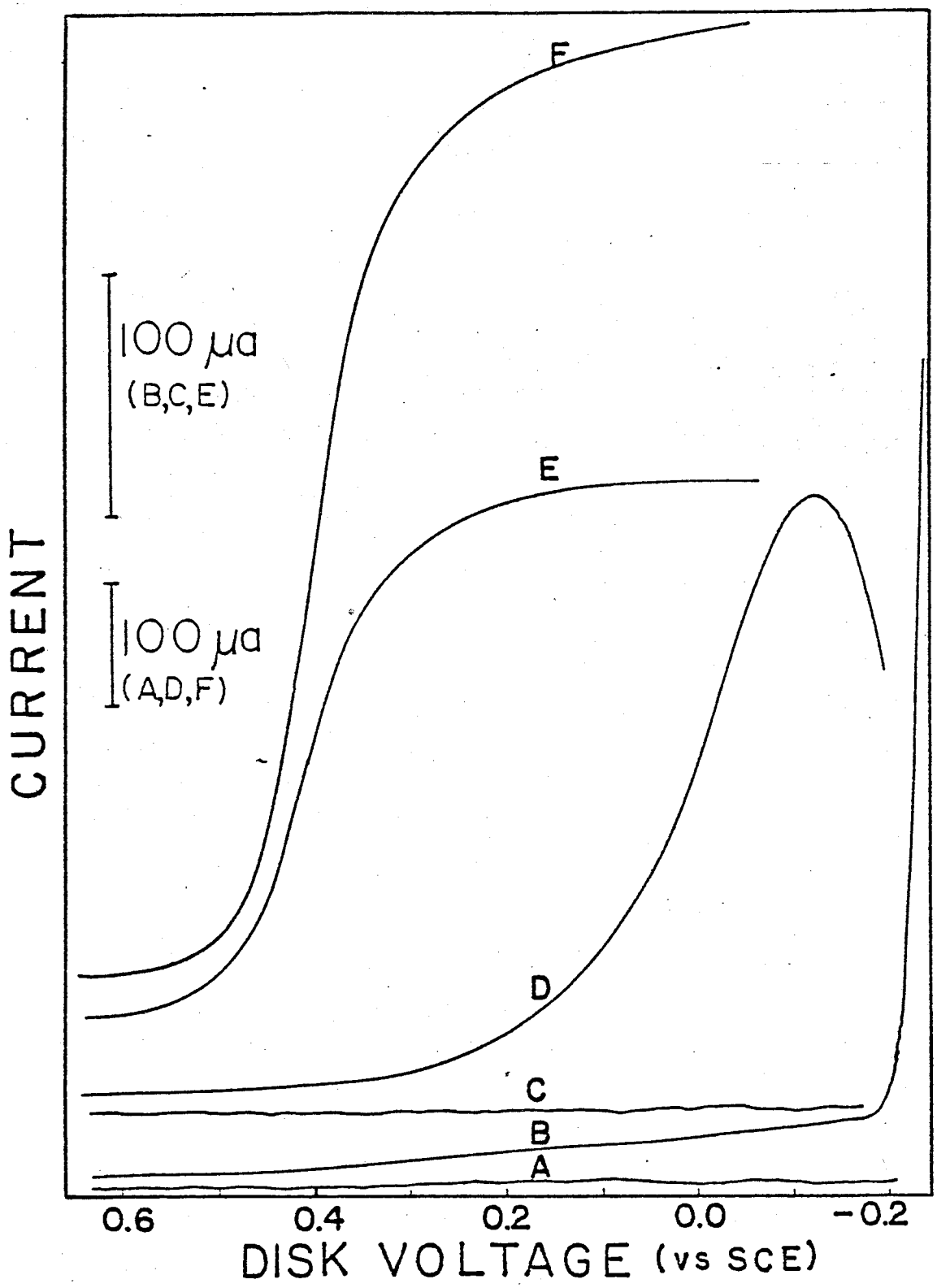
F
100 μa
(B,C,E)
E
100 μa
(A,D,F)
CURRENT
D
C
B
A
0.6
0.4
0.2
0.0
-0.2
DISK VOLTAGE (vs SCE)

FIGURE 10A: CURRENT VS ROTATION RATE IN Fe(III)/H_2O_2/2.0M HCl AT 25°C

i_D^{WO} and i_R^{WO} are disk and ring current, respectively, in 6.40 mM $FeCl_3$;

i_D^{W} and i_R^{W} are disk and ring currents, respectively in 6.40 mM $FeCl_3$/12.8 mM H_2O_2

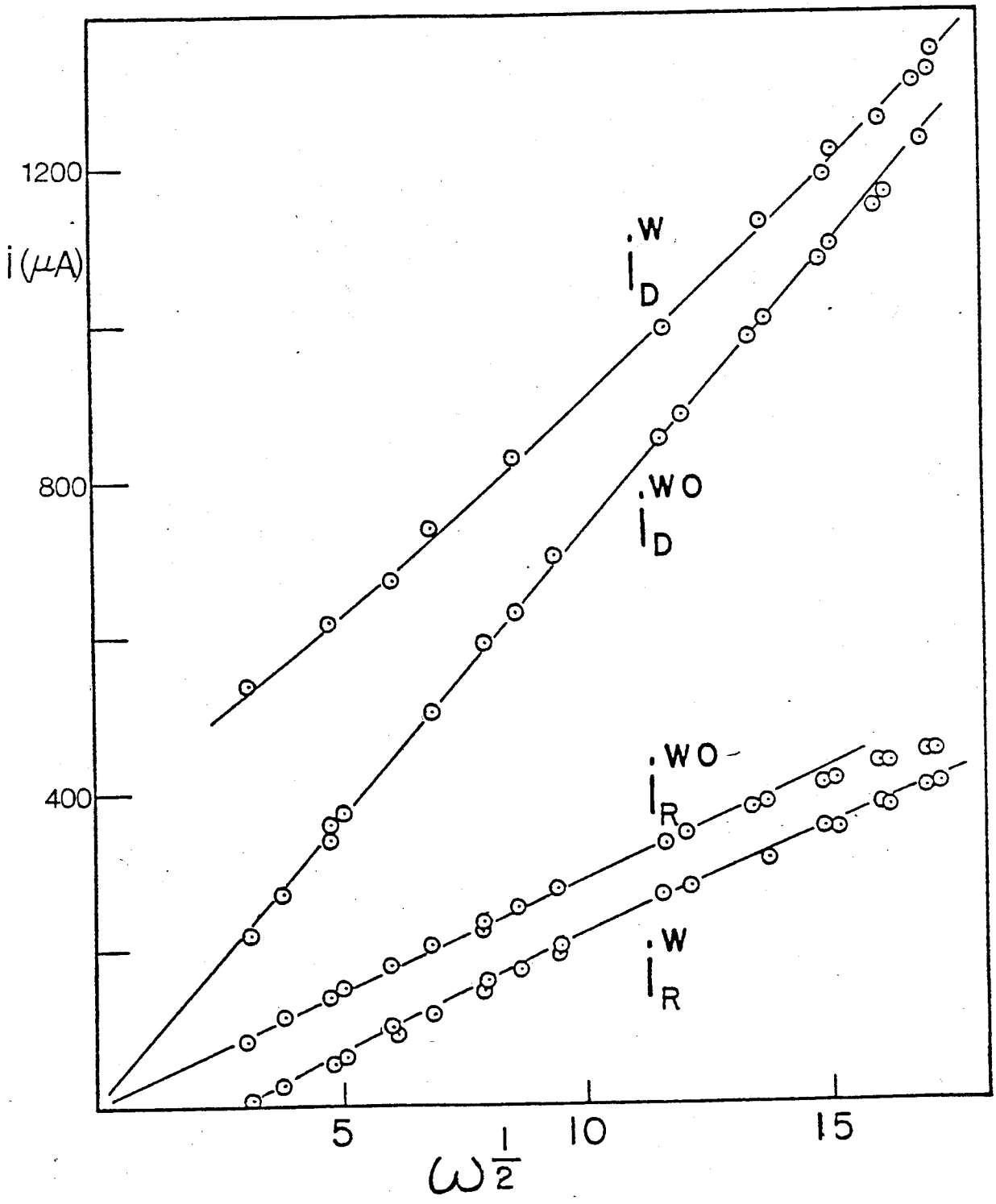
1200
800
400
i (μA)
.W
I_D
.WO
I_D
.WO
I_R
.W
I_R
5
10
15
$\omega^{\frac{1}{2}}$

TABLE 4

RRDE DATA FOR 6.48 mM Fe(III)/6.40 mM H_2O_2

(rad/sec)	N_k	XKTC	k_1 (M^{-1} Sec^{-1})
9.4	0.064	5.18	191
22	0.167	1.99	173
36	0.215	1.34	187
62	0.246	1.01	246
90	0.295	0.60	210
137	0.320	0.43	228
182	0.344	0.28	199
222	0.356	0.21	185
258	0.353	0.23	232
290	0.350	0.25	281
299	0.367	0.16	184
			k_1 (average) = 2.1×10^2

TABLE 5

RRDE RESULTS FOR Fe(III)/H_2O_2/2.0M HCl AT 25°C

Conc. of $FeCl_3$ (mM)	Conc. of H_2O_2 (mM)	k_1 (average) (M^{-1} sec^{-1})
3.30	3.30	$2.2 \times 10_2^2$
6.45	12.80	$2.5 \times 10_2$
6.45	1.28	$2.5 \times 10_2$
12.94	1.28	$2.3 \times 10_2$
1.31	12.8	3.1×10

In the publication of their digital simulation technique for the analysis of RRDE data, Bard and Prater (50) reported a value of 105 ± 5 M^{-1} sec^{-1} for the reaction

$$Fe^{2+} + H_2O_2 \longrightarrow Fe^{3+} + HO^- + HO\cdot$$

at 25°C in 2 M HCl. Recalculation of their data with the form of the program described in the Experimental Section using m = 0.5 working curve with the dimensions of their electrode gave k_1 = 202 ± 15, in agreement with the values in Tables 4 and 5.

There are numerous literature values for k_1 for the Fe(II)/H_2O_2 reaction in a wide variety of supporting electrolytes. For the purpose of using the present results to test the digital simulation, a review of the literature has been made.

Barb et al (60) reported a value of 53 M^{-1} sec^{-1} at 25°C in acidic perchlorate, sulfate or chloride. Sutin (61 - 62) reported values of 58 -64 in chloride-perchlorate mixtures, while Wells (19) gave values of 50, 54 and 69 in 1M $NaClO_4$, 1M $HClO_4$ and 1M NaCl, respectively.

There have been four studies reported where Fe(II) was generated electrochemically from Fe(III), with the peroxide reaction catalytically regenerating the Fe(III). In a polarographic study at the dropping mercury electrode, Delahay (63) reported values at 0.6°C and 31.4°C in 0.25M H_2SO_4 from which a value of approximately 59 can be interpolated for 25°C. At a gold rotating disk electrode, Haberland (27) calculated a value of 92 at 25°C in 0.1M HCl using a rotating palladium disk electrode.

Several points need to be made in regard to the rate constants presented in Tables 4 and 5. Reaction concentrations have been varied from

a ten-fold excess of cation (m = 0.1), to concentrations equimolar in cation and peroxide (m = 1.0), to a ten-fold excess of peroxide (m = 10). Assuming that the reaction is first-order in each reactant, a one hundred-fold increase in reaction rate would be expected between the slowest and fastest cases. The computer simulation gives k_1 values (average over a run), which are in general agreement over this wide range of concentrations. However, the overall average value of 240 M^{-1} sec^{-1} for the Fe(II)/H_2O_2 reaction is three or four times the literature values. Reasons for this discrepancy could be experimental in origin, or could result from some of the approximations made in deriving the computer simulation.

In the Fe(II)/H_2O_2 reaction it should be considered that the H_2O_2, in addition to being reduced by Fe(II) in solution, is partially or completely reduced directly at the electrode. This will give a larger disk current than would be found for the disk reaction of Fe(II) alone. In a RDE study of the Fe(II)/H_2O_2 reaction, Beran (28) found such considerable reduction of H_2O_2 at a platinum electrode in 0.1 M HCl that a satisfactory measurement could not be made, while neither Haberland (27), using a gold RDE, nor Bard (50), using a carbon paste RRDE made any reference to the problem for the solutions studied. Bard did report the appearance of bubbles at the electrode for very high H_2O_2 concentrations.

The current potential sweep for H_2O_2 in HCl in Fig. 10 clearly shows evidence of H_2O_2 reduction at the disk. Attempts were made to correct the current magnitude due to the direct electrode reduction of H_2O_2. The correction does decrease k_1, from 210 M^{-1} sec^{-1} to 160 M^{-1} sec^{-1}, but this value remains considerably larger than the values 50 - 70 M^{-1} sec^{-1} reported in the literature.

The computer simulation depends on the method of calculating the changes in concentrations of electroactive species in the volume elements beneath the electrodes. The effect of solution reactions is taken into account by the DEL terius in Eqs. [38 - 40]. If one arbitrarily introduces a factor of 3 or 4 before the DEL terms in Eqs. [38] and [39], a steeper working curve results, giving smaller k_1 values for a given ω. This arbitrary change has the effect of increasing the rate of change of the concentrations of Fe(III) and Fe(II), relative to the rate of disappearance of H_2O_2, in the reaction volume beneath the electrode. Indeed, when the working curve (Fig. 5) is normalized to yield $k_1 = 60\ M^{-1}\ sec^{-1}$ for all ω, a similarly steeper curve can be obtained. These results suggest that in the simulation the dependence of the disk and ring currents on the reaction kinetics may need further study, especially the treatment of the volume of solution immediately below the disk electrode as a single "box" in the (J, K) grid.

1.3.4. Redox Reactions of $Fe(II)/S_2O_8^{=}$ and $Fe(C_2O_4)_3^{-4}/S_2O_8^{=}$

While the electro-reduction of H_2O_2 at the disk electrode is possible, there is no direct electro-reduction of $S_2O_8^{=}$ in the potential range of interest. This is evident by data presented in Fig. 7 where only Cu(II) is reduced. The rate constant obtained for the $Cu(I)/S_2O_8^{=}$ reaction, however, cannot be compared unequivocally with the value reported by Kolthoff et al (58) in the sole study using a dropping mercury electrode. Experiments were performed with the system $Fe(II)/S_2O_8^{=}$, which had previously been studied by King and Steinbach (66) and by Fordham and Williams (67) using spectroscopic techniques. The data in Table 6 provide the rate constants obtained in this work. The average rate constant is 62 M^{-1} sec^{-1} at 10°C, while Fordham et al reported k = 42.6 M^{-1} sec^{-1} at 10°C and King et al reported k = 83.3 M^{-1} sec^{-1} at 25°C.

The reactions of $S_2O_8^{=}$ with Fe(II) yielded a much lower rate of formation of free radicals than those obtained with Cu(I). Attempts were made to increase the rate of reaction by complexing the Fe(II) ions and the systems $Fe(C_2O_4)_3^{=}$ and $Fe(CN)_6^{=}$ were employed. The rate of reaction was essentially unaffected in the ferricyanide complexes but was increased in the oxalate complexes. The range of potential at which the reductions take place and the magnitude of the currents showed that it is the complexed ions rather than the Fe(II) ions that take part in the electrochemical reactions and in the subsequent reactions with $S_2O_8^{=}$. The data for oxalate are summarized in Table 7.

TABLE 6

RRDE DATA FOR $Fe(III)/S_2O_8^{=}$ SYSTEM

ω (rad/sec)	Disk Current i_d (μ A)	Ring Current i_r (μ A)	N_k	XKTC	ω (XKTC)
45.0	252	90	0.357	0.11	5.0
62.8	330	121	0.367	0.08	5.0
108.4	436	164	0.376	0.06	6.5
131.4	476	181	0.380	0.05	6.6
172.3	554	213	0.385	0.04	6.9
209.4	616	240	0.389	0.03	6.3
				average	6.1

k_1 (average) $= 62\ \ell\ mole^{-1}\ sec^{-1}$

Conditions: Temp = 10°C 5 mM Fe(III)/5 mM $S_2O_8^{=}$

Supporting electrolyte: 0.5 M HCl

$D_A = 5 \times 10^{-6}\ cm^2/sec, \quad \nu = 1 \times 10^{-2}\ cm^2/sec$

TABLE 7

RRDE DATA FOR $Fe(C_2O_4)_3^{-3}/S_2O_8^{=}$ SYSTEM

(rad/sec)	Disk Current i_d (μ A)	Ring Current i_r (μ A)	N_k	XKTC	ω (XKTC)
108.4	568	190	0.335	0.17	18.4
131.4	618	220	0.356	0.11	14.5
151.8	636	228	0.359	0.10	15.2
191.1	660	250	0.378	0.06	11.5
				average	14.9

k_1 (average) $= 150\ \ell\ mole^{-1} sec^{-1}$

Conditions: Temp = 25°C Supporting electrolyte 0.5 M $K_2C_2O_4$

1.3.5. Redox Initiation of Aqueous Polymerization

An interesting set of reactions takes place upon the addition of monomer to a solution containing Cu(I) and $S_2O_8^{=}$. The reaction of $SO_4^{\cdot-}$ with monomer

$$SO_4^{\cdot-} + M \xrightarrow{k_3} {}^{-}SO_4M^{\bullet} \qquad [47]$$

competes with reaction [30] in the following reaction scheme

$$Cu^{+} + S_2O_8^{=} \xrightarrow{k_1} Cu^{+2} + SO_4^{\cdot-} + SO_4^{=} \qquad [29]$$

$$Cu^{+} + SO_4^{\cdot-} \xrightarrow{k_2} Cu^{+2} + SO_4^{=} \qquad [30]$$

Essentially, the presence of monomer reduces the electrocatalytic contribution to the disk current.

Typical sweeps showing reduction and re-oxidation of Cu(II) in the presence and absence of $S_2O_8^{=}$ and acrylonitrile are shown in Fig. 11. The solid curve A is obtained with Cu(II) only. When $S_2O_8^{=}$ is added the disk current increases and curve B is obtained. On addition of monomer, the competition of Cu(I) and acrylonitrile for $SO_4^{\cdot-}$ reduced the electrocatalytic effect and curve C is obtained. Corresponding behavior is evident from the curves of ring currents.

Plots of i_d and i_r vs $\omega^{1/2}$ are presented in Fig. 12 for various concentrations of acrylamide, while Fig. 13 shows the effect of increasing concentrations of acrylic acid on i_r. It can be seen that the currents are significantly affected by the addition of $S_2O_8^{=}$. i_d and i_r reach their maximum and minimum values respectively as a result of the homogeneous reactions [29] and [30] . When monomer is added, reaction [47] competes with reaction [30] and corresponding increases in i_r and decreases in i_d are observed. With excess monomer, reaction [30] will be suppressed completely

FIGURE 11: TYPICAL RRDE VOLTAMMOGRAMS FOR REDUCTION OF Cu(II) IN THE PRESENCE AND ABSENCE OF $S_2O_8^=$ AND MONOMER

(A) 2 mM Cu(II)

(B) (A) with 2 mM $S_2O_8^=$

(C) (B) with 0.286 M AN

ω = 81 rad/sec, supporting electrolyte: 0.5 M KCl, temperature : 25°C

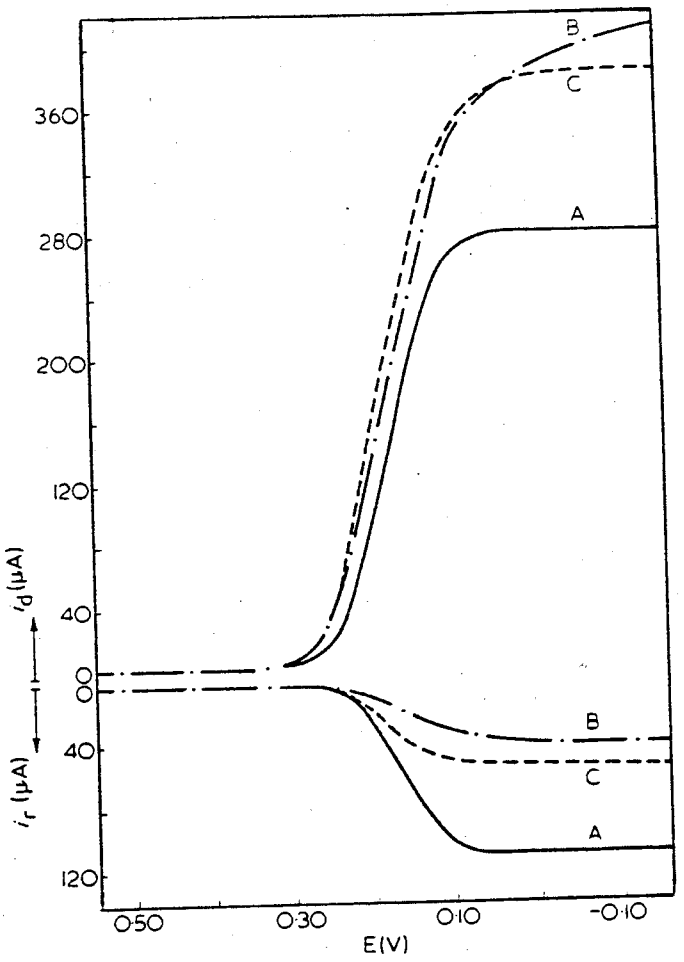
B
C
A
360
280
200
120
40
0
0
40
120
i_d (μA)
i_r (μA)
B
C
A
0·50
0·30
0·10
-0·10
E(V)

FIGURE 12: RING AND DISK CURRENTS VS ROTATION RATE FOR VARIOUS CONCENTRATIONS OF ACRYLAMIDE

All solutions : 2 mM Cu(II)/2 mM $S_2O_8^{=}$/0.5 M KCl/25°C except Cu(II) blank run

Monomer concentrations :

○ 0.0M	■ 0.176M
▼ 0.132M	▲ 0.088M
□ 0.044M	△ 0.022M

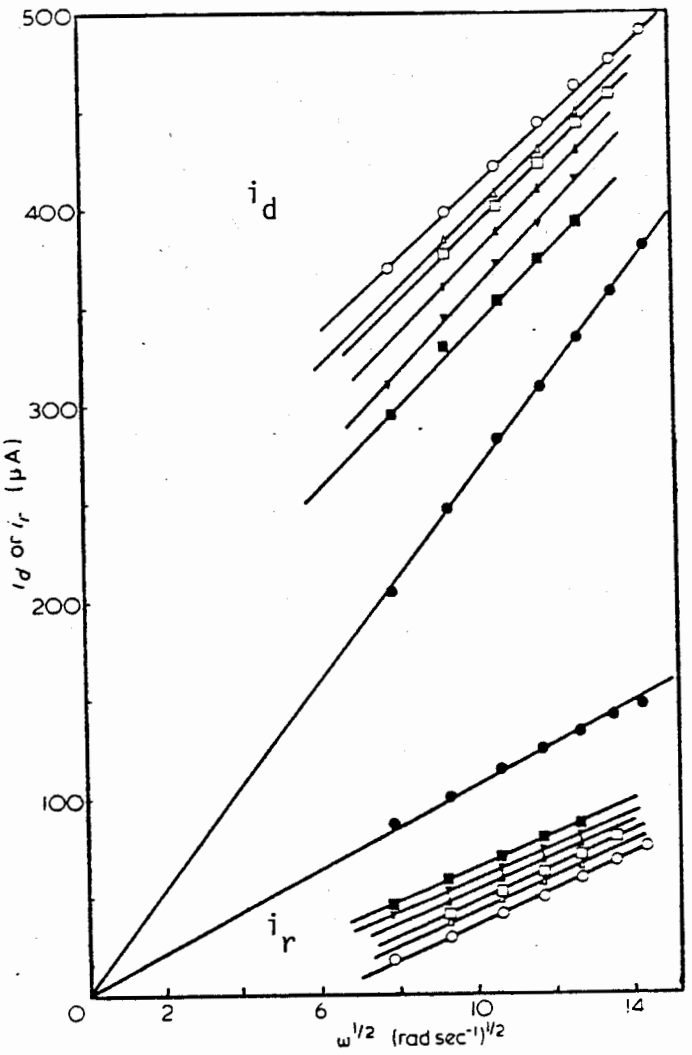
500
400
300
200
100
0
2
6
10
14
i_d
i_r
i_d or i_r (μA)
$\omega^{1/2}$ (rad sec^{-1})$^{1/2}$

FIGURE 13: EFFECT OF INCREASING ACRYLIC ACID CONCENTRATION ON RING CURRENT

All solution : 5 mM Cu(II)/5 mM $S_2O_8^{=}$/0.5 KCl/25°C except Cu(II) blank run (■)

Monomer concentrations: ●, 0.39 M; □, 0.30 M; ▲, 0.18 M; ○, 0.10 M; △, 0.00 M.

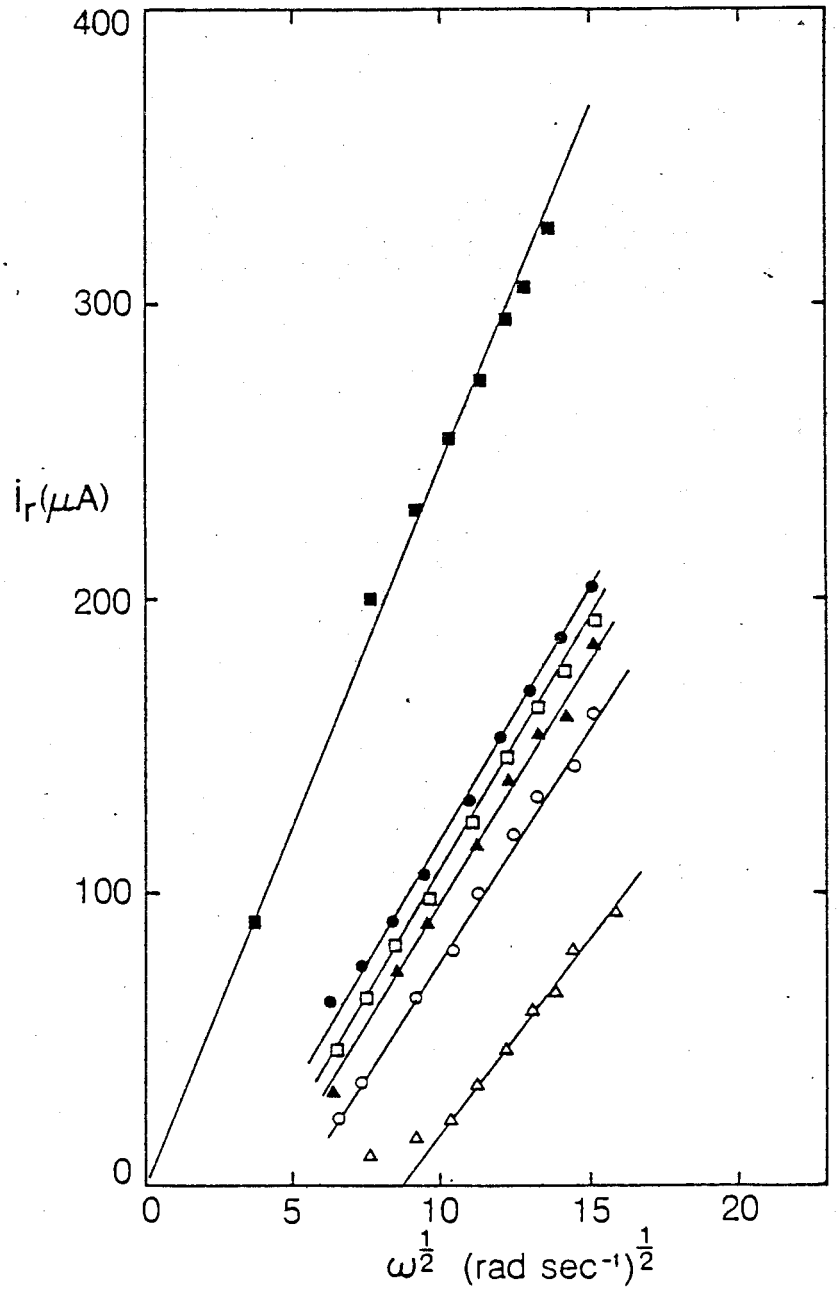
400
300
200
100
0
$i_r(\mu A)$
0
5
10
15
20
$\omega^{\frac{1}{2}}$ (rad sec^{-1})$^{\frac{1}{2}}$

and only reaction [29] will be effective. Under these conditions the changes in i_r and i_d will be one half of the catalytic effect due to $S_2O_8^=$ alone, because the rate determining step [29] is independent of monomer concentration.

At monomer concentrations intermediate between these two extremes the changes in i_r and i_d reflect the competitive effects of reactions [30] and [47].

Thus when the rates of [30] and [47] are equal catalytic current should be 1/2 of the maximum attainable change, i.e.:

$$k_2[SO_4^{-\bullet}][Cu(I)] = k_3[SO_4^{-\bullet}][M] \qquad [48]$$

or

$$\frac{k_2}{k_3} = \frac{[M]}{[Cu(I)]} \qquad [49]$$

This expression is identical to that obtained by Baxendale (48) from a stationary state method. Orr and Williams (67) studied the $Fe(II)/H_2O_2$ and $Fe(II)/S_2O_8^=$ systems and found:

$$\frac{R_2}{R_3} = \frac{k_2\ [Fe(II)]}{k_3\ \ [M]} \qquad [50]$$

where R_2 and R_3 are the fractions of the total radicals produced which have reacted in steps [30] and [47] respectively. When $R_2 = R_3$ equations [49] and [50] are identical.

The fractional change in ring current ($\Delta i_r / {}^1/_2 \Delta i_r$ cat) with varying concentrations of acrylic acid, acrylamide, methacrylic acid, and acrylonitrile are shown in Fig. 14.

FIGURE 14: FRACTIONAL CHANGE IN RING CURRENT WITH MONOMER CONCENTRATION

● acrylic acid; ○ acrylamide;

▲ methacrylic acid; ▽ acrylonitrile

2 mM Cu(II)/2mM $S_2O_8^{=}$/0.5 M KCl/25°C with various concentrations of monomers

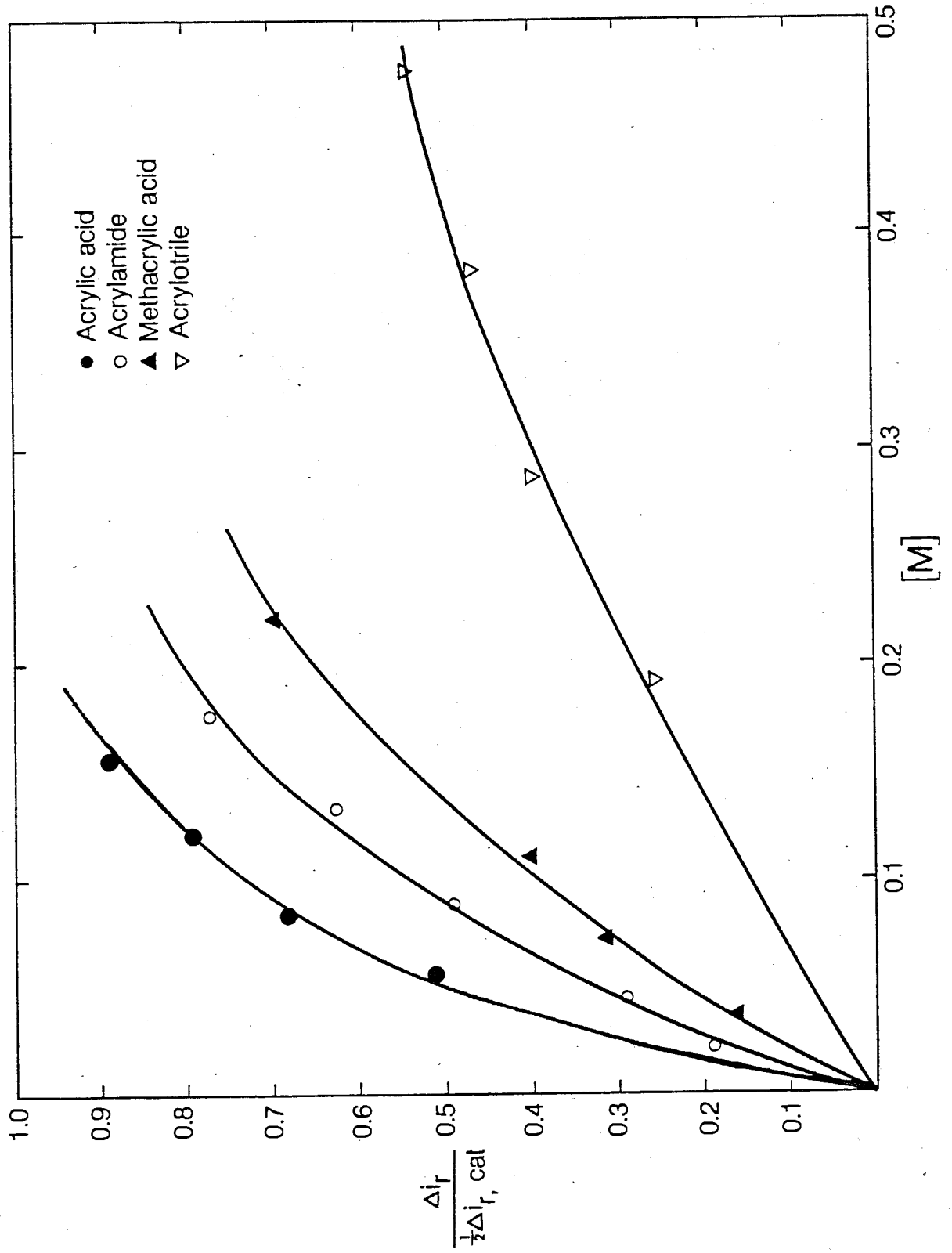
Acrylic acid
Acrylamide
Methacrylic acid
Acrylotrile
$\frac{\Delta i_r}{\frac{1}{2}\Delta i_{r,\,cat}}$
[M]
0.1
0.2
0.3
0.4
0.5
0.6
0.7
0.8
0.9
1.0

The Cu(I) concentration varies throughout the diffusion layer in the region between the ring and disk electrodes. However, the steady state assumption is applicable at each point in the diffusion layer because the concentration is invariant with time. The ring and disk currents serve to evaluate Cu(I) concentration at the electrodes. Thus the rates of reactions [47] and [30] may be compared at the ring electrode. At acrylic acid concentration of 0.115 M, the concentration of Cu(I) at the ring electrode was measured as 2.1 mM for the system containing 5mM Cu(II), 5mM $S_2O_8^{=}$, and acrylic acid; the ratio of $\Delta i_r / {}^1/_2 \Delta i_{r,cat}$ was 0.5. The ratio of k_2/k_3 was calculated to be 55 for acrylic acid. The ratio of k_2/k_3 for acrylamide, methacrylic acid, and acrylonitrile are compiled in Table 8

TABLE 8

RELATIVE REACTIVITIES OF MONOMERS WITH $SO_4^{\cdot -}$

MONOMER	k_2/k_3	k_3 RELATIVE
Acrylic acid	55	1
Acrylamide	78	0.71
Methacrylic acid	123	0.45
Acrylonitrile	363	0.15

The relative reactivities listed in Table 8 are indicative of the initiation step in the polymerization. The quantification of this effect in contradistinction to the effectiveness of the initiator has been reported for only a few systems. The RRDE technique is well suited to this probing of the mechanism. It allows the study to be performed without sensible change in the monomer concentration and avoids the buildup of ionic species which may alter the polymerization process and introduce further complexities into the reaction mechanism.

CHAPTER II

ELECTRO-INITIATED GRAFT COPOLYMERIZATION

2.1. INTRODUCTION

Addition polymerization are initiated by reactive species such as free radicals, carbanions, or carbonium ions. Usually the reactive species are generated in the system via suitable chemical processes. Such processes include the formation of free radicals by thermal decomposition of peroxides, the generation of radical anions by a transfer of electron to monomers, and by many other reactions.

When a reactive species capable of initiating a polymerization is formed by an electron transfer process occurring at the electrodes, the reaction is referred to as an electrolytically initiated polymerization. The earliest mention of an electro-initiated polymerization appeared in an article published by Szarvasy (68) at the turn of this century. No further results appeared until 1947, when a Ph.D. thesis by Rembold (69) mentioned the polymerization of methyl methacrylate by electrolytic initiation. In 1949, Wilson (70) made reference to the polymerization of acrylic acid while studying the electro-reduction of various organic compounds. It was not until the late fifties and the early sixties, however, that this new type of initiation began to be recognized and utilized by polymer chemists. Since then, activity in the field has been growing rapidly as is reflected in the number of published papers (1-4, 71-72, and references cited therein).

Electrolytic initiation often implies a significant degree of control over the rate of initiation reaction. It has been shown that the total charge passed to a solution may be directly related to the concentration of initiating species and that the electrode potential determines the formation of the type of initiating species (73, 74). Under appropriate conditions, polymerization may proceed by a free radical, anionic or cationic mechanism. In an anionic polymerization, the formation of initiating species and the termination of growing chain ends may be further affected by simply switching the current polarity (75, 76). The rate of reaction can thus be controlled by programming the current-time profile (77). Quantitative control of anionic polymerization has been demonstrated to produce polymers with desirable molecular weights and molecular weight distributions (78).

While the synthetic potential of electrochemically initiated polymerizations has been explored extensively for many monomer systems, the application of the electrochemical technique to the modification of polymer structure has received little attention. Apart from the few phenomenological studies concerning the grafting of monomers onto cellulose (79,80) and polyacrylic acid (81) in aqueous media, no work has been reported on electrochemical studies of polymers. This may be partly due to the low solubility of polymers in many of the solvents used in electrochemical studies. However, extensive work for small molecule systems has been carried out in recent years in organic media with suitable supporting electrolytes, which should allow investigations of a number of substituent electroactive groups on polymers.

For polymers bearing electroactive substituent groups it is conceivable that the direct electron transfer processes, analogous to those occurring in small molecule systems, should result in the formation of macromolecular initiators and could provide a means of controlled synthesis. Most recently, Guillet et al (82) took a similar approach, employing polymers containing chromophoric groups in the photosynthesis of polymers with new structures.

The aim of the present investigation was to examine the possibilities of forming graft copolymers by an electrolytic method. Electroactive benzophenone groups were attached to a backbone polymer and subsequently activated at a cathode electrode by a passage of current. The resulting polyradical anions were used to initiate graft copolymerization.

2.1.1. Graft Copolymers

Graft copolymers are macromolecules consisting of a polymer backbone with attached polymer branches:

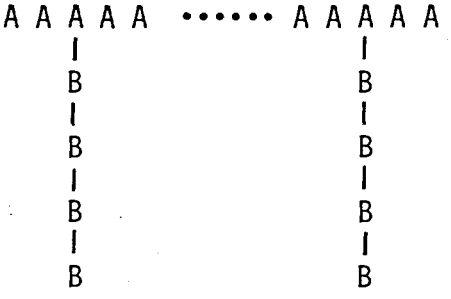

This class of polymers together with block copolymers belong to sequential copolymers which provide the basis of a number of commercially important polymers, such as high impact polystyrene, acrylonitrile-butadiene-styrene

(ABS) copolymer, and methacrylate-butadiene-styrene (MSB). They offer useful properties which are often superior to the blends of the corresponding homopolymers and frequently represent a unique combination not attainable by other materials.

The earliest and simplest method for preparing graft polymers utilized chain transfer to polymer. In this preparation, monomer is polymerized in the presence of a pre-formed polymer of a different composition. During polymerization, an occasional free radical may remove a hydrogen atom or other labile group and thus leave a free radical on the polymer chain which can later add monomers to form a graft copolymer. The preparation of graft copolymers by chain transfer is, however, usually inefficient and generates only a few grafts.

Studies of the preparation, purification, and characterization of better defined graft copolymers have followed two main lines. The initial approach was to prepare graft copolymers by more random methods such as radiation and mechanical degradation. The polymers thus formed were then purified and characterized as well as possible. More recently the emphasis has shifted to the preparation of purer and better defined graft copolymers. Specifically the use of "living anions" in preparing graft coplymers has made the preparation of well-defined copolymers possible.

In general, grafting may be achieved by one of the following methods:

(a) Grafting onto - grafting onto occurs if a growing polymer chain attacks another polymer and thereby a branch is attached to a pre-formed backbone.

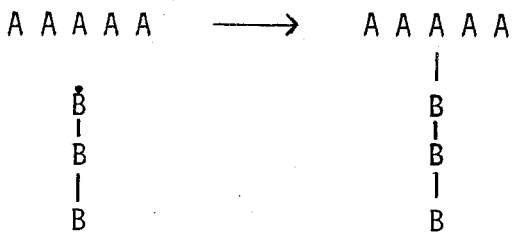

[51]

(b) Grafting from - grafting from occurs if an active site generated along a polymer backbone starts to propagate monomer in the system and thus produces branches.

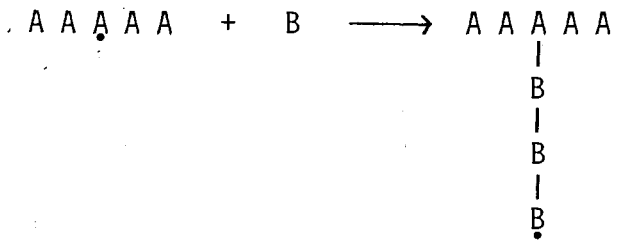

[52]

(c) Step growth - polymer molecules containing functional groups such as hydroxyl, carboxyl, amine, etc., may be chemically linked to form graft copolymers by a condensation reaction.

Among the methods described, the "grafting from" technique offers a better control of structure and less homopolymer contamination. The technique generally involves the introduction of functional groups at positions along the length of a polymer chain. The functional groups are activated by chemical, thermal or photochemical reactions or by radiation and mechanical degration to generate free radicals, anions or cations. The "grafting onto" method usually results in some unreacted homopolymer, and the step-growth graft copolymerizations, due to their di- or multi- functional nature, would produce cross-linked systems.

A number of surveys dealing with graft and block coplymerizations have been published (83 - 87) and it is hence unnecessary to provide a comprehensive review within the scope of this text.

2.1.2. Anionic Graft Copymerization

The synthesis of well-defined block copolymers was first described by Szwarc (88). The reaction of metallic sodium with an aromatic hydrocarbon such as naphthalene, in tetrahydrofuran, under proton donors free conditions, yields a soluble naphthyl radical anion. Addition of styrene to the system leads to electron transfer from the naphthyl radical anion to the monomer to form a reddish styryl radical anion. The reaction is generally believed to proceed as follows:

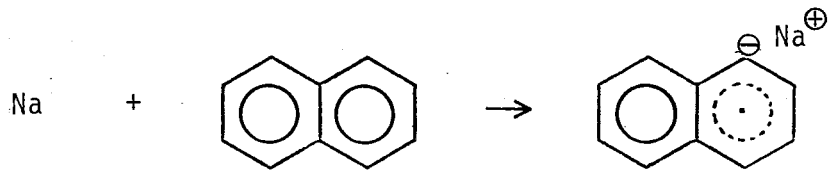

[53]

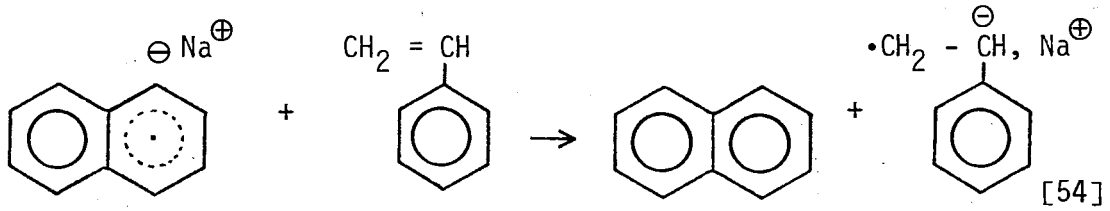

[54]

the initiation step is apparently not completed until dimerization of radicals take place:

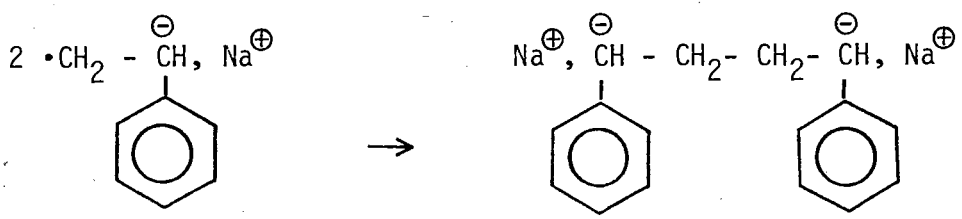

[55]

Propagation therefore proceeds at both ends by an anionic mechanism. It was demonstrated that the polymer solution so formed still contained active polymer chains even when all the monomer had been consumed. The addition of further monomer to the "living" anions resulted in the formation of a block copolymer.

By analogy to the polymerization with the sodium-naphthalene complex, Rembaum et al (89) demonstrated that the aromatic moieties in a polymer chain undergo the same reaction. Poly (4-vinylbiphenyl) was allowed to react with sodium in ether-type solvents to form biphenyl radical anions. The polyvinylbiphenyl sodium complex so formed was found to initiate the polymerization of styrene, isoprene, α-vinylnaphthalene, and ethylene oxide. With ethylene oxide, graft copolymers were obtained.

Following along the same lines, Goutiere et al (90) prepared the complex of poly (vinyl-2-fluorene) with alkali metal in anhydrous tetrahydrofuran. The metalized polymers thus obtained, especially those containing lithium were capable of anionically initiating the graft copolymerization of vinyl monomers.

Greber and Egle (91) prepared polymeric ketyls by reacting sodium with poly (vinylbenzophenone) at room temperature. Using this complex, grafting was initiated with acrylonitrile, methyl methacrylate, and 4-vinylpyridine.

Soluble organometallic macromolecules were also formed by the introduction of an alkali metal into halogen-containing polymer molecules (92). Thus the chlorine in poly (p-chlorostyrene) was exchanged for sodium by reaction of sodium naphthalene in tetrahydrofuran and the complex used to initiate the grafting of anionically polymerizable monomers. The grafted branches were reported to remain "live" and permitted further polymerization of added monomers to form a block-graft network.

Direct introduction of alkali metal sites on polymers by trans-metalation has been reported (93). Lithiated polydienes have been prepared by direct metalation of the diene polymers with sec-butyllithium and N,N,N',N' - tetramethylethylenediamine. Reaction of the polylithiodienes with styrene or α-methylstyrene formed graft copolymers with high grafting efficiencies (94, 95). Coupling reactions of lithiated polymers with polymers containing certain end groups such as hydroxymethyl group (96, 97) and chlorinated group (98) have also been utilized for the formation of graft copolymers.

2.2 EXPERIMENTAL

2.2.1. Chemicals and Their Purifications

Styrene (ST), acrylonitrile (AN), and methyl methacrylate (MMA) were dried over calcium hydride and vacuum distilled. The central cuts were then"flash"distilled in a vacuum line and stored in flasks filled with purified nitrogen.

N,N-dimethylformamide (DMF) was distilled from barium oxide at reduced pressure in a purified N_2 atmosphere and was collected over molecular sieve type 4A and finally redistilled before use.

Tetrahydrofuran (THF) was purified by a method described by Morton (99) and was stored in a vacuum line. It was "flash" distilled into the cell when used.

Benzoyl chloride and nitrobenzene were similarly distilled.

Tetraethylammonium perchlorate (TEAP) was recrystallized from water and dried at 80 - 100°C under reduced pressure for 48 to 96 hours (100).

Sodium tetraphenylboride, $NaPh_4B$, and other supporting electrolytes were of highly purified commercial grades and were dried in vacuo prior to use.

2.2.2. Polymerization Procedure

Poly(styrene) was prepared by anionic polymerization of styrene in benzene with n-butyllithium as initiator. In some cases, styrene was polymerized in bulk by a thermal method.

Poly(vinylbenzophenone-co-styrene), PVBP/ST, was prepared by allowing poly(styrene), anhydrous aluminum chloride, and benzoyl chloride to react in dry nitrobenzene for 20 hours. The polymer was precipitated in methanol and purified.

The apparatus for galvanostatic electrolysis consisted of a divided H type electrolysis cell to which a co-monomer holder was attached. The electrodes were square platinum sheets, 2.5 cm X 2.5 cm. The cell used to conduct potentiostatic electrolysis was of a similar design, except that an additional compartment was provided for accommodating a reference electrode. The reference electrode was Ag/AgCl spiral in DMF saturated with tetraethylammonium chloride. In the constant potential electrolysis, poly(vinylbenzophenone) radical anions were generated in the presence of co-monomers.

A KEPCO ABC1000 was used as a constant current supply. Controlled potential electrolysis was carried out using a Princeton Applied Research Model 170 Electrochemical System (PAR 170). This instrument was capable of providing up to 5 amps and the maximum voltage output of 90 volts between the working and counter electrodes. It was sufficient for work carried out in the relatively high resistance non-aqueous solvents used here.

In a typical experiment, the required amounts of poly(vinylbenzophenone-co-styrene) and supporting electrolyte were placed into the cell. The cell was attached to a vacuum line and evacuated for 24 hours with intermitting heating. Solvent was then distilled into the cell from a graduated cylinder. The contents of the cell were then thoroughly mixed and distributed to anode and cathode compartments. Current was passed through the cell until a persistent blue color, characteristic of $PVBP^{\cdot-}$, was formed at the cathode. This indicated the complete removal of reactive impurities. Current reversal destroyed the radical anions and thus zero concentration of the radical anion could be achieved by this process of electrochemical titration. A known

charge was passed through the solution until the solution turned dark blue. The concentration of $PVBP^{\cdot-}$ was determined by titration with dilute HCl. To this solution, monomer, previously purified and degassed by alternate freeze-and-thaw cycles, was added. The polymerization was allowed to proceed for 2 to 10 hours.

2.2.3. Voltammetry

Cyclic voltammetric measurements were carried out with a PAR Model 170 Electrochemical System in a three-compartment cell, similar to the one described in the previous chapter. The working electrode was a platinum disk sealed in soft glass and polished on a surface of ground glass. The reference electrode was Ag/AgCl or, in cases when only potential differences were measured, a silver wire reference was employed.(101). A coil of platinum wire served as the counter electrode. About 10 g neutral alumina were added to 50 ml solution to be measured and the mixture was stirred while it was flushed with purified N_2 prior to voltammetric measurements (102).

The rotating ring-disk electrode and its associated apparatus are the same as those described in Section 1.2.1. The detailed experimental procedure will be described in the next chapter.

2.2.4. Characterization Procedure

Visible spectra of the radical anions were determined with a Cary 17 spectrophotometer using a closed quartz cell equipped with a spacer for adjusting the absorbance and a self-sealing rubber cap for the introduction of the radical anion solution by syringe. The cell was dried in vacuo and flushed with dry argon.

Ultraviolet spectra of poly(vinylbenzophenone-co-styrene) were also recorded on a Cary 17 spectrophotometer using benzene as a solvent.

Infrared spectroscopic analysis of the copolymers was carried out on a Perkin-Elmer 457 IR spectrophotometer employing the KBr pressed disk technique.

Elemental analysis of the polymers was performed on a Perkin-Elmer Elemental Analyzer M240.

Intrinsic viscosity of the polymer solutions before and after electrolysis was measured in a Ubbelohde suspended level dilution viscometer in DMF at 30 ± 0.05°C.

Gel permeation chromatograms were obtained from a modified Waters Associates Model GPC/ALC301 using dilute polymer solution in either THF or DMF at flow rate of 1 ml/min. The chromatograph was equipped with a pump, a U6K injector and a differential refractive index detector. It contained four μ-styragel columns packed to the nominal exclusion limit of 10^6, 10^5, 10^5, 10^4 Å and was operated at ambient temperature.

2.3 RESULTS AND DISCUSSION

2.3.1 Preparation of Poly(vinylbenzophenone-co-styrene) (PVBP-ST)

Poly(vinylbenzophenone-co-styrene) used in the electrolysis experiments was prepared by the Friedel-Crafts reaction (103) of polystyrene with benzoyl chloride and aluminum chloride in nitrobenzene.

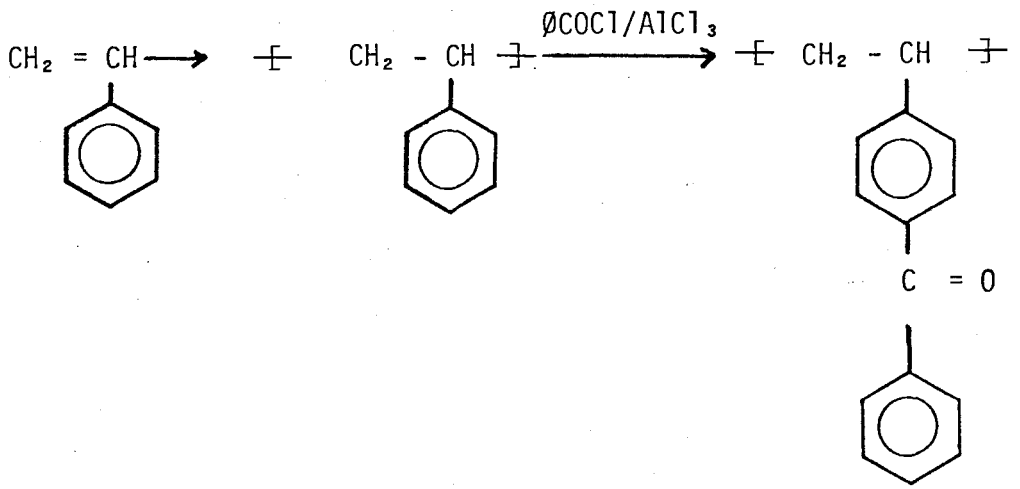

[56]

The polymer was precipitated in methanol and washed with excess methanol until it was free from nitrobenzene. The product obtained can be considered as a copolymer of styrene and 4-vinylbenzophenone. The benzophenone content of the polymer was controlled by adjusting the stoichiometric ratio of the reactants. The compositions were determined from the UV spectra as well as elemental analyses, corresponding to 80%, 50%, 35%, and 15% vinylbenzophenone.

2.3.2. Electro-reduction of Poly(vinylbenzophenone)

Cyclic voltammograms of poly(vinylbenzophenone) in DMF solution containing 0.12M TEAP at a micro-platinum electrode are shown in Figs. 15 and 16. When the sweep is limited to the range corresponding to the addition of one electron, a symmetrical trace is obtained. This is typical of a reversible one-electron transfer reaction which forms a product with sufficient stability to leave the diffusion layer. The experimental trace is shown in Fig.15. With a more cathodic bias a peak is formed which corresponds to the addition of a second electron, but this peak has no anodic counterpart(Fig.16). This indicates that the reduction of the benzophenone radical anion attached to the polymer chain is accompanied by a rapid irreversible protonation reaction. It is possible that the electron transfer step is reversible. These results are consistent with the mechanism proposed for the reduction of unsubstituted benzophenone and can be represented as

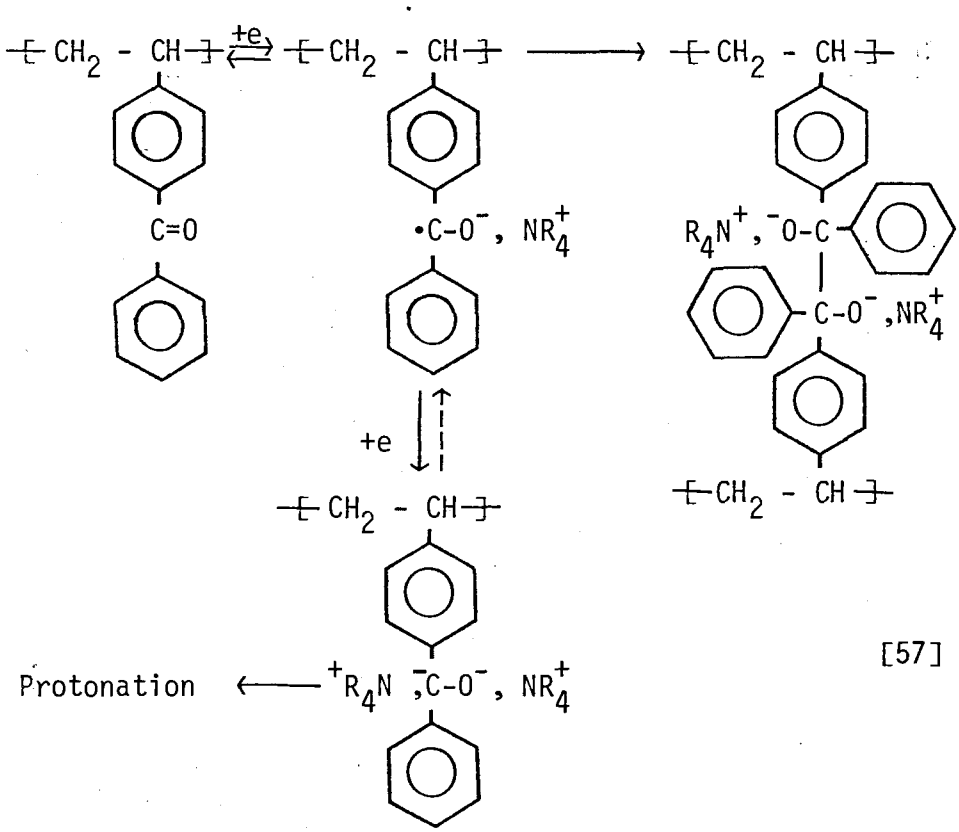

[57]

FIGURE 15: CYCLIC VOLTAMMOGRAM OF POLY(VINYLBENZOPHENONE) FOR THE FIRST ONE- ELECTRON TRANSFER REDUCTION

4.8 mM based on benzophenone residue in DMF with 0.12 M TEAP in the presence of suspended alumina; sweep rate = 250 mV/sec.

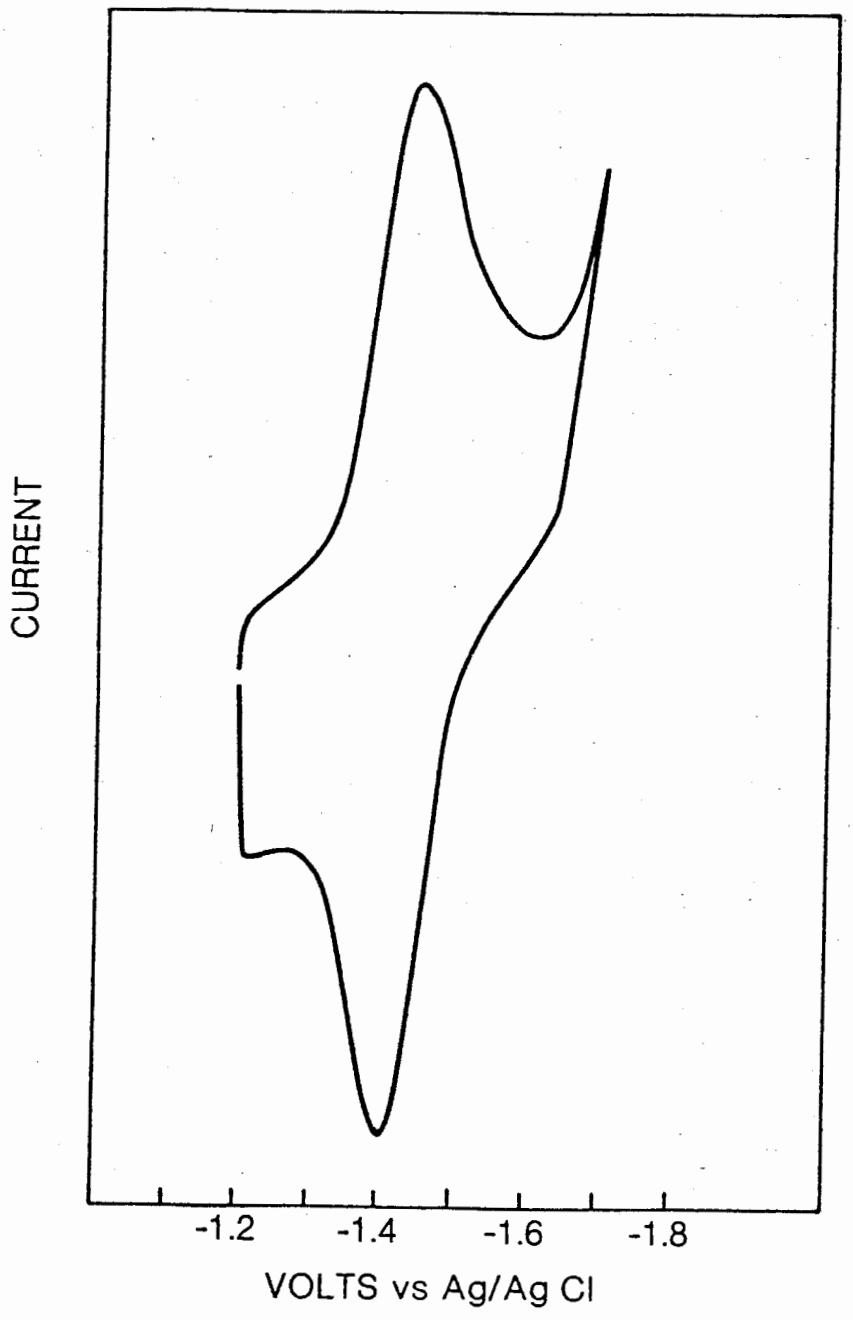
CURRENT
-1.2
-1.4
-1.6
-1.8
VOLTS vs Ag/Ag Cl

FIGURE 16: CYCLIC VOLTAMMOGRAM OF POLY(VINYLBENZOPHENONE) FOR THE FIRST AND SECOND ONE- ELECTRON REDUCTIONS

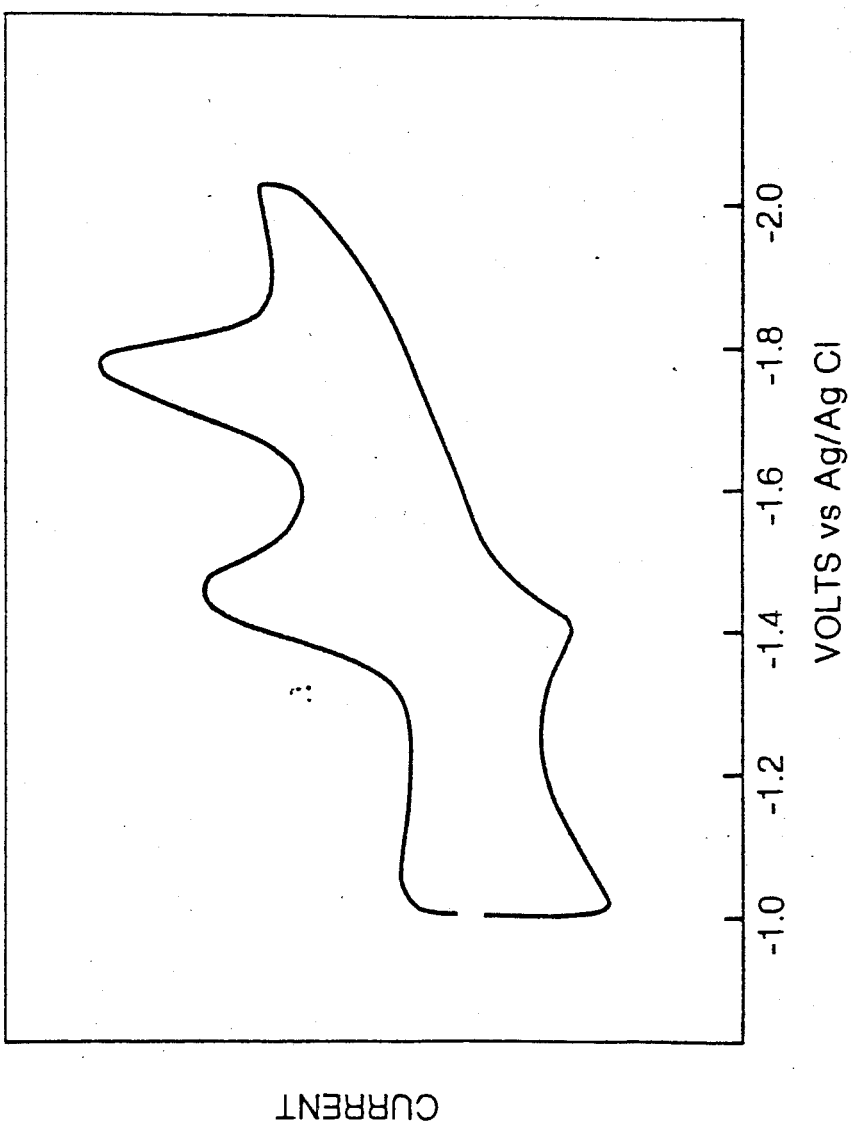
CURRENT
-1.0
-1.2
-1.4
-1.6
-1.8
-2.0
VOLTS vs Ag/Ag Cl

Difficulties were encountered when attempts were made to carry out voltammetric measurements for PVBP in THF with $NaPh_4B$. Although it was possible to measure the peak potentials for the two one-electron transfers at low concentrations of $NaPh_4B$ and the values were comparable to those found in DMF, the amount of salt could not be increased significantly without encountering serious problems with deactivation of the electrode which resulted in very irreversible voltammograms, thus rendering the measurements meaningless.

Macro-electrolyses were also conducted either in DMF with tetraethylammonium perchlorate (TEAP) as a supporting electrolyte or in THF with sodium tetraphenylboride as a supporting electrolyte. In both cases, the characteristic dark blue color of the polyradical anion formed immediately at the cathode. The reversibility of the electron transfer reaction was evident by the disappearance of the characteristic color when the current polarities were reversed. When a sufficiently high current was passed to the solution of PVBP with $NaPh_4B$ in THF, the reddish-violet colored PVBP dianion was formed at the cathode electrode. Current reversal caused the color to change from reddish violet to blue and then colorless. The electro-reduction of PVBP that undergoes two consecutive reversible one-electron transfers is thus evident.

2.3.3. Synthesis of Graft Copolymers

$PVBP^{\cdot-}$ was produced in DMF with TEAP through potentiostatic electrolysis at -1.5 V vs Ag/AgCl or through galvanostatic electrolysis at 10 - 15 mA. The $PVBP^{\cdot-}$ generated in this medium appears to be fairly stable and retains its activity for a considerable time. When acrylonitrile was added to the

blue solution, an instantaneous color change was observed. The dark orange solution that formed yielded yellow polyacrylonitrile polymer. This coloration is attributed to the cyclization of the -C≡N groups, an effect well established for anionically prepared polyacrylonitrile. Methyl methacrylate was less rapidly polymerized as shown by the gradual change of the characteristic blue to a light yellow. The quantitative evaluation of effective concentration of radical anion (grafting site) in DMF was complicated by the occurrence of side reactions. Although coulometric experiments indicated that all benzophenone moieties were reduced, it was estimated that less than half of the PVBP$^{\cdot-}$ remained active at the end of the electrolysis. The radical anions can dimerize to give pinacolate, or their concentrations may be gradually decreased by scavenging effects of slowly reacting impurities, of the solvent (DMF) or of the tetraalkylammonium perchlorate. The dimerization was, however, thought to be insignificant as, otherwise, cross-linked insoluble gels would be expected.

Galvanostatic electrolysis was also performed with PVBP in THF with $NaPh_4B$. The polyradical anions generated in this medium were very stable and no decomposition could be detected experimentally. With prolonged electrolysis, the polydianion was produced as indicated by the appearance of the reddish-violet color characteristic of the benzophenone dianion. It was thus possible to control the conversion of PVBP to PVBP$^{\cdot-}$ by adjusting the conditions of electrolysis. It was found that, as a result of intermolecular dimerization, a considerable amount of dark blue gel precipitated out in the course of electrolysis in cases where polymers containing 80% vinylbenzophenone were used as backbone polymers. These insoluble gels, although as active as the

soluble $PVBP^{\cdot}$, made it difficult to study the subsequent graft copolymerization. However, when the vinylbenzophenone content of the copolymer was less than 35%, little or no gel was detected in the solution even at high conversion to $PVBP^{\cdot}$. Intramolecular cyclization was also not detectable as evidenced by the constancy of the intrinsic viscosities before and after electrolysis.

The visible spectrum of $PVBP^{\cdot}$ produced electrochemically in $THF/NaPh_4B$ exhibits a maximum at 645 nm (Fig. 17). A slight difference in the maxima can be seen when the spectrum of $PVBP^{\cdot}$ is compared with that of $BP^{\cdot}$. This change, attributed to the decrease in interatomic separation of the radical anion and its counter ion, reflects the decrease in the chemical reactivity of the radical anion and the increase in electron affinity of the BP when substituted on a vinyl polymer backbone (106).

The results of grafting experiments are compiled in Table 9.

FIGURE 17: VISIBLE SPECTRA OF BENZOPHENONE AND POLY(VINYLBENZOPHENONE) RADICAL ANIONS IN THF

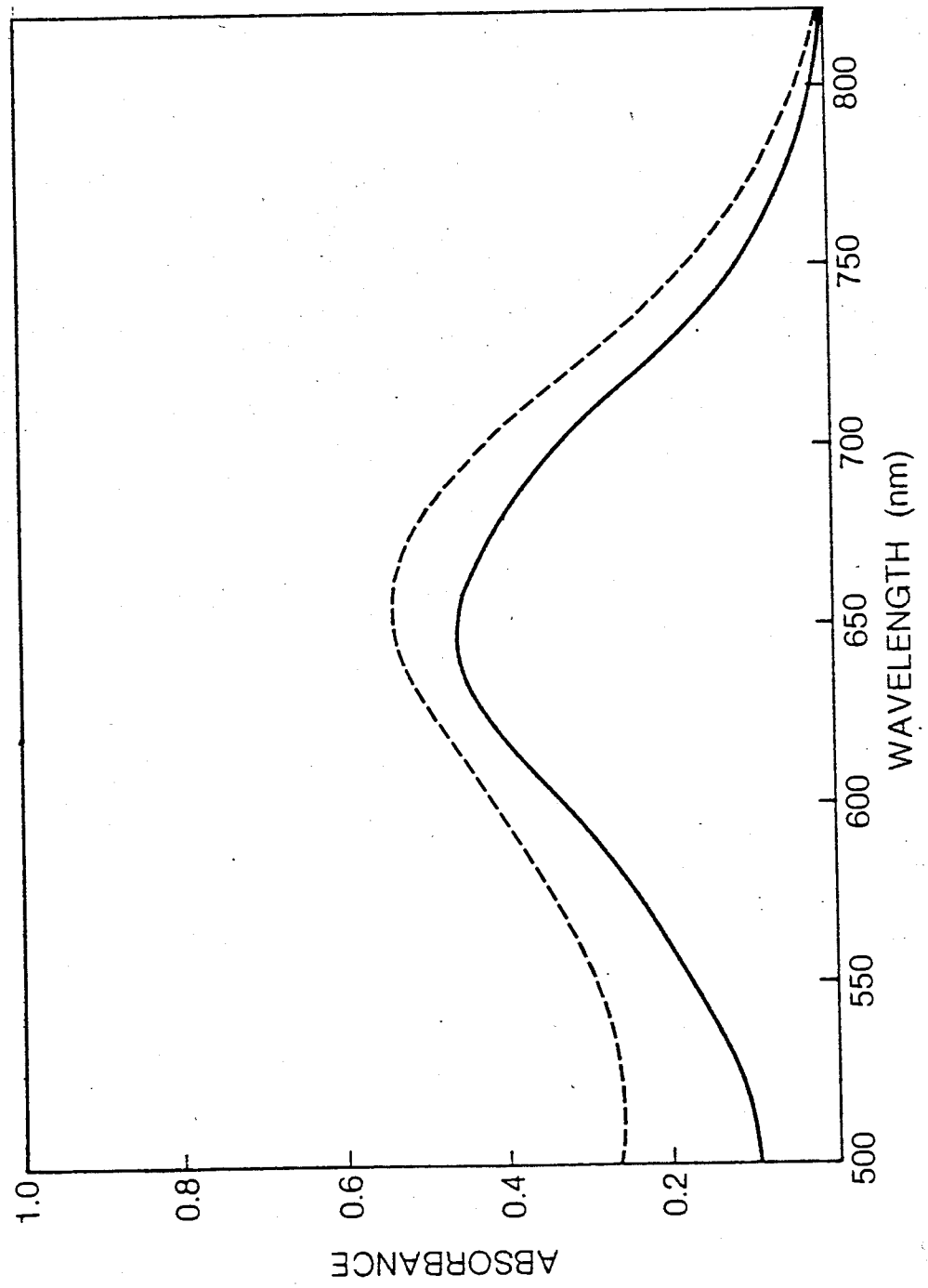
ABSORBANCE
1.0
0.8
0.6
0.4
0.2
500
550
600
650
700
750
800
WAVELENGTH (nm)

TABLE 9

GRAFT COPOLYMERIZATION BY POLYVINYLBENZOPHENONE RADICAL ANION

BACKBONE POLYMER	SOLVENT	SUPPORTING ELECTROLYTE	CURRENT	MONOMER	APPROXIMATE YIELD
80% PVBP 0.120 g	DMF	0.12 M TEAP	10 mA	2.4 g AN	50%
80% PVBP 0.110 g	DMF	0.12 M TEAP	15 mA	0.8 g AN	40%
80% PVBP 0.213 g	DMF	0.12 M TEAP	15 mA	2.7 g MMA	5%
35% PVBP 0.250 g	THF	2.5×10^{-2} M $NaPh_4B$	7 mA	2.3 g MMA	70%*
35% PVB 0.250 g	THF	2.5×10^{-2} M $NaPh_4B$	20 mA	2.3 g MMA	100%*
15% PVBP 0.450 g	THF	2.5×10^{-2} M $NaPh_4B$	5 mA	1.5 g MMA	50%*
50% PVBP 0.420 g	THF	2.5×10^{-2} M	5 mA	2.6 g MMA	90%†

Polymerization conducted at 10°C.

Reaction Time: 10 hours.

* Product contaminated with poly MMA.

† Graft copolymerization was conducted in a separate flask after removal of metallic sodium from polyradical anion solution. Only graft copolymer was obtained.

With the system PVBP/AN/TEAP/DMF yields of up to 50% based on AN monomer were observed. However, only low yields were obtained with MMA in the same reaction medium of TEAP/DMF. The lower reactivity of MMA as contrasted to AN towards anionic initiators is probably the explanation for this difference in yield. A greatly improved yield was obtained with MMA when $NaPh_4B$ was employed as a supporting electrolyte and high concentration of $PVBP^{\cdot-}$ could be generated and maintained. The polymerization was, however, complicated by the presence of Na which was simultaneously generated during the electrolysis and competed with $PVBP^{\cdot-}$ for MMA, resulting in the formation of homo PMMA. Upon removing the Na from the system, only graft copolymer was formed.

2.3.4. Characterization of Polymers

When the polymers resulting from the interaction of $PVBP^{\cdot-}$ with acrylonitrile were subjected to Soxhlet extraction with chloroform, a good solvent for PVBP and a non-solvent for PAN, for 48 hours, little or no homopolymer could be extracted. The IR spectra of the polymer before and after extraction showed absorption bands at 2240 cm^{-1} (-C ≡ N), 1660 cm^{-1} (benzophenone) and 700 cm^{-1} (substituted benzene), suggesting that the copolymer of ST/VBP-g-AN was formed (Fig. 18). Further evidence for the formation of graft polymers appears in the gel permeation chromatograms of the reaction crude product and of the backbone polymer as shown in Fig. 19. Although the chromatograms obtained from DMF solvent are somewhat skewed, the results clearly confirmed that AN was successfully grafted to the base polymer. The grafted product lacked the peak characteristic of the ungrafted substrate and displayed a new peak displaced far toward the high molecular weight

FIGURE 18: INFRARED SPECTRA OF A, POLY(VINYLBENZOPHENONE) BACKBONE, AND B, POLY(VINYLBENZOPHENONE-G-ACRYLONITRILE)

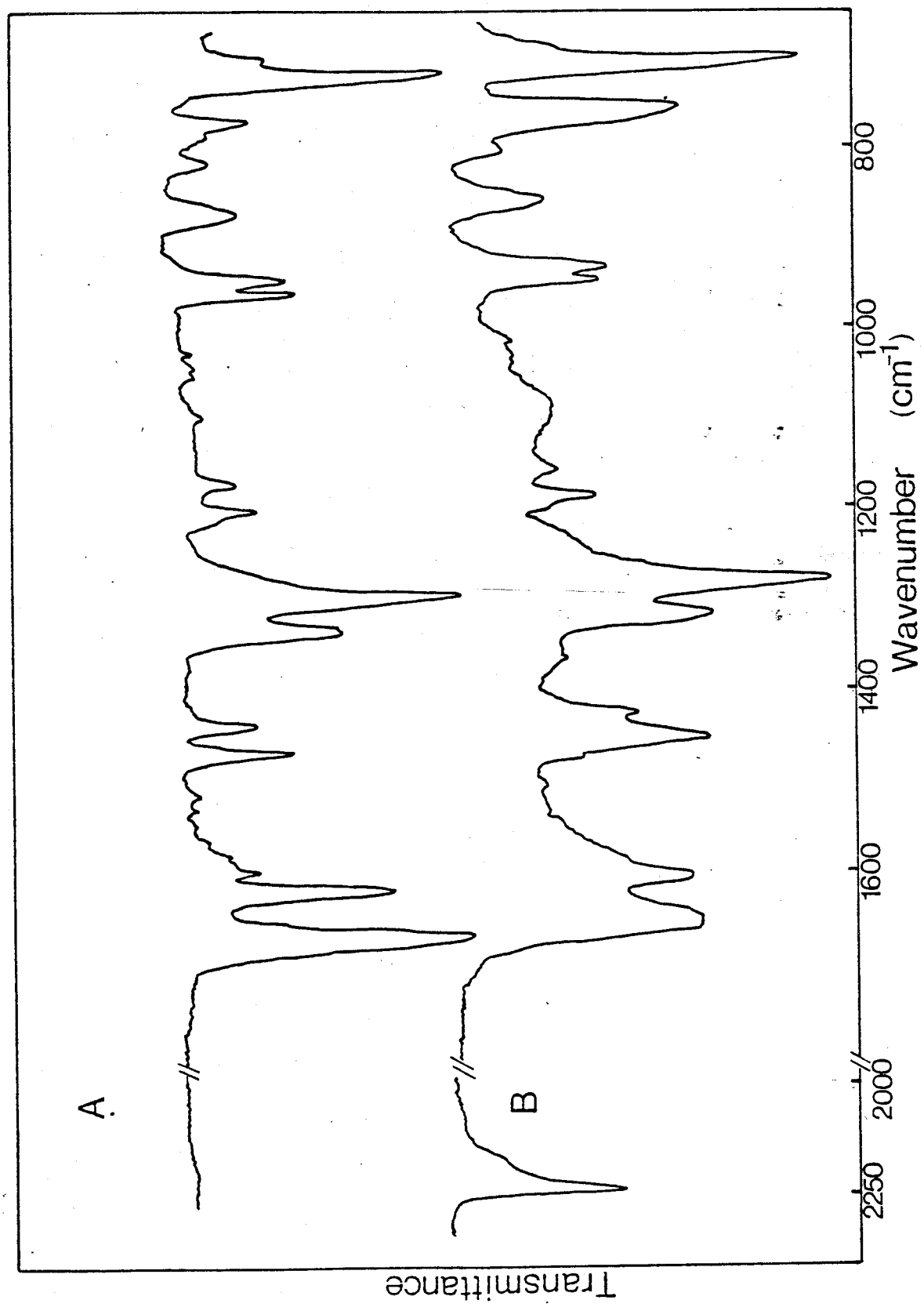
A
B
Transmittance
2250
2000
1600
1400
1200
1000
800
Wavenumber (cm^{-1})

FIGURE 19: GEL PERMEATION CHROMATOGRAMS OF
A, POLY(VINYLBENZOPHENONE) BACKBONE, AND
B, POLY(VINYLBENZOPHENONE-G-ACRYLONITRILE)

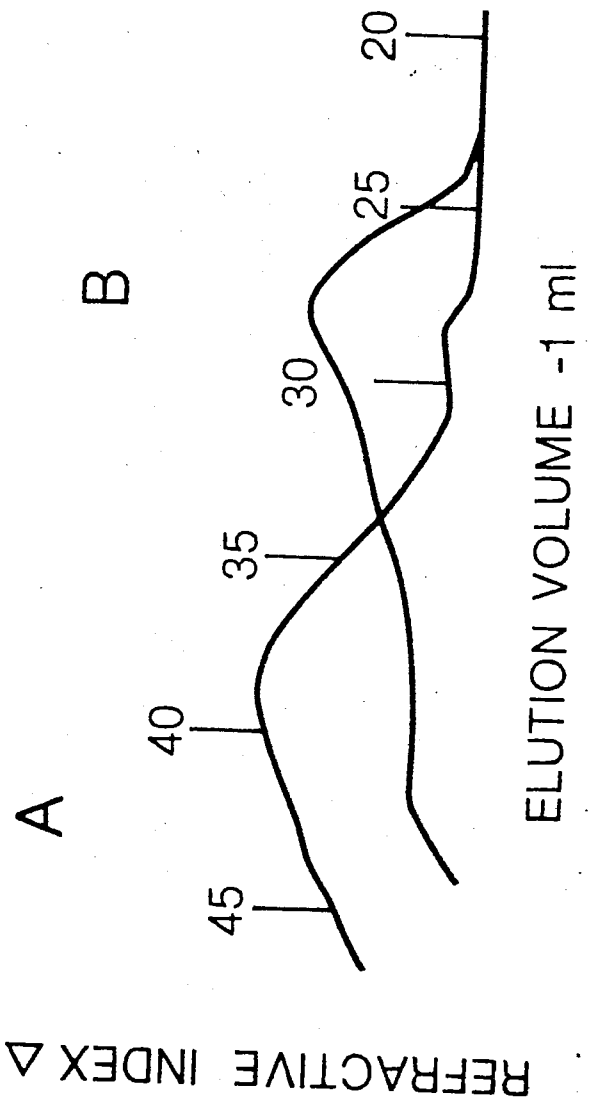
A
B
40
35
30
25
20
45
REFRACTIVE INDEX Δ
ELUTION VOLUME -1 ml

region. It is quite significant that the GPC of the reaction product showed a single peak on material not subjected to further purification to remove homopolymer of PAN. This result points to a high grafting efficiency in the reaction.

The IR spectrum of the reaction product from PVBP/TEAP/DMF/MMA possessed absorption band at 1725 cm^{-1}, characteristic of acrylate, and 1660 cm^{-1} (benzophenone) as well as 700 cm^{-1} (monosubstituted benzene) (Fig. 20). Extraction of the reaction product with hot acetonitrile (a solvent for PMMA and a non-solvent for PVBP) gave no soluble fraction. This indicates that the acrylate groups are chemically bonded to the base polymer. The GPC of the reaction product has a single broad peak at an elution volume slightly less than that of the base polymer and exhibits a high molecular weight tail. This pattern substantiates the formation of graft polymer (Fig. 21).

The gel permeation chromatogram of the samples prepared from PVBP/$NaPh_4B$/THF/MMA exhibits a bimodal distribution shown in Fig. 22; evidently the samples were mixtures of PMMA and copolymer of ST/VBP-g-MMA. Attempts to extract homo PMMA with hot acetonitrile resulted in a hazy solution, which was difficult to separate. The formation of homopolymer of MMA was not surprising for this reaction system. The electrochemical reduction of PVBP to its radical-anion may lead to the concurrent reduction of $NaPh_4B$ to free Na.

$$Na^+ + e \xrightarrow[\text{cathode}]{\text{at}} Na \qquad [58]$$

$$Na + CH_2 = \underset{\underset{COOCH_3}{|}}{\overset{CH_3}{\overset{|}{C}}} \longrightarrow CH_2\text{-}\underset{\underset{COOCH_3}{|}}{\overset{CH_3}{\overset{|}{C}}}{}^- \xrightarrow{MMA} \text{Polymer} \qquad [59]$$

FIGURE 20: INFRARED SPECTRUM OF POLY(VINYLBENZOPHENONE-G-METHYL METHACRYLATE)

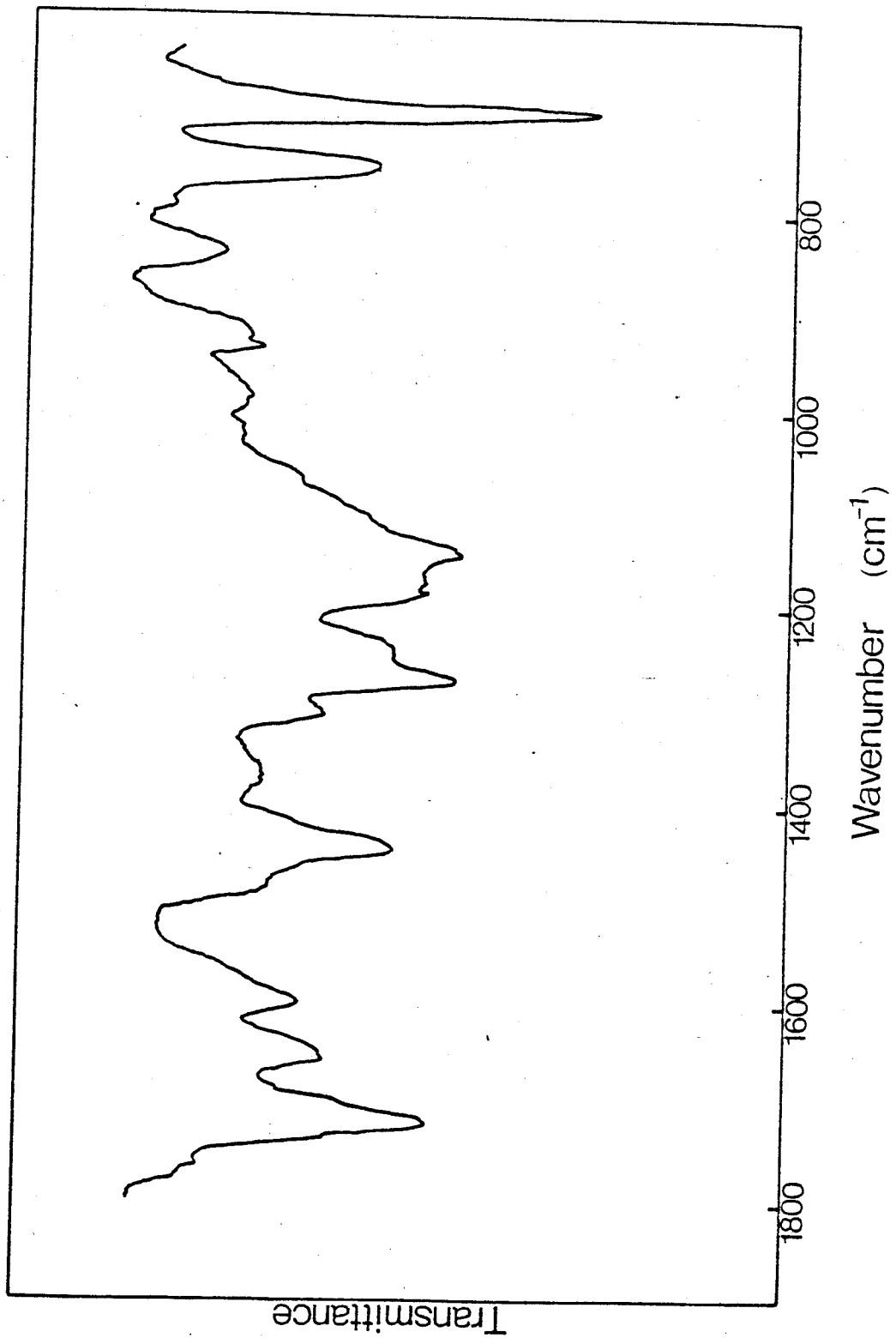
Transmittance
1800
1600
1400
1200
1000
800
Wavenumber (cm-1)

FIGURE 21: GEL PERMEATION CHROMATOGRAMS OF

A, POLY(VINYLBENZOPHENONE)

B, PRODUCT OBTAINED FROM PVBP/MMA/TEAP/DMF

Solvent: THF

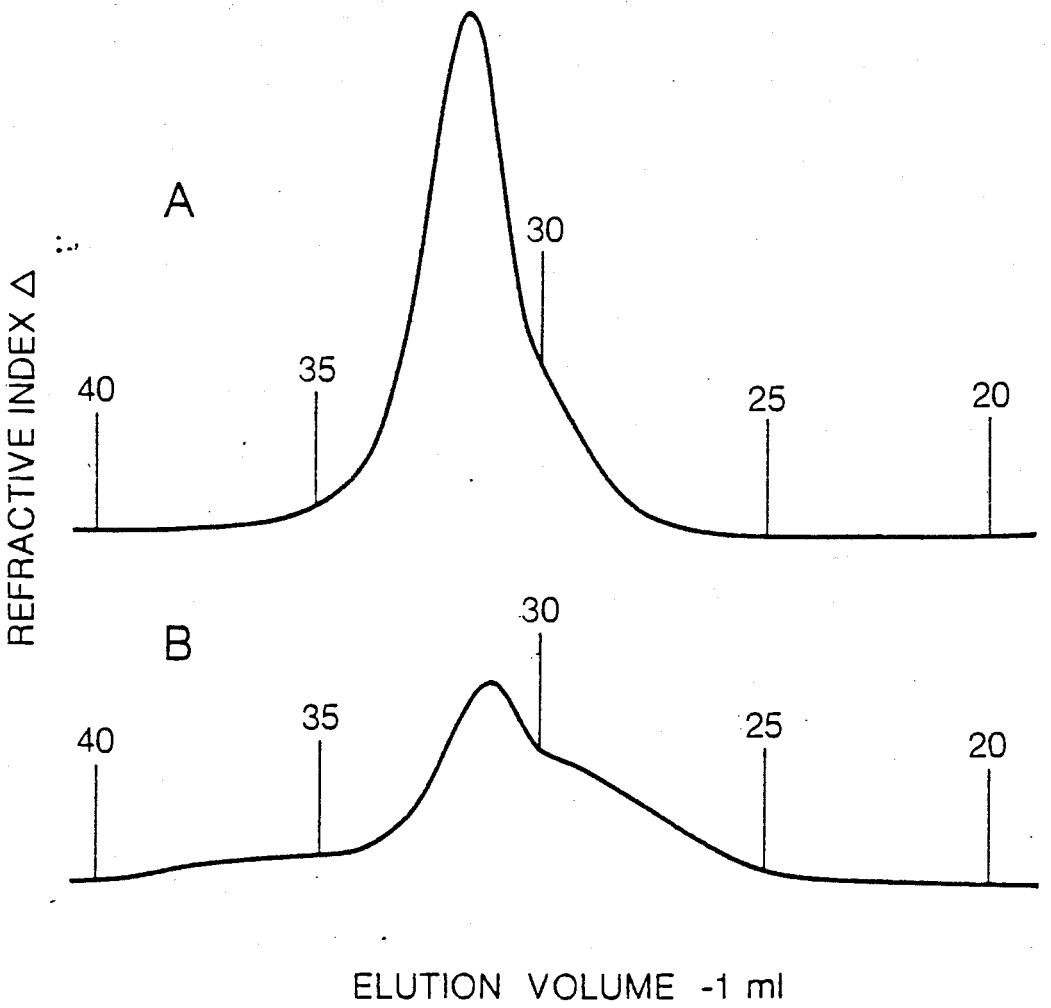
A
B
30
35
40
25
20
30
35
40
25
20
REFRACTIVE INDEX Δ
ELUTION VOLUME -1 ml

FIGURE 22: GEL PERMEATION CHROMATOGRAMS OF

A, POLY(VINYLBENZOPHENONE)

B, PRODUCT OBTAINED FROM PVBP/MMA/$NaPh_4B$/THF

Solvent: THF

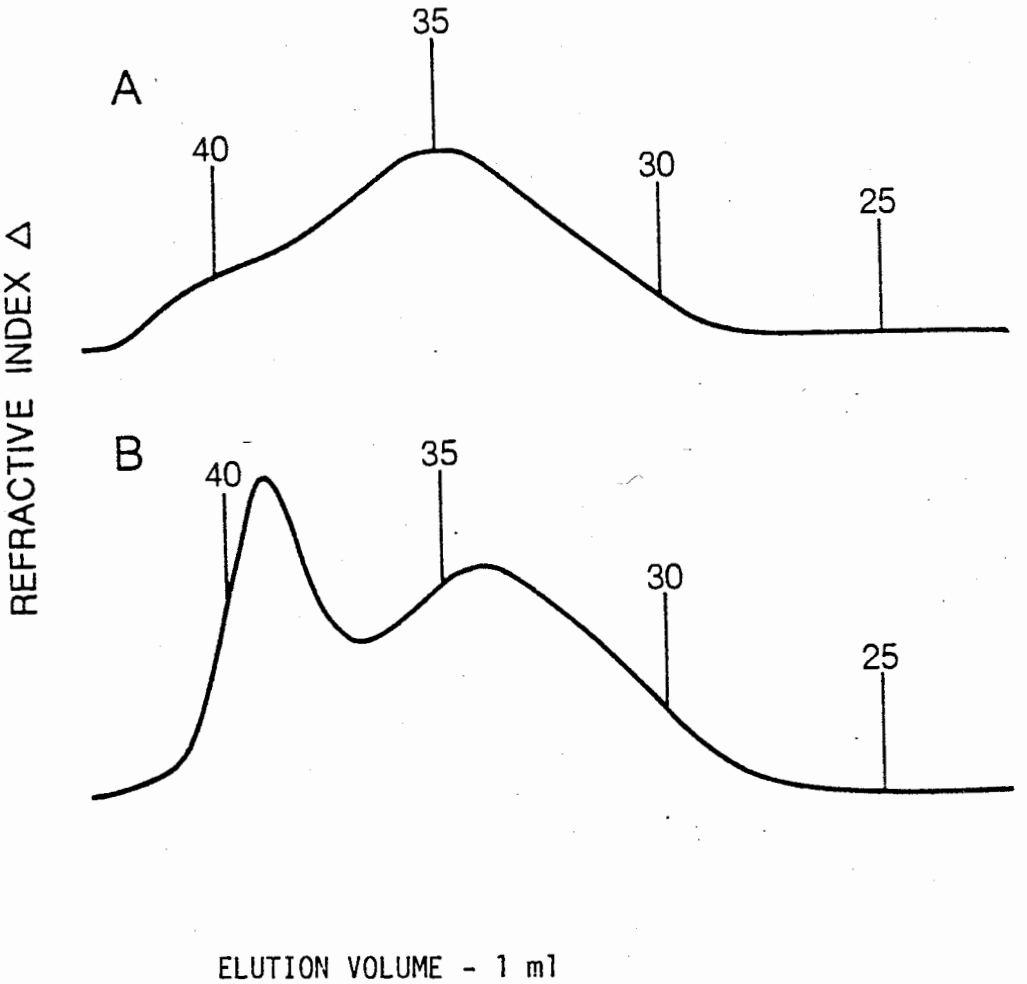
A
35
40
30
25
B
40
35
30
25
REFRACTIVE INDEX Δ
ELUTION VOLUME - 1 ml

In the galvanostatic electrolysis, the potential is not controlled and this competitive reduction can be expected.

To corroborate this view, a graft copolymerization was conducted in a second flask containing MMA, to which polyradical anion was filtered and transferred in a closed system. The GPC trace of the samples obtained in this manner, which is shown in Fig. 23, indeed gives a single peak at the high molecular weight region with the complete absence of the second peak previously attributed to the initiation by metallic sodium.

2.3.5. Initiation Mechanism of Polyvinylbenzophenone Radical Anion with Methyl Methacrylate

The formation of graft copolymer is consistent with the mechanism that the initial step is the formation of the adduct between the alkoxide anion and a vinyl monomer as suggested by Greber (91) and Braun (107).

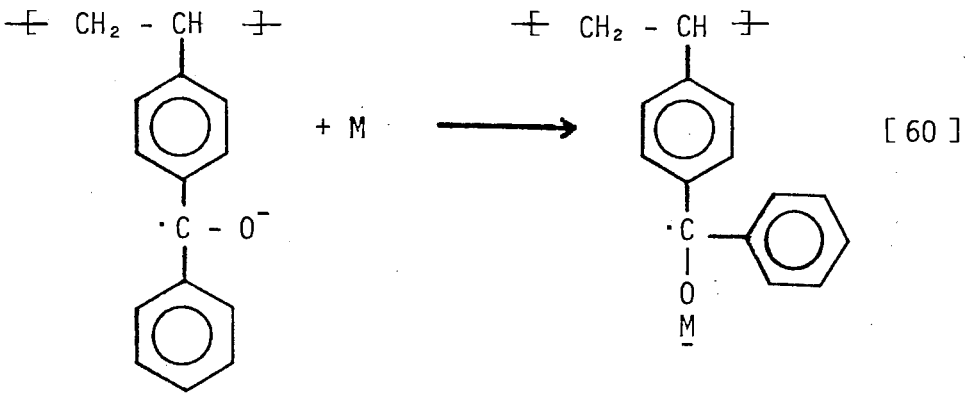

[60]

The radical end is considered to be too stable to attack the double bond of the monomers and is probably destroyed by hydrogen abstration (108).

Although a number of studies have been made on anionic polymerization initiated by benzophenone radical-anions (10, 108 - 112), they have led to two conflicting views on the initiation mechanism of this polymerization.

FIGURE 23: GEL PERMEATION CHROMATOGRAMS OF

A, POLY(VINYLBENZOPHENONE)

B, POLY(VINYLBENZOPHENONE-G-METHYL METHACRYLATE

Solvent: THF

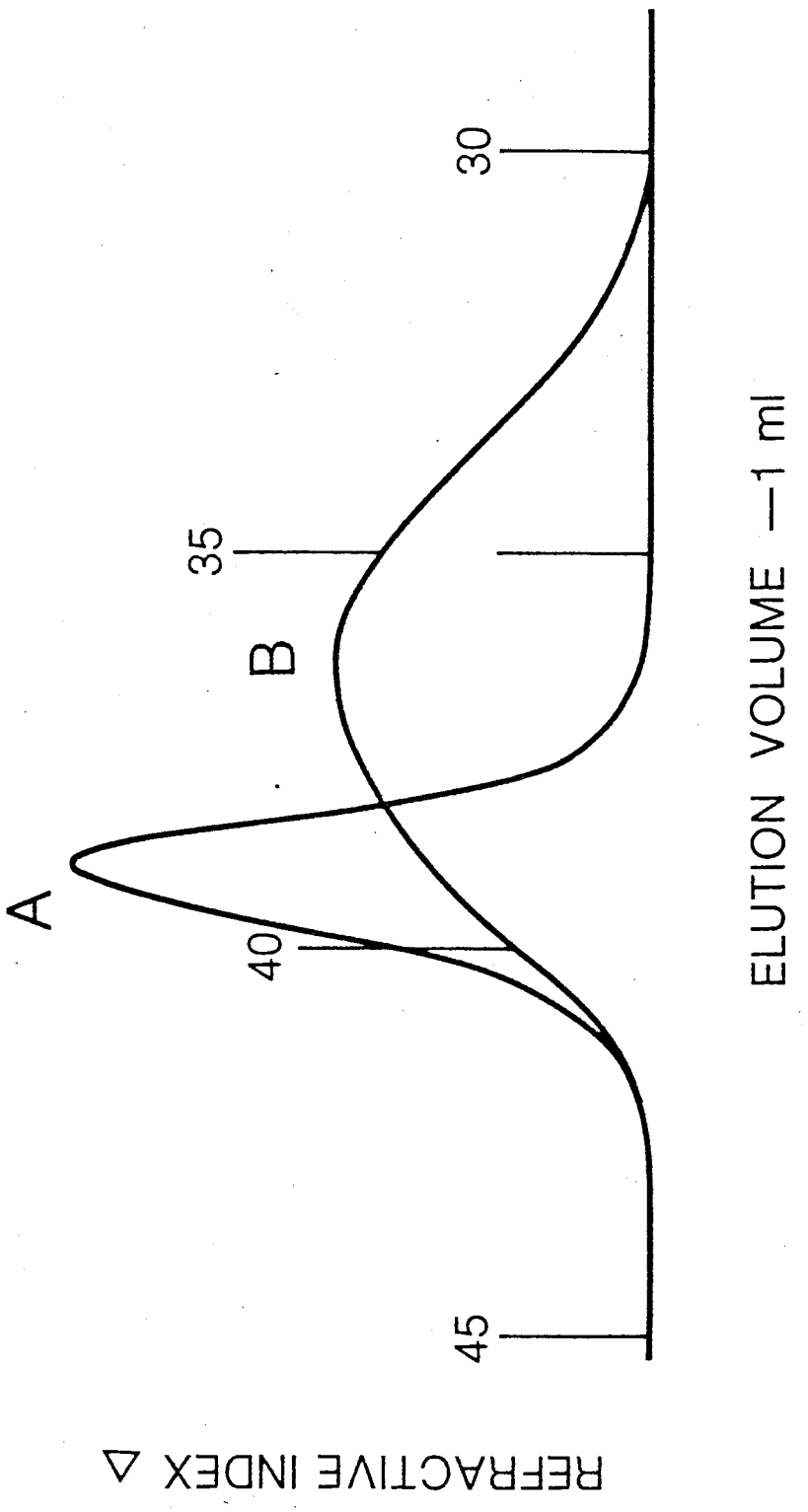
A
B
40
35
30
45
REFRACTIVE INDEX Δ
ELUTION VOLUME —1 ml

Mengoli (10), in a study of the interaction between $BP^{-\bullet}$ and MMA, suggested that electron transfer to monomer from a dianion, which was formed by dismutation of $BP^{-\bullet}$ ($BP^{-\bullet} + BP^{-\bullet} \rightleftharpoons BP^{=} + BP$), was the intiating step. Zilkha (110) and Ogasawara (111), on the other hand, favored the adduct mechanism.

The results obtained from the present study strongly indicate that the adduct formation is the initial reaction as graft polymers would not be formed by the electron transfer mechanism. However, an alternative mechanism, postulated by Panayotov (112), of electron transfer to monomer from $BP^{-\bullet}$, followed by the interaction of growing polymeric anion with benzophenone, is compatible with the graft formation (Eqs. [61] to [63]).

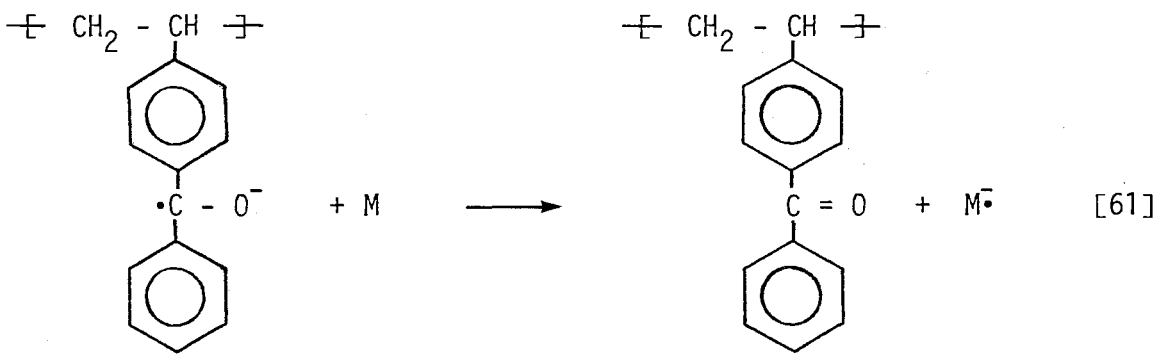

[61]

[62]

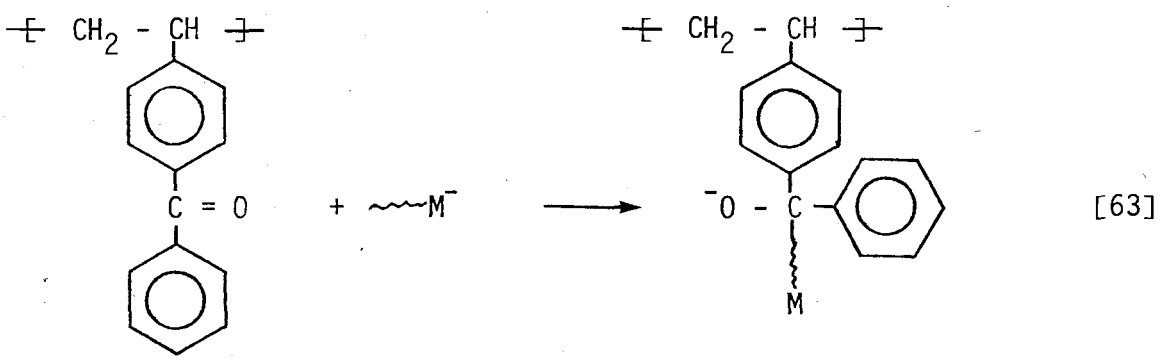

[63]

To differentiate the two possible initiation mechanisms, i.e. Eq. [60] and Eqs. [61] through [63], polymethyl methacrylate anions ($PMMA^-$) were allowed to react with PVBP and the resulting product was compared with the product obtained from the reaction between $PVBP^-$ and MMA. The reactions were carried out using vacuum line techniques with break seal system as illustrated in Fig. 24.

Poly MMA anions were obtained from the reaction of methyl methacrylate with a predetermined amount of sodium-naphthalene in THF at -70°C. A yellow colored viscous solution, characteristic of poly MMA anion, was formed immediately after the MMA was mixed with sodium-naphthalene. The addition of PVBP to the poly MMA anion solution brought about a sudden change in color of the solution from yellow to green which slowly turned to yellow again. The electron transfer reaction [64] was evidently taking place.

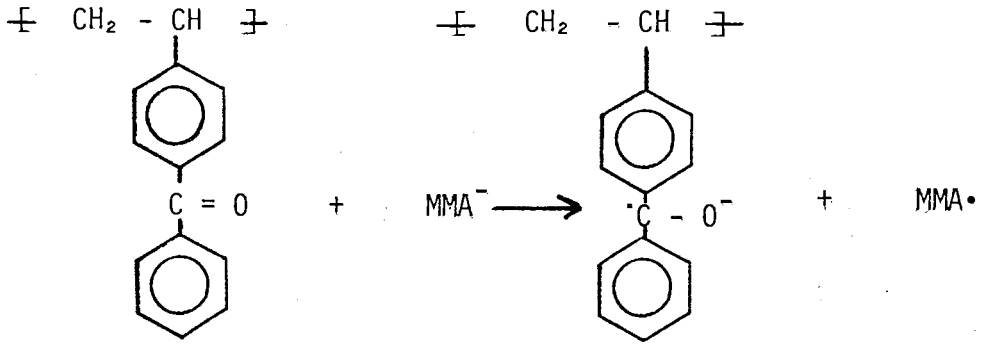

[64]

The gel permeation chromatographic analysis of the reaction product showed no change in elution volume of PVBP. This indicated that the addition reaction between PVBP and poly MMA anion Eq.[63] did not occur.

A parallel experiment was conducted for the reaction of $PVBP^-$ and monomeric MMA under similar conditions. The dark blue color of the $PVBP^-$ in THF, free from metallic sodium, gradually disappeared after MMA was added

FIGURE 24: APPARATUS FOR MECHANISTIC STUDIES OF GRAFTING REACTIONS

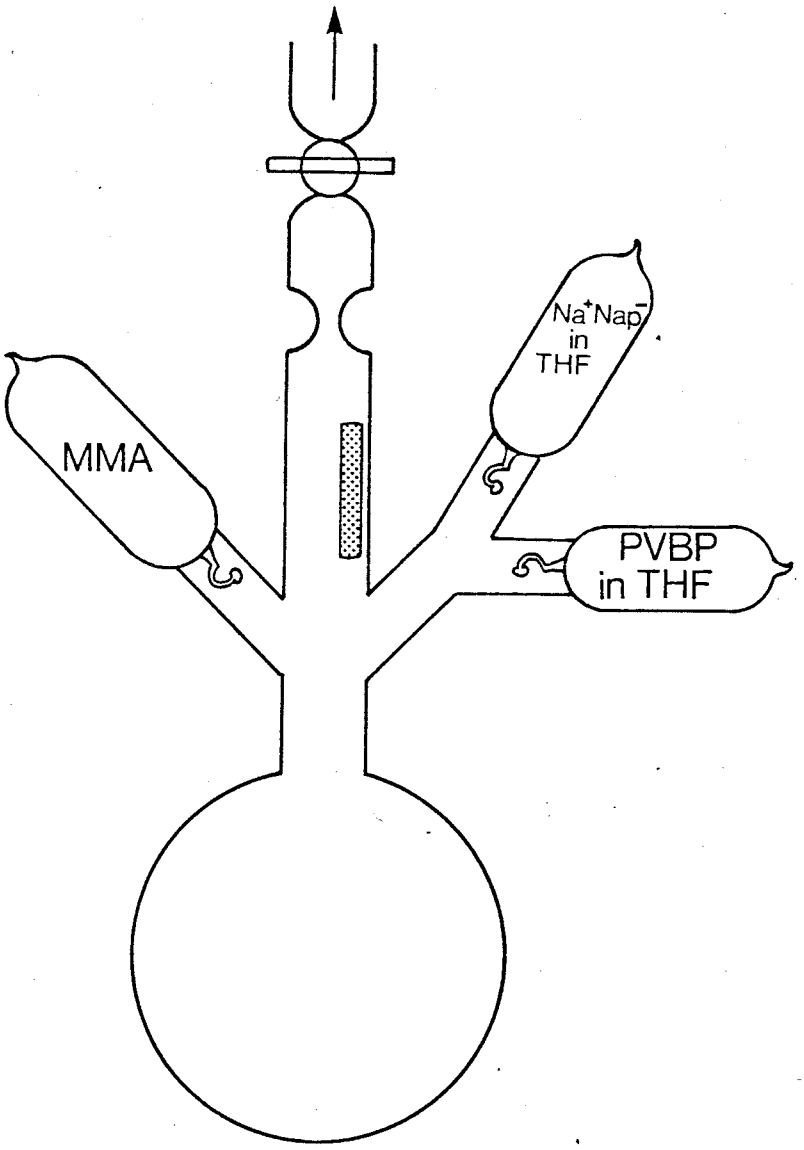
MMA
Na^+Nap^-
in
THF
PVBP
in THF

to the solution, resulting in a highly viscous solution. A substantial increase in molecular weight of the reaction product in comparison with that of the parent PVBP indicated the formation of graft copolymer. The results thus show quite conclusively that the adduct mechanism (reaction [60]) is the most likely route for the initiation reaction.

2.3.6. Interaction of Benzophenone Radical Anion with Acrylonitrile

The rotating ring disk electrode (RRDE) was also employed in attempts to elucidate the kinetic and mechanistic aspects of the reaction between PVBP$^{\cdot-}$ and AN. For simplicity, benzophenone was utilized in place of poly(vinylbenzophenone), although identical results were obtained with PVBP. The detailed account of the electrochemical behavior of BP and BP substituted onto a polymeric chain will be given in Chapter 3.

The RRDE voltammogram of 5 mM BP with 0.1 M TEAP in DMF is shown in Fig. 25. The disk potential was swept negatively from -1.30 volts to -2.10 volts vs. a Ag reference electrode and the limiting disk current corresponded to the one-electron transfer of BP to BP$^{\cdot-}$. The ring potential was maintained at -1.00 volts so that all the BP$^{\cdot-}$ reaching the ring was oxidized to BP. The collection efficiency under this condition was identical to the value expected from the electrode geometry, indicating the absence of any secondary reactions within the time scale of measurements.

When 6.5 mM of AN were added to the solution, a decrease in disk current (i_d) commencing at approximately -2.0 volts was observed. The magnitude of the ring current at this potential decreased accordingly. This is shown in Fig. 25 with curve B. A further increase in the concentration of AN

FIGURE 25: RRDE VOLTAMMOGRAMS OF

A : 5 mM BENZOPHENONE/0.10 M TEAP/DMF AND

B : 5 mM BENZOPHENONE/6.5 mM ACRYLONITRILE/

0.10 M TEAP/DMF

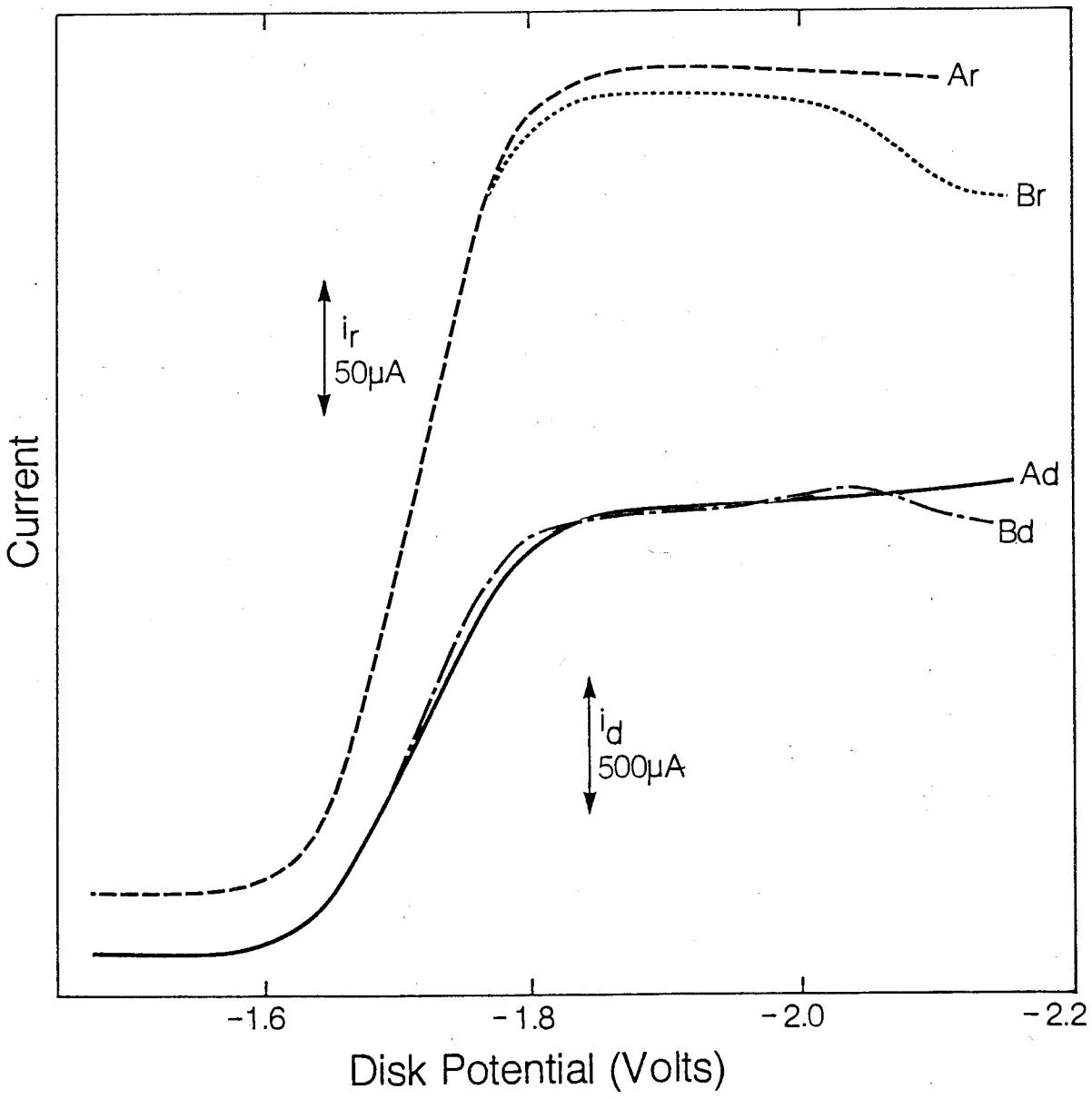
Ar
Br
i_r
50μA
Ad
Bd
i_d
500μA
Current
-1.6
-1.8
-2.0
-2.2
Disk Potential (Volts)

to 13.1 mM resulted in a significant change in the current-potential curves as illustrated in Fig. 26 (curve A). The i_d exhibits a short limiting current plateau after which the current drops considerably. By extending the potential beyond -2.1 volts, at which the AN began to be reduced, the i_d increased as a result of the electro-reduction of AN. However, the increase in i_r at the disk potential corresponding to the reduction of AN was also observed. It is known that the electrochemical reduction of AN is irreversible. A RRDE study with AN only produced a disk current at the similar potential with no ring current. The increase in i_r at the potential where AN is reduced is evidently due to the formation of $BP^{\cdot-}$ from the solution reaction of BP with AN^{-}. An increase in conc. of AN to 40 mM only gave a current maximum followed by the total disappearance of the current in the current-potential curve (Fig. 26, curve B).

The decreases in the disk and ring currents at the potentials where only benzophenone can be reduced (Fig. 25, 26) are somewhat unexpected. A decrease of current with increasing potential has been observed in the case of electrode passivation (113). Passivation is the inhibition of an electrochemical process due to changes of the electrode surface. However, blank runs conducted with AN and TEAP in DMF did not show such decreases in currents in the potential range under investigation. In addition, repetitive runs of the solution containing BP, AN, and TEAP in DMF gave reproducible current-potential curves. These results suggest that neither adsorption nor polymer coating is the factor contributing to the observed voltammetric behavior.

FIGURE 26: EFFECT OF ACRYLONITRILE CONCENTRATION ON REDUCTION OF BENZOPHENONE IN DMF

Ar and Ad : Ring and disk currents of solution containing
5 mM Benzophenone/13.1 mM Acrylonitrile/
0.10 M TEAP/DMF

Br and Bd : Ring and disk currents of solution containing
5 mM Benzophenone/40 mM Acrylonitrile/
0.10 M TEAP/DMF

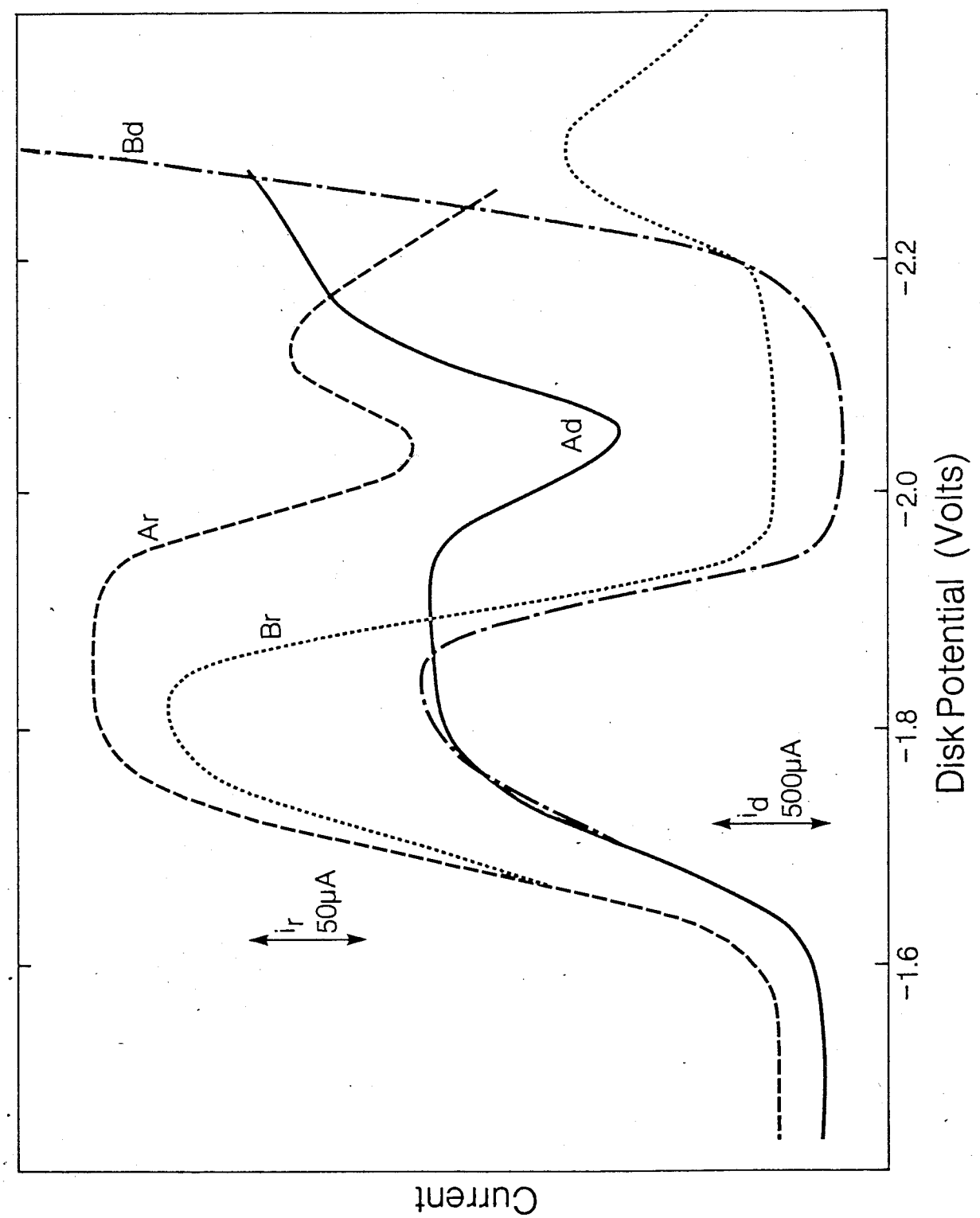
Current
Disk Potential (Volts)
-1.6
-1.8
-2.0
-2.2
Bd
Ar
Br
Ad
i_r 50μA
i_d 500μA

The fact that the decrease in current is dependent upon the concentration of AN implies the existence of a chemical stage involving the interception of incoming benzophenone molecules to the disk electrode. The reactions taking place at the electrodes and in solution may be represented by the following scheme:

$$\text{at the disk} \quad BP + e \longrightarrow BP^{\cdot -} \qquad [65]$$

$$\text{in solution} \quad BP^{\cdot -} + AN \longrightarrow \cdot BPAN^{-} \xrightarrow{AN} \sim\sim AN^{-} \qquad [66]$$

$$AN^{-} + BP \longrightarrow AN\cdot + BP^{\cdot -} \qquad [67]$$

$$\text{at the ring} \quad BP^{\cdot -} \longrightarrow BP + e \qquad [68]$$

The AN anion formed through reaction [66] can react with benzophenone supplied to the electrode by convective diffusion, regenerating $BP^{\cdot -}$. The detection of $BP^{\cdot -}$ at the ring electrode when AN is directly reduced at the disk electrode is direct evidence for the occurrence of the electron transfer reaction [67]. A similar reaction was observed in the reaction of poly MMA anion with PVBP, while Iwakura (114) reported the electron transfer reaction of α-methylstyrene anion to benzophenone.

It is obvious that, in the limiting current region, the rate of electrode reaction is diffusion controlled, and that in the region of minimum current, the rate is kinetically controlled. To show that the anomalous current-potential curve in the presence of AN is associated with the kinetics of the solution reactions, the scan rate of the disk potential was varied. At a low scan rate (10 mV/sec), a rapid decrease in current was observed (Fig. 27, curve A). At moderate scan rate (50 mV/sec) the decrease in current commenced at a more negative potential, and at a fast scan rate (500 mV/sec) the current-potential curve was close to normal (curve C). It can be visualized

FIGURE 27: EFFECT OF SCAN RATE ON LIMITING DISK CURRENT

A : 10 mV/sec

B : 50 mV/sec

C : 500 mV/sec

in solution containing 8 mM Benzophenone/28 mM Acrylonitrile/0.12 M TEAP/DMF/25°C

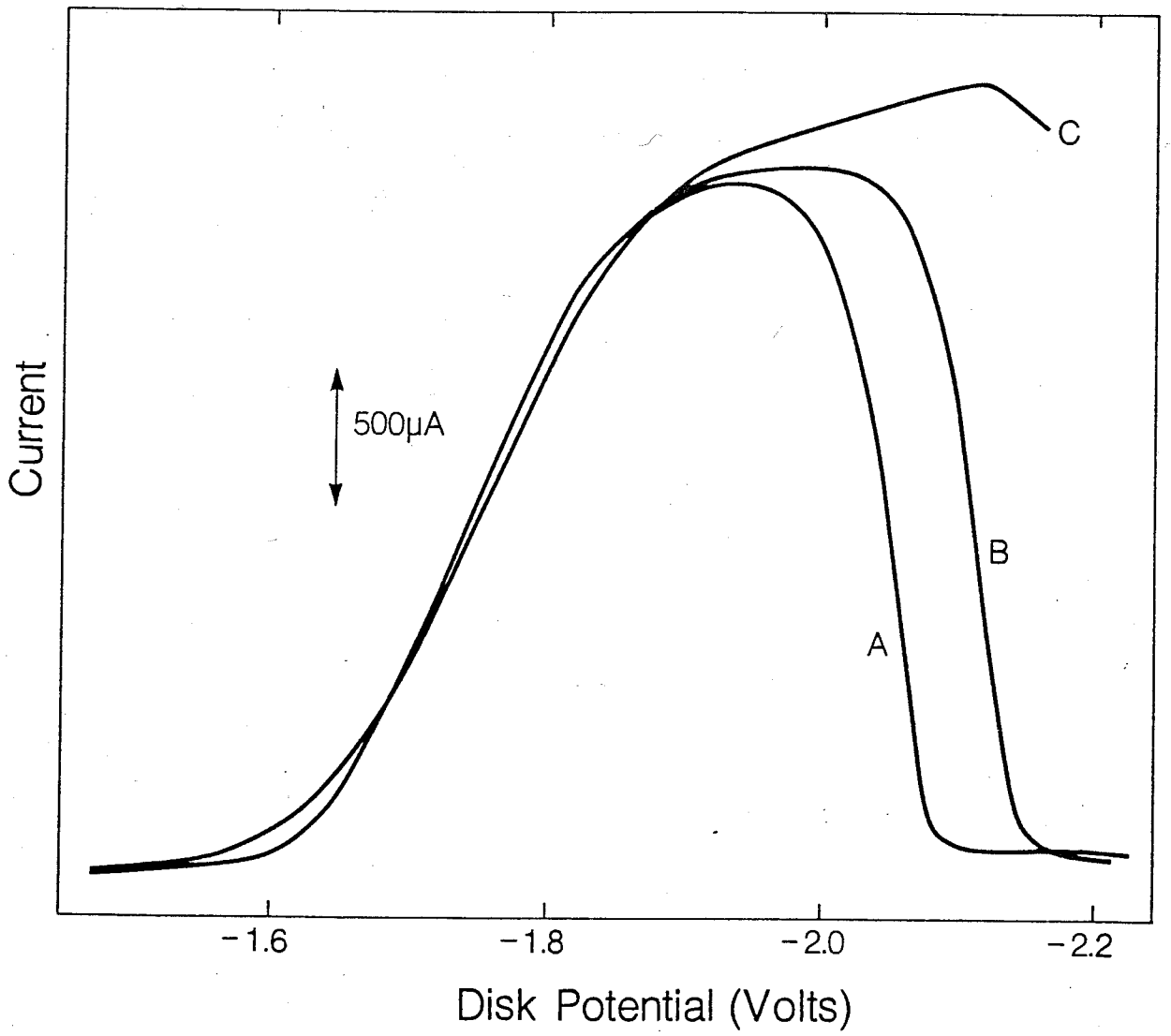
Current
500μA
C
B
A
−1.6
−1.8
−2.0
−2.2
Disk Potential (Volts)

that, at sufficiently slow rates, diffusion processes are able to follow the changes of concentrations at areas immediately below the electrode. If chemical processes are faster than diffusion processes, a decrease in current can be expected.

The results obtained thus suggest that, in the presence of AN, the electro-reduction of BP is followed by a series of fast chemical reactions (EC processes) which interfere with the subsequent electrode reaction. The $BP^{\cdot-}$ generated initially at the disk electrode reacts with AN to form AN^{-} which, in turn, reacts with BP. Under certain conditions, it is possible that BP is supplied to the electrode at a rate equal to that of chemical reaction (Eq. [67]); reactions [67] and [66] take place in turn, resulting in a rapid decrease in disk current.

The electrochemical formation of graft copolymers and the use of electrochemical methods to probe the reaction mechanism were demonstrated. The work points to a number of possibilities of electrochemical synthesis of polymers with specific structures. For example, polymers with suitably placed electroactive groups may be employed to form block , star , and comb polymers in a manner similar to that described in this chapter. If a base polymer molecule contains both electro-reducible and oxidizable groups, polyradical anions and cations may be generated at suitable stages to incorporate monomers that are polymerizable only by anionic and cationic mechanisms into the molecular framework. The full control of the electrochemical modification of polymers such as the number and the length of branches, however, requires a system that combines resonable conductivity, chemical compatibility, and adequate solubility characteristics. As the

choice of solvents and of supporting electrolytes is still limited, many promising electrochemical systems have not been utilized under ideal conditions.

CHAPTER III

ELECTROCHEMICAL BEHAVIOR AND CHARACTERIZATION OF POLY(VINYLBENZOPHENONE)

3.1. INTRODUCTION

Electroactive polymers possess groups susceptible to electron transfer reactions at electrodes. For reversible electron transfer, the polymers are classified as electron-transfer or redox polymers.

Studies of the behavior of electroactive or redox groups incorporated into macromolecular structures or polymer systems are of both theoretical and practical importance. The presence of the macromolecular structure may confer new, distinctive, and sometimes unusual properties on the functional group and on the molecule. These are exemplified by the ability of a single molecule to accept or release a large number of electrons, by the changes in reactivity and in electrochemical behavior of the functional group (120, 123 - 125), and by the development of polymer modified electrodes (129 -131). This type of polymer may also be considered as electroactively tagged polymers and electroanalytical techniques may be used to characterize them.

An important approach to the study of this type of reactive polymer has been based on the comparison of the electrochemical behavior of the polymeric molecule and the small molecule of analogous structure. Investigations on oligomeric molecules containing certain redox groups have indicated that the functional behavior and chemical stability of a molecule are remarkably affected by various structural, configurational and environmental

factors. The greater degree of regularity, and the lower degree of flexibility of the macromolecular structure, compared with a random association of monomeric units, may exert an effect on the interconversion of the redox couple in the polymer system. The neighboring group interaction, the molecular weight, the length of inert bridging which separtes the active centers and the solubility of polymers have all been shown to affect the electrochemical behavior of the functional groups attached to the backbone of the macromolecule. On the other hand, for polymers containing multiple, non-interacting redox centers, a recent report (127) indicated that electrochemically the active centers behaved independently and were not influenced by the macromolecular environment.

Electron transfer processes may be investigated experimentally by voltammetric and coulometric methods. The electrode in these methods may be viewed as analogous to a "molecule" that has a continuously adjustable chemical potential. Intramolecular effects, such as neighboring group interactions, may be evident in the voltammetric behavior of dilute polymer solutions, in comparison with monomeric model compounds. The positions of peak potentials, their symmetry and reversibility, and the magnitudes of limiting currents can serve to probe the structure of the macromolecule; these parameters can be interpreted through well established electrochemical theory. Intermolecular effects due to dimerization, entanglement, viscosity, and related phenomenological effects may become evident in a more concentrated solution.

This chapter deals with the electrochemical behavior and characterization of benzophenone, poly(vinylbenzophenone) and poly(vinylbenzophenone-co-styrene) at solid electrodes. The extent of neighboring group interactions

was studied for polymers of identical chain length with varied spacing between the electroactive centers. The number of electro-reducible groups was investigated as a function of the chain length of polymers. The relationship between limiting current, measured at a rotating disk electrode, and molecular weight of the polymer was examined quantitatively and the molecular weight dependence of the diffusion coefficient was determined.

3.1.1. Electrochemical Studies of Oligomeric Molecules

The electrochemical behavior of the quinone-hydroquinone couple is perhaps the most widely studied organic system. The electro-reduction of p-benzoquinone can be represented by the following series of reaction equations:

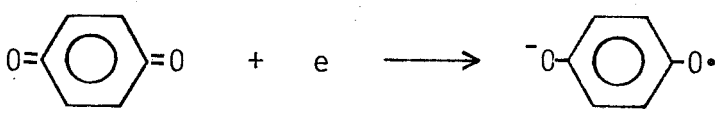

[69]

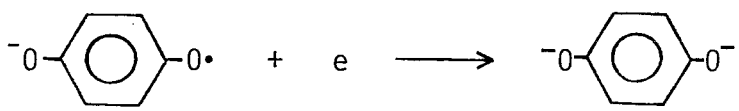

[70]

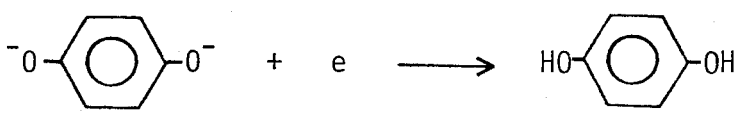

[71]

Reactions [69] and [70]occur as discrete steps under aprotic conditions. In aqueous solutions, the second step [70] shifts to more positive potentials and merges with the first to produce the reversible two-electron transfer process (115).

Potentiometric studies show that the titration curve for many polymeric quinones deviates considerably from the shape of a normal two-electron

curve of monomeric quinones (116, 117). Several investigators have studied the properties of dimers, trimers, and very small polymers of the quinone-hydroquinone types with a view towards simplifying the problem of interpreting polymer behavior. Hunt, Lindsey, Savill, and Peover (118 - 120) studied the electrochemical behavior of mono-, di-, tri-, and polyfunctional quinones with structures corresponding to those thought to be present in polyquinones derived from quinone-formaldehyde condensates. Polarographic reduction of the quinone segments in aqueous-enthanolic solution indicated that two-electron additions were made successively to each quinone unit. The triquinone (I) showed a

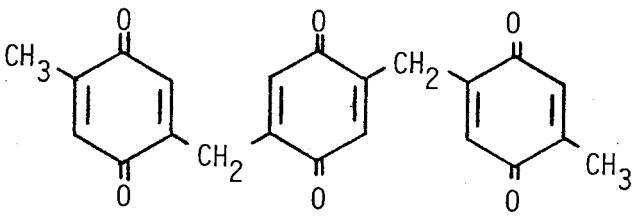

(I)

two-electron step and a complex four-electron wave, which could be analysed into two-electron components. In aprotic solvents such as acetonitrile, reductions of the mono-, di-, and

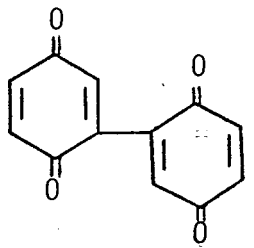

(II)

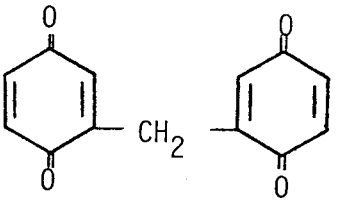

(III)

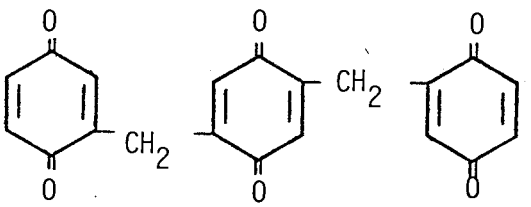

(IV)

tri-quinones proceeded by one-electron additions with formation of multi-radical structures. For the diquinones (II, III), the first two one-electron additions were clearly resolved; for triquinones (I, IV), the three one-electron steps could be separated. The fact that the diquinone (II) exhibited a considerably enhanced potential (-0.35V for the first electron addition) in comparison with p-benzoquinone (-0.51V) led Lindsey et al to suggest that a strong electronegative inductive effect of the quinone "substituent" was operating. It was concluded that the anomalous behavior observed during titration of polyquinones could be qualitatively interpreted in terms of nearest-neighbor interactions.

Moser and Cassidy (121, 122) carried out electrochemical studies on oligomeric hydroquinone. During potentiometric oxidation, the hydroquinone groups reacted independently when the connecting bridge contained five or more consecutive methylene units. The data for the series of oligomers studied are summarized in Table 10.

TABLE 10

REDOX TITRATIONS OF VARIOUS OLIGOMERIC P-BENZOQUINONES (121,122)

BRIDGE (R^a)	E_1 (V)	E_2 (V)	$E_2 - E_1$ (mV)
$(CH_2)_2$	0.636	0.669	33
$(CH_2)_3$	0.638	0.667	28
$(CH_2)_5$	0.655	0.655	0
SD-3[b]	0.616	0.616	0

a.

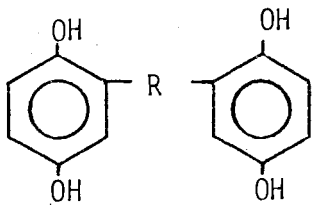

b.

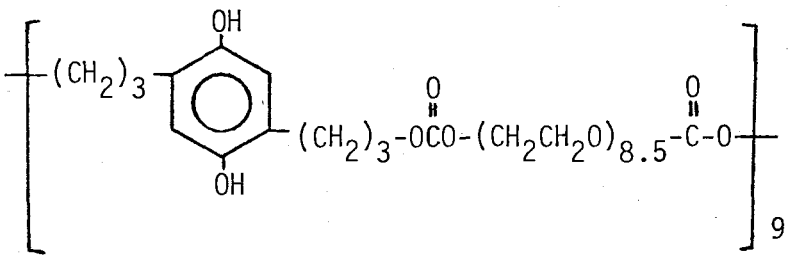

More recently, Brown (123) and LeVanda (124) studied the electro-oxidation of 1, 1- poly(ferrocene) and found that successive ferrocenes were oxidized in a series of resolvable waves with values of $E_{1/2}$ separated by hundreds of millivolts. On the other hand, Morrison et al (125), in an electrochemical study of several biferrocenes, obtained single polarographic waves with diffusion currents corresponding to a two-electron transfer process when certain bridging groups connected the two ferrocene centers (C_2H_4, $(CH_3)_2C\text{-}C(CH_3)_2$, and $-CH=CH-C_6H_4-CH=CH-$) but separated waves with one-electron diffusion currents resulted with other bridging groups.

The studies mentioned above thus indicated that the functional behavior of active centers embedded in oligomer (or polymer) frameworks is dependent on various structural, configurational, and environmental factors and is reflected in the difference in potential between the half reactions of the successive electron transfers.

3.1.2. Electrochemical Studies of Polymers

Despite several investigations on electroactive oligomers, knowledge of the electrochemical and physicochemical behavior of polymers is still limited. Previous work is confined to a few recent papers (126 - 128). In a study of the electrochemical oxidation of poly(vinylferrocene) in hexamethylphosphoramide, Smith et al (126) observed multi-electron transfers producing voltammetric waves with the overall shape of a one-electron transfer reaction. The half-wave potentials of ferrocene and vinylferrocene polymers were compared and shown to have similar values. However, the low values of the diffusion coefficients obtained experimentally, in comparison with those calculated theoretically, led them to suggest that only "isolated" ferrocene residues were oxidized in the macromolecular environments. It was shown that the number of oxidizable ferrocene residues on a polymer chain decreased with increasing chain length of the polymers and the difficulty in oxidizing the substituted ferrocene was attributed to the inaccessibility of the active groups to the electrode.

In view of the limited research carried out in the field of the electrochemical behavior of polymers, the present work has been directed towards a more fundamental study of this type of reaction. Experiments were devised to investigate possible interference effects attributable to the neighboring group interactions and the macromolecular environments.

While the present work was in progress, Flanagan et al (127) reinvestigated the same poly(vinylferrocene) utilized by Smith (126). Results from normal pulse voltammetry and coulometry indicated that almost every ferrocene group could be oxidized. They also recalculated the results of Smith, employing a more refined approximation for the dependence of diffusion

coefficient on the molecular weight,and concluded that 40 to 75% of the ferrocece residues may have been oxidized in Smith's study. A theory was further formulated for electron transfer for reactants with multiple non-interacting centers. It was shown that molecules containing a number of identical, non-interacting centers will exhibit current-potential responses having the same shape as those obtained with the corresponding molecules containing a single center, and the successive electron transfer will follow simple statistics.

A variety of factors could, however, cause departures from the current-potential response predicted from the model derived on the basis of the statistics: interactions between adjacent reducible centers; slow electron transfer at the electrode; i.e. non-Nernstian behavior; structural changes in the polymer which accompany its reduction; absorption or precipitation of reactants or products at the electrode surface. Yet, it was shown that a general treatment for the prediction of current-potential responses can be derived, applicable to polymers in which inductive effects or other forms of specific interactions between active sites are absent. The equations derived are of considerable interest for the characterization of electroactive polymers and are thus briefly described.

3.1.3. Theory of Electron Transfer with Reactants Having Multiple Active Centers (127)

When a polymeric molecule contains n independent centers each of which is capable of accepting or donating one electron and has the same standard potential (E_m^o), there is a corresponding half-reaction for each center as follows;

$$\cdots\cdots X\ X\ O\ X\ X\cdots\cdots + e \underset{}{\overset{E_m^o}{\rightleftharpoons}} \cdots\cdots X\ X\ R\ X\ X\cdots\cdots \quad [72]$$

$$\cdots\cdots X\ X\ X\ X\ O\cdots\cdots + e \underset{}{\overset{E_m^o}{\rightleftharpoons}} \cdots\cdots X\ X\ X\ X\ R\cdots\cdots \quad [73]$$

where O and R represent the electroactive center at its oxidized and reduced states, respectively, and X represents a center in either oxidation state or an inert bridging unit. Assuming that the Nernst equation is applicable independently to each center in the molecule, the probability that any site, i, is reduced at potential E with which the multi-centered molecule is in equilibrium may be expressed by

$$P = \frac{[R]}{[O] + [R]} = \frac{1}{1 + \theta} \quad [74]$$

where

$$\theta = \frac{[O]}{[R]} = \exp \frac{F}{RT}(E - E_m^o) \quad [75]$$

The application of standard binomial distribution leads to

$$f_j = \left(\frac{n!}{j!(n-j)!}\right) \left(\frac{\theta}{1 + \theta}\right)^{(n-j)} \left(\frac{1}{1 + \theta}\right)^{j} \quad [76]$$

where f_j is the fraction of the polymer molecules present containing j reduced centers and (n-j) oxidized centers at each value of θ. $\theta/(1+\theta)$ and $1/(1+\theta)$ are the probabilities that any particular monomeric center is oxidized or reduced, respectively.

If C_p is the bulk concentration of polymers, the equilibrium concentration, C_j, of molecules containing exactly j reduced sites (produced, for example, by controlled potential electrolysis of the solution at potential E) is given by

$$C_j = C_p f_j \qquad [77]$$

where f_j has the value corresponding to the potential E.

Fig. 28 shows calculated fractional concentration-potential curves for the reduction of a two-centered molecule. The three curves represent the fractions, f_0, f_1, and f_2, of unreduced, half reduced, and fully reduced molecules respectively. The curves intersect at the potentials where $f_0 = f_1$ and $f_1 = f_2$. These are identified in Fig. 28 as E_1^F and E_2^F. For molecules containing n non-interacting reducible centers it is possible to calculate the formal potentials corresponding to each pair of successive oxidation states of the polymer by noting that at E_j^F, $f_j = f_{j-1}$

$$f_j = \frac{n!}{j!\,(n-j)!}\left(\frac{\theta}{1+\theta}\right)^{n-j}\left(\frac{1}{1+\theta}\right)^{j}$$

$$= \frac{n!}{(j-1)!(n-j+1)!}\left(\frac{\theta}{1+\theta}\right)^{n-j+1}\left(\frac{1}{1+\theta}\right)^{j-1}$$

$$= f_{j-1}$$

$$\theta = (n-j+1)/2 \qquad [78]$$

Substituting Eq. [78] to Eq. [75] leads to

$$E_j^F = E^o - \ln\left[\frac{j}{n-j+1}\right] \qquad [79]$$

FIGURE 28: CALCULATED FRACTIONAL CONCENTRATION-POTENTIAL CURVES FOR REACTANT WITH TWO REDUCIBLE CENTERS

Fractional Concentrations of Unreduced (1), Half-Reduced (2), and Fully-Reduced (3) Reactant

E_1^F and E_2^F are the formal potentials corresponding to the transfer of the first and second electrons to the molecule, respectively

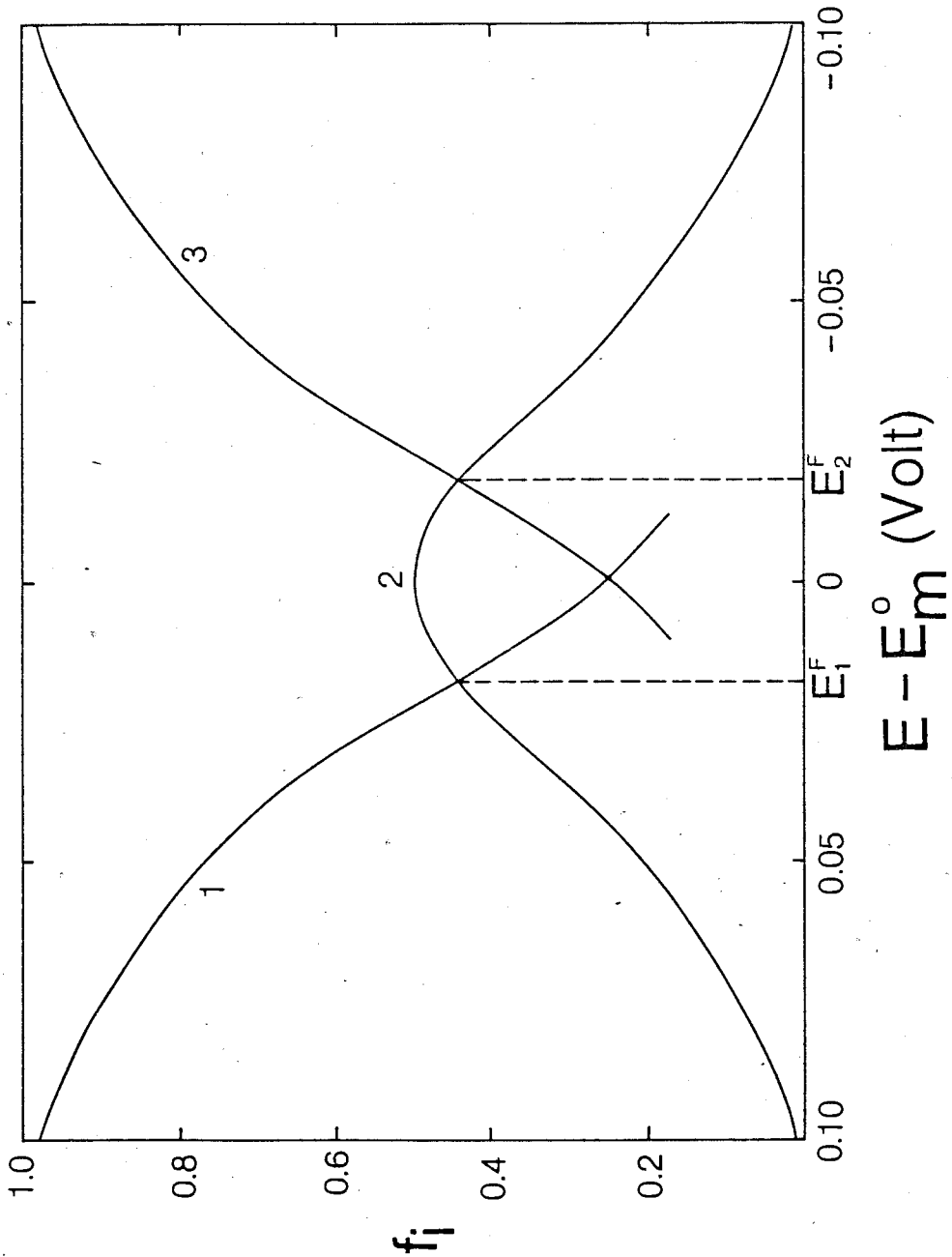
1.0
0.8
0.6
0.4
0.2
f_i
0.10
0.05
0
-0.05
-0.10
E_1^F
E_2^F
$E - E_m^o$ (Volt)
1
2
3

The formal potentials for the first and last pair of oxidation states in a molecule with n reducible centers are represented in Eqs. [80] and [81] respectively.

$$E_1^F = E^o - \frac{RT}{F} \ln\left(\frac{1}{n}\right) \qquad [80]$$

$$E_n^F = E^o - \frac{RT}{F} \ln(n) \qquad [81]$$

The difference between the formal potentials for the molecule is therefore

$$E_1^F - E_n^F = \frac{2RT}{F} \ln(n) \qquad [82]$$

For large n this means that there will be a large overlap of the concentration of the various partially reduced species at potentials in the rising portion of a polarization curve, i.e., that the successive formal potentials will fall increasingly close to each other as n increases.

The final relation of the current-potential responses derived for one-center and n-center molecules was shown to have the form:

$$i_n(\theta) = n\, i_1(\theta) \left(\frac{D_n}{D_1}\right)^p \qquad [83]$$

where i_n is the current obtained at each value of θ with a polymer and i_1 the corresponding current for a monomeric sample. D_n and D_1 are diffusion

coefficients for polymer and monomer, respectively, and the exponent P depends on the voltammetric technique employed. Eq. [83] thus implies that molecules containing a number of identical, non-interacting centers will exhibit current-potential responses having the same shape as that response obtained with the corresponding molecule containing a single center, i.e. only the magnitudes but not the shapes are affected by the number of centers the reactant contains.

3.1.4 Evaluation of Diffusion Coefficient by Electrochemical Methods

An electrochemical reaction generally involves three consecutive steps: transport of reactants to the electrode surface, electrolytic reaction, and transport of products away from the electrode. Three mass-transfer modes are normally encountered: migration, convection, and diffusion. In most electrochemical work, migration of electroactive material is minimized by the use of a large excess of supporting electrolyte. Convection is important in stirred solutions, whereas diffusion is perhaps the most widely studied means of mass transport process. For example, much information is derived from limiting current measurements which are often determined under diffusion controlled conditions. Therefore the evaluation of the diffusion coefficient of electroactive species under study is of prime importance.

Because of the narrow molecular weight ranges spanned by most monomers, their diffusion coefficients are almost identical. However, in the case of macromolecules, diffusion coefficients can be many times smaller than those of simple molecules and the variation of diffusion coefficient with chain length has to be determined experimentally.

The diffusion coefficient (D) can be determined by various electrochemical and non-electrochemical methods. The latter include, among others, isotopic tracers, optical, ultracentrifuge and, more recently, laser light spectroscopy. Electrochemical methods are widely used to determine the D. At a stationary electrode, diffusion is considered as the sole means of mass transport. During the reaction at the electrode surface, material is depleted and a concentration gradient is established. Reactants from the bulk of solution then diffuse toward the electrode in response to this gradient. The

measurement of $it^{1/2}$ curves at constant potential, limiting current measurement from peak voltammetry, and chronopotentiometry have been used to determine the diffusion coefficient at stationary electrodes.

At a rotating disk electrode, forced convection is used as a means of mass transport. The reactants are carried along by the moving liquid. When a potential is applied so that the concentration at the electrode surface is maintained at zero, the reactant is transported to the electrode as a result of the concentration gradient. These two mass-transfer processes, molecular diffusion and convective transfer, exist simultaneously in forced convection; one or the other may predominate in magnitude. In forced convection it can be visualized that diffusion has the minor contributions if the entire solution is considered. However, in a restricted region very close to the electrode, both convection and diffusion play major roles. The limiting current equation at the rotating disk electrode has been rigorously derived from hydrodynamic treatment and mass-transfer equations by Levich (35) and modified by others (38-40), and it is known that the dependence of limiting current on several factors in the equation can be verified experimentally to ± 1%. The final equation is

$$i_L = 0.62\, nFACD^{2/3}\upsilon^{-1/6}\omega^{1/2} \qquad [84]$$

where

i_L = limiting current (mA)

n = number of electrons transferred

F = 96487 columbs/faraday

A = area of the electrode (cm^2)

C = concentration of electroactive species (mole/l)

D = diffusion coefficient (cm^2/sec)

ν = kinematic viscosity (cm^2/sec)

ω = angular velocity of the disk (rad/sec)

The dependence of limiting current on the diffusion coefficient of the electroactive species has led to the use of voltammetry with the RDE as a reliable tool for the determination of D. D values of 3, 3'- dimethoxy benzidine were determined with excellent precision by Glaus et al (132) using the RDE and are in good agreement with values obtained from other methods. Gostisa-Mihelcic (133) determined the diffusion coefficient of the proton in a RDE and the results compared well with the literature data.

3.1.5. Relationship Between Diffusion Coefficient and Molecular Weight

The relationship between diffusion coefficient (D) and molecular weight (M) is well established in the Stokes-Einstein equation:

$$D = \frac{RT}{6\pi\eta r N_o} \qquad [85]$$

where N_o = Avogadro's number

η = the viscosity of solution

r = the radius of sphere

For spherical molecules the radius may be related to the molecular weight by

$$\frac{M\bar{v}}{N_o} = \frac{4}{3}\pi r^3 \qquad [86]$$

where $\bar{v}$ is the specific volume of solute molecule.

A combination of Eqs. [85] and [86] gives

$$D = \frac{RT}{N_o\, 6\pi\eta}\left(\frac{4\pi N_o}{3M\bar{v}}\right)^{1/3} \qquad [87]$$

The diffusion coefficient thus is inversely proportional to the cube root of the molecular weight.

While the radius of a small, spherical molecule can be relatively well defined (134), a polymer chain in a dilute solution has no preferred structure and can only be pictured as a coil changing its shape continuously. Consequently meaningful chain dimension can only be values averaged over the many conformations assumed. Two commonly employed averages are:
(a) the average root mean square distance between the chain ends $\langle \bar{r}^2 \rangle^{1/2}$;
(b) the average root mean square radius of gyration $R_G = \langle \bar{s}^2 \rangle^{1/2}$ which is a measure of the average distance of a chain element from the center of gravity of the coil. The two quantities are related in the absence of excluded volume effects by

$$\langle \bar{r}_0^2 \rangle^{1/2} = 6 \langle \bar{s}^2 \rangle^{1/2} \qquad [88]$$

where $\langle \bar{r}_0^2 \rangle^{1/2}$ denotes the value in the absence of long range and short range effects.

In a very dilute solution each molecule will tend to exclude all others from the volume which it occupies. This leads to a net effect of increasing $\langle \bar{r}^2 \rangle^{1/2}$. To take this into account, Flory and Fox (135) introduced an empirical expansion factor, α,

$$\langle \bar{r}^2 \rangle^{1/2} = \alpha^2 \langle \bar{r}_0^2 \rangle^{1/2} \qquad [89]$$

$\langle \bar{r}^2 \rangle^{1/2}$ may be related to the molecular weight by (136)

$$\langle \bar{r}^2 \rangle = \beta^2 M/M_0 \qquad [90]$$

where β is a constant characteristic of the nature of the polymer; M is the molecular weight of the polymer; M_0 is the molecular weight of the structural unit.

Thus

$$R_G^2 = \langle \bar{r}^2 \rangle / 6 = \alpha^2 \beta^2 M/6M_o \qquad [91]$$

When the hydrodynamic particle resulting from a polymer molecule is considered as a sphere, this equivalent sphere (Re) has the radius

$$R_e = \xi_f R_G \qquad [92]$$

where ξ_f is a universal constant equal to 0.665. The frictional coefficient of such a sphere is (Stokes' equation):

$$f = 6\pi\eta R_e = 6\pi\eta\xi_f R_G \qquad [93]$$

Using Einstein relation, we obtain

$$D = \frac{KT}{f} = \frac{KT}{6\pi\eta\xi_f R_G} \qquad [94]$$

Combining Eqs. [93] and [94] leads to the relation between diffusion coefficient (D) and molecular weight (M) as:

$$D = \frac{KT\, M_o^{1/2}}{6^{1/2}\pi\eta\alpha\beta\, \xi_f\, M^{1/2}} \qquad [95]$$

It has been shown that α varies approximately as $M^{0.05}$ from an average poor solvent to good solvent, and β and ξ_f are independent of the molecular weight (136), Eq.[95] predicts that D should be proportional to $1/M^{0.5}$ in a poor solvent and as $1/M^{0.55}$ in an average good solvent. In a study of the diffusion process of poly(methyl methacrylate) in acetone, this prediction was entirely confirmed by Meyerhoff et al (137).

There have been numerous studies of the diffusional behavior of macromolecules in solution (138 - 141). Experimental work in particular has been stimulated by the recent development of a laser light scattering technique (142 - 144). The use of electrochemical methods has, however, received relatively little attention. The only studies are those of Drushel (145) and Smith (126). On the basis of information from the anodic polarograms of model compounds and knowledge of the effect of molecular weight upon the average diffusion coefficients of aliphatic sulfides, Drushel suggested a method to estimate the diffusion coefficient of aliphatic sulfides in petroleum by a polarography. Smith et al studied a series of poly(vinyferrocene) at a RDE. It is, however, believed that the success of applying electrochemical methods in determining the diffusion coefficients of small molecules should and can be applied to polymer systems and should also provide a new means of characterising polymers.

3.2. EXPERIMENTAL

3.2.1. Chemicals

Chemicals and their purifications are the same as those described in Section 2.2.1.

Poly(styrene) with low polydispersity was prepared by anionic polymerization of styrene with either n-butyllithium in benzene or with sodium naphthalene in tetrahydrofuran. The stringent conditions of purity and preparation required for polymerization in "living" anionic systems were met. Poly(vinybenzophenone-co-styrene) (PVBP-ST) and poly(vinylbenzophenone) (PVBP) were prepared by reacting poly(styrene) with appropriate amounts of benzoyl chloride and aluminum chloride in nitrobenzene in the same manner as those described in Section 2.3.1.

3.2.2. Determination of Molecular Weights and Compositions

Molecular weights and polydispersities of the polymers were determined with the aid of gel permeation chromatograph (Waters Associates Model GPC/ALC 301). Five μ-styragel columns of the following pore dimensions: 10^6, 10^5, 10^5, 10^4, and 10^3 Å were used, and measurements were carried out in tetrahydrofuran with a constant flow rate of 1 ml/min. The columns were calibrated using a series of N.B.S. poly(styrene) standards. A plot of the molecular weights of the standards against their peak elution volumes is shown in Fig. 29. The University of Waterloo MWD I computer program was used to calculate the molecular weights of the polymer samples.

The benzophenone content of the polymers was determined by infrared spectroscopic analysis using a Perkin Elmer 599B. Poly(vinylbenzophenone) and poly(styrene) blends of known composition were used to construct a calibration curve (Fig.30). The finely powdered blends were first dissolved

FIGURE 29: PRIMARY CALIBRATION CURVE FOR GEL PERMEATION CHROMATOGRAPHY

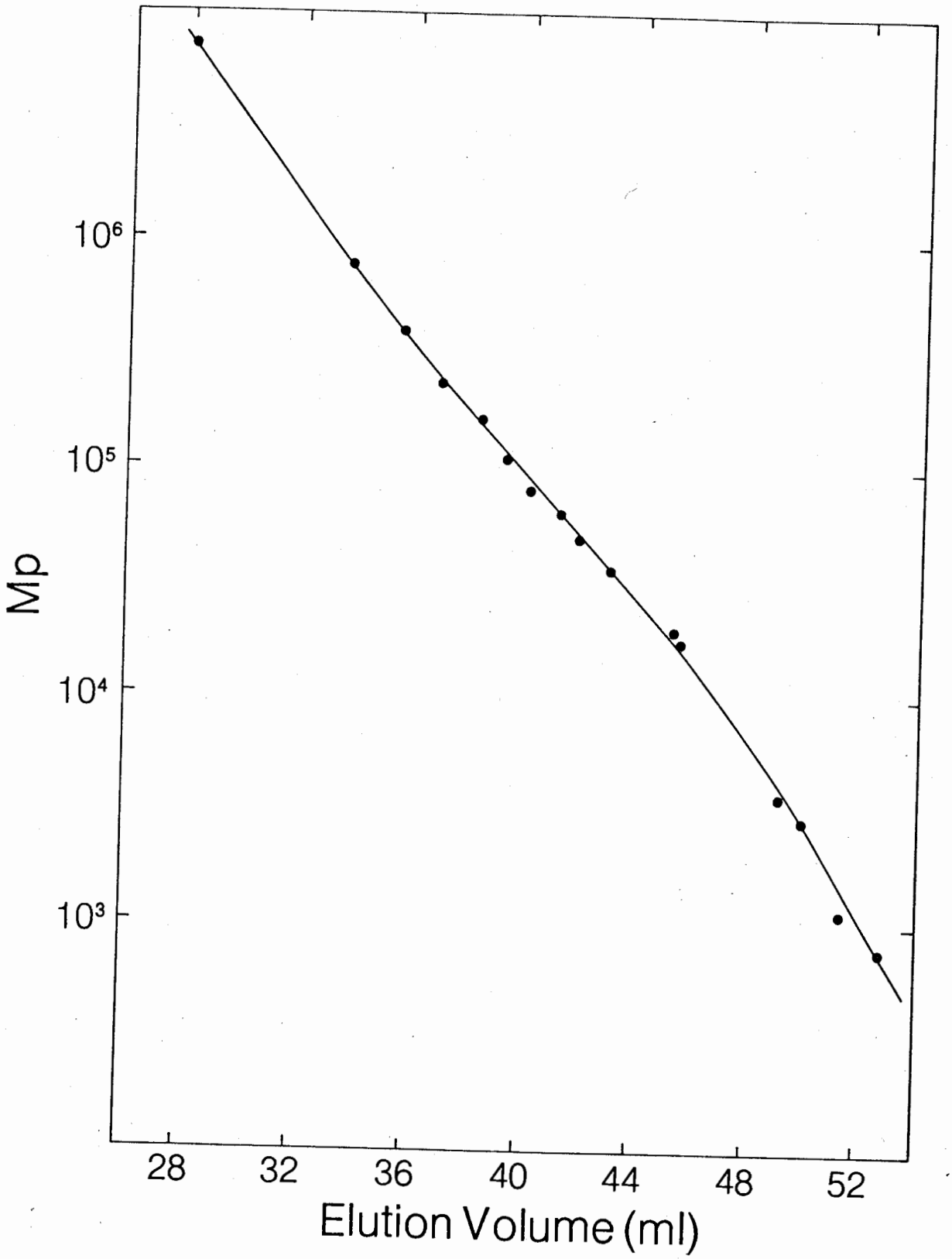
Mp
10⁶
10⁵
10⁴
10³
28
32
36
40
44
48
52
Elution Volume (ml)

FIGURE 30: CALIBRATION PLOT FOR INFRARED SPECTROSCOPIC ANALYSIS OF VINYLBENZOPHENONE CONTENT IN POLYMER

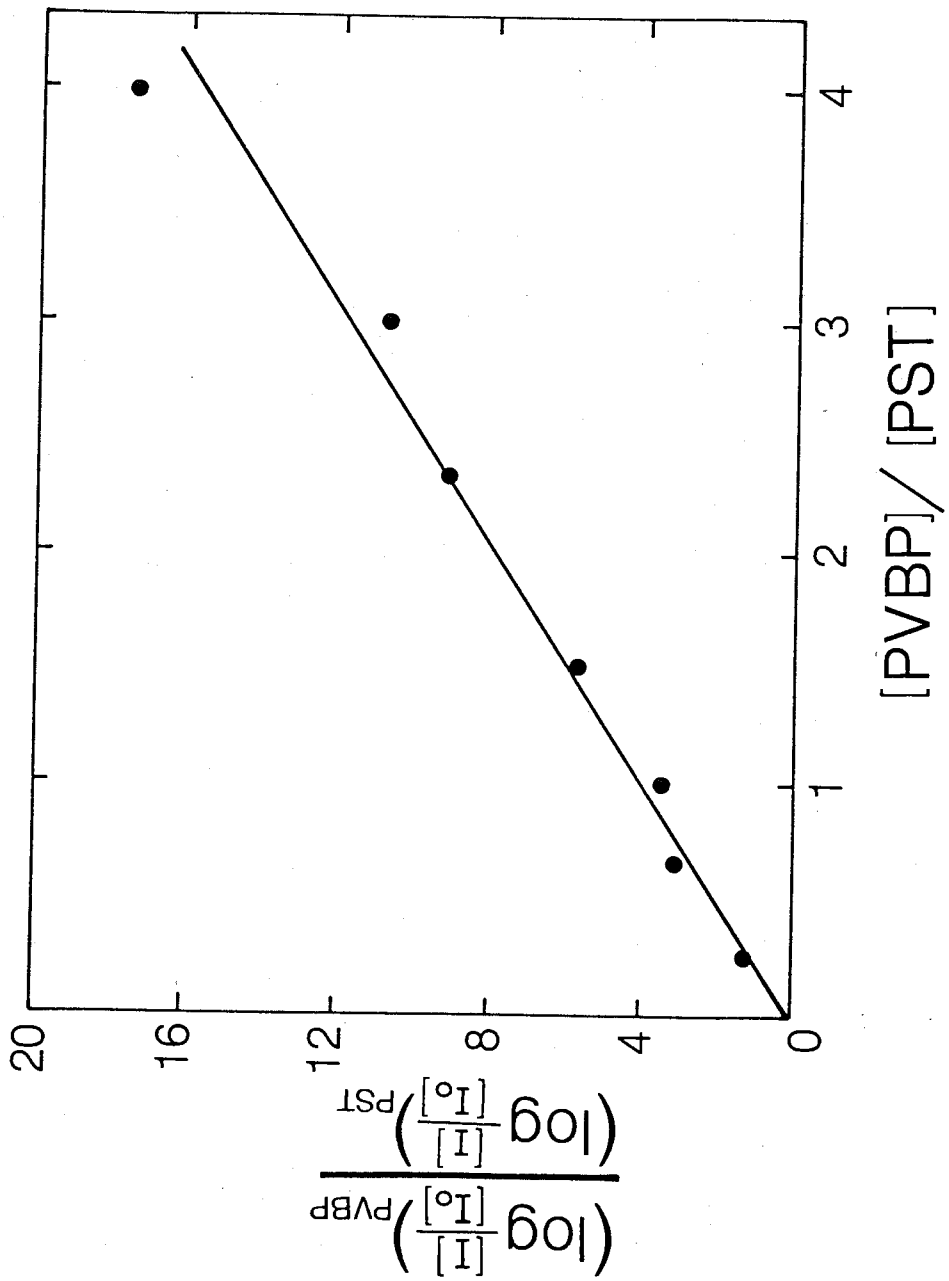
$\frac{(\log \frac{[I]}{[I_o]})_{PVBP}}{(\log \frac{[I]}{[I_o]})_{PST}}$
0
4
8
12
16
20
1
2
3
4
[PVBP]/ [PST]

in benzene and then freeze-dried in vacuo. The absorptivity was measured by noting the absorbance of PVBP at 1655 cm^{-1} and PST at 1490 cm^{-1}. The polymer blends were further analysed on a Cary 17 ultraviolet spectrograph. Fig. 31 shows the calibration plot of PVBP in benzene at 343 nm. The composition of the polymers determined from the two spectroscopic methods are in good agreement.

Molecular weights, polydispersities, and compositions of the polymers employed in this study are summarized in Table 11.

TABLE 11

MOLECULAR WEIGHT, MOLECULAR WEIGHT DISTRIBUTION, AND COMPOSITION OF PVB AND PVBP/ST

POLYMERS	$\bar{M}n$	$\overline{DP}n$	$\overline{M}w/\overline{M}n$	% VBP
P2A	3.22×10^3	22.5	1.16	37.4
P2C	4.68×10^3			100
P5A	7.38×10^3	51.9	1.20	36.7
P5B	9.33×10^3			72.8
P8A	9.82×10^3		1.22	30.8
P8B	1.33×10^4	72.2		76.9
P8C	1.42×10^4			88.6
P12A	1.46×10^4			30.7
P12B	1.80×10^4	107.7	1.14	60.9
P12C	2.11×10^4			88.6
P40A	5.27×10^4			22.5
P40B	6.52×10^4	413.5	1.16	51.5
P40C	8.62×10^4			100
P200A	3.00×10^5			32.5
P200B	3.55×10^5	2173.1	1.35	57.1
P200C	4.52×10^5			100
P300A	3.49×10^5	2740.4	1.12	22.5
P300B	5.02×10^5			76.2

FIGURE 31: CALIBRATION PLOT FOR ULTRAVIOLET SPECTROSCOPIC ANALYSIS OF POLY(VINYLBENZOPHENONE-CO-STYRENE)

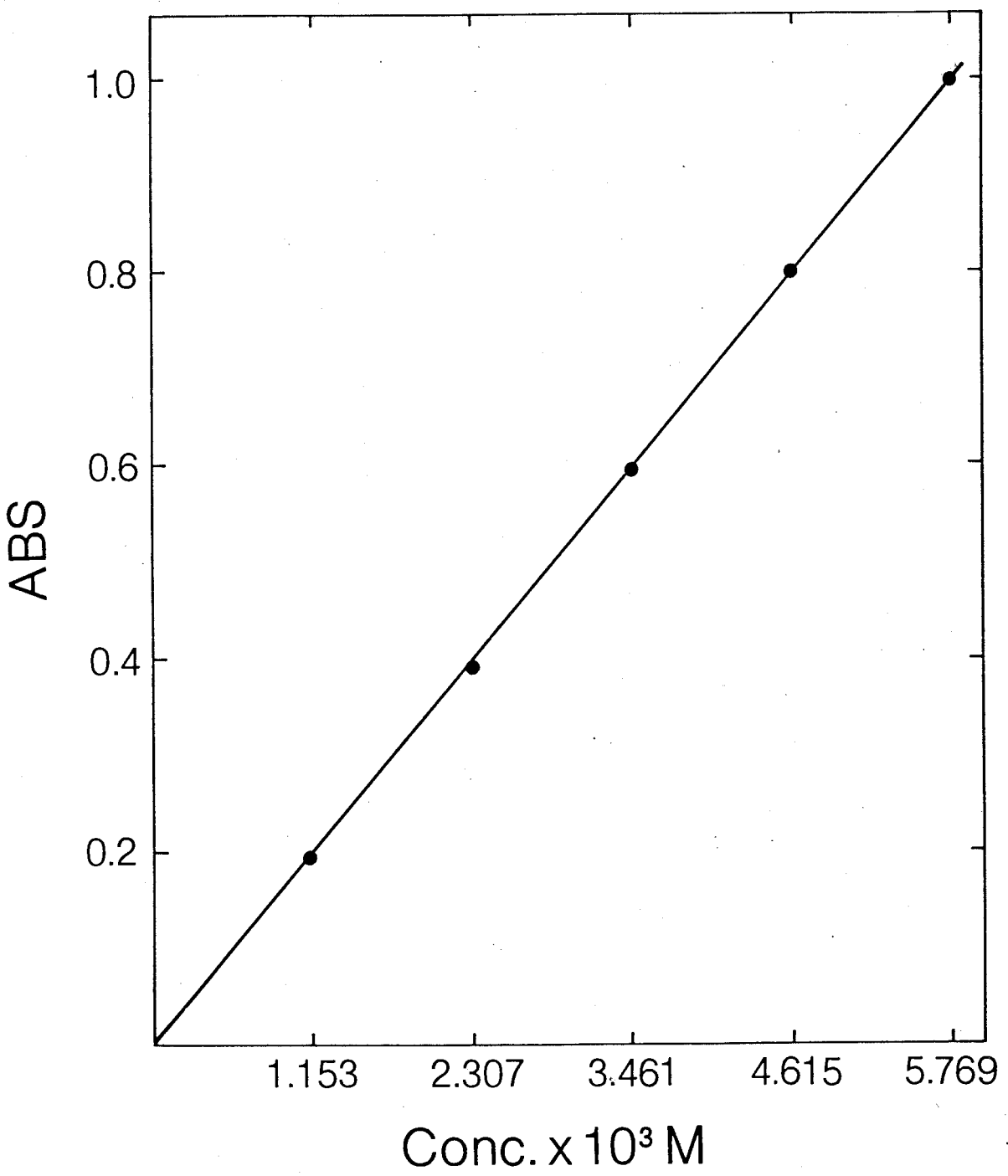
1.0
0.8
0.6
0.4
0.2
ABS
1.153
2.307
3.461
4.615
5.769
Conc. x 10³ M

3.2.3. Voltammetry with Rotating Ring Disk Electrode

The rotating ring disk electrode (RRDE) assembly has been described in Section 1.2.1. The platinum electrode used in this study was manufactured by Pine Instrument Co. and had dimensions of r_1 = 0.383 cm, r_2 = 0.399 cm, and r_3 = 0.422 cm. The counter and reference electrodes were coils of platinum wire and silver wire respectively.

The area of the electrode was determined by evaluating the potential step response of the known $K_4Fe(CN)_6$ system. The kinematic viscosity was determined with the aid of a capillary viscometer. The specific gravity of the solutions and the density of the polymers were measured using a specific gravity bottle and a density gradient formed from two liquids (methanol and formic acid) respectively. All concentrations in electrochemical measurements were expressed in moles of benzophenone residue per liter. The RRDE electrode was pretreated in DMF with TEAP while a potential sweep was applied at the disk electrode.

In a typical experiment, the required amounts of polymer and supporting electrolyte (TEAP) were placed into a flask which was attached to a vacuum line and evacuated for 18 hours. N,N'-dimethylformamide, previously redistilled, was transferred into the flask and the contents were mixed. The solution was then transferred directly into the electrochemical cell under an inert nitrogen atmosphere. The electrochemical measurements were carried out at 25 $\pm$ 0.1°C (unless otherwise specified) in cells maintained under a positive pressure of nitrogen.

3.2.4. Determination of Intrinsic Viscosity

The viscosity measurements for the determination of the Mark-Houwink constants for PVBP-ST in DMF with 0.10M TEAP were carried out in an Ubbelohde suspended level viscometer at 25 $\pm$ 0.01°C. The flow times were

measured at five concentrations; the intrinsic viscosity was calculated by the least square method according to the Huggins equation

$$\eta_{sp}/C = [\eta] + K' [\eta]^2 C \qquad [96]$$

The values of $[\eta]$ determined from this equation along with the molecular weights obtained from the gel permeation chromatography were used to determine the K and a values of the Mark-Houwink equation

$$[\eta] = KM^a \qquad [97]$$

3.3. RESULTS AND DISCUSSION

3.3.1 Comparative Voltammetric Studies of Molecular Benzophenone and of Benzophenone Moieties in a Polymer Chain

A rotating ring disk voltammogram (RRDE) of benzophenone (BP) in N,N'-dimethylformamide (DMF) containing 0.1 M tetraethylammonium perchlorate (TEAP) as supporting electrolyte is shown in Fig. 32. The disk current, i_d, exhibits two well-defined one-electron reduction waves which correspond to the formation first of a radical anion and then of a dianion (curve a). The reoxidation is shown in curve b, where the ring current, i_r, is shown as a function of disk potential, E_d, with the ring potential E_r maintained at -0.5V vs. a poised Ag wire reference. The limiting ring current (curve b in Fig. 32) is readily identified as due to the reoxidation of benzophenone radical anion, $BP^{\cdot -}$, to BP. At the region where the oxidation of the dianion $BP^{=}$ was expected, there was a sharp decrease in i_r. This shows that the dianions formed at the disk had reacted before they reached the ring electrode. These results are consistent with data from cyclic voltammetry (147) and from dropping mercury polarography (148) and may be represented by the following reaction scheme:

$$Ph_2\,C{=}O \underset{-e}{\overset{+e}{\rightleftharpoons}} Ph_2\dot{C}{-}O^- \xrightarrow{+e} Ph_2{}^-C{-}O^- \qquad [99]$$

$$Ph_2{}^-C{-}O^- + \text{proton donor} \longrightarrow Ph_2CH{-}O^- \qquad [100]$$

FIGURE 32: RRDE VOLTAMMOGRAMS OF 2.9 mM BP IN 0.1 M TEAP/DMF

ω = 202 rad/sec;

(a) disk current

(b) ring current

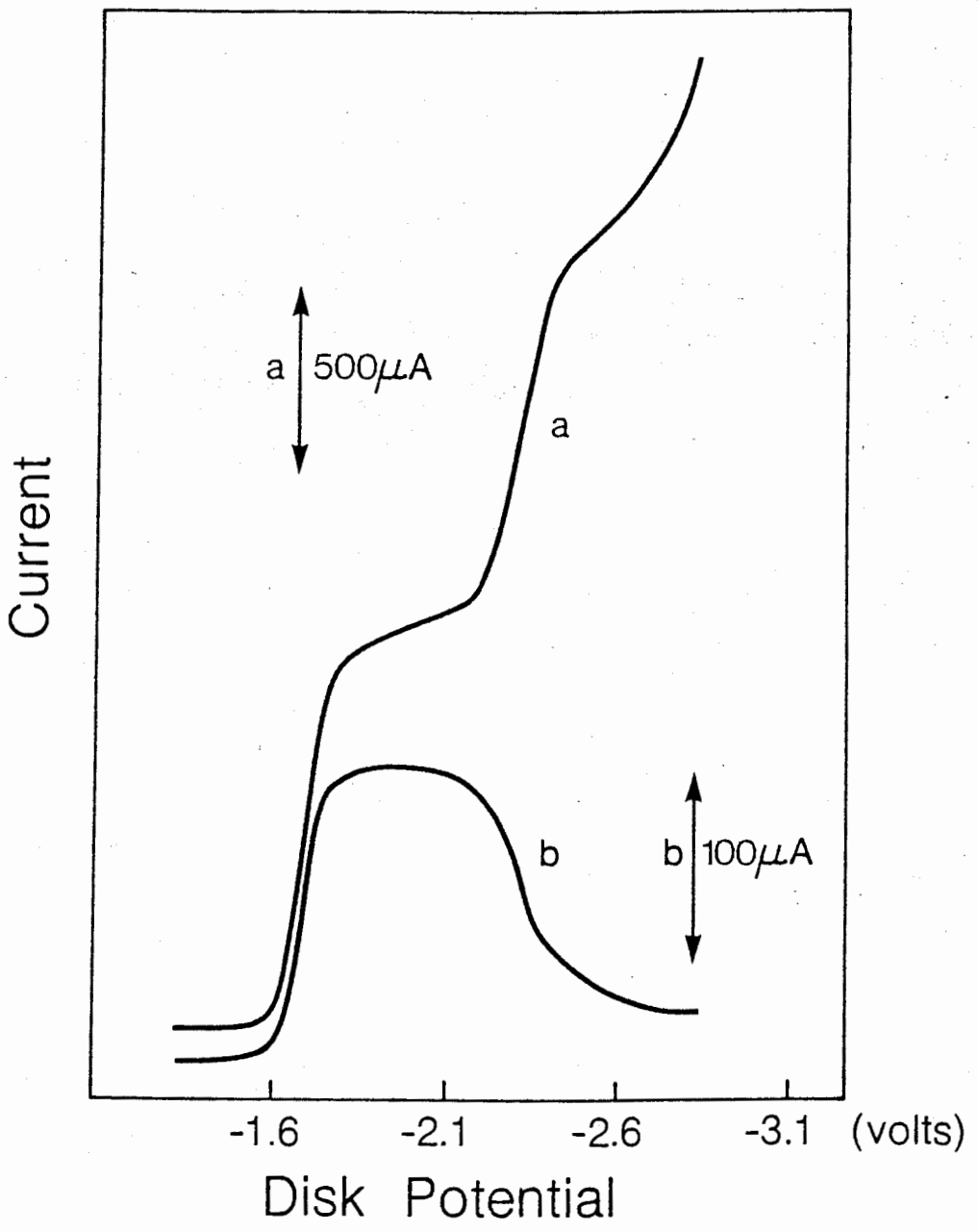
Current
a
500μA
a
b
b
100μA
-1.6
-2.1
-2.6
-3.1
(volts)
Disk Potential

The collection efficiency, N_o, (ratio of i_r/i_d) for the first reduction and oxidation waves at various rates of rotation yield a constant value of 0.179 from the data in Fig. 33. This can be compared with N_o =0.1785 calculated by the procedure of Albery et al (36) and with N_o = 0.1762 obtained by a digital simulation method (49). This close agreement of N_o values determined experimentally with the theoretical efficiency and the constancy of N_o with rotation rate indicate that the first stage reduction and reoxidation reactions are free of kinetic complications due to competing reaction paths.

The cyclic voltammogram of poly(vinylbenzophenone-co-styrene)(PVBP-ST) with an $\bar{M}n = 6.25 \times 10^4$ at a stationary microplatinum electrode in DMF with 0.1 M TEAP (Fig. 34) is quite similar to that of molecular benzophenone (Fig. 34b) despite the fact that the former requires hundreds of electrons per polymer molecule for the electron transfer process. The peak potential separation ($E_{Pa} - E_{Pc}$) is about 65 mV. This wave is characteristic of a Nernstian one-electron reduction to form a stable product.

The RRDE voltammogram of PVBP-ST ($\bar{M}n = 1.8 \times 10^4$ and % VBP = 61) exhibits the shape expected for an isolated non-interacting BP residue (Fig. 35), but the limiting current is much smaller than that of benzophenone. This obviously is due to the much smaller rate of diffusion of the polymeric species as the limiting current is directly proportional to the diffusion coefficient of the electroactive species. It was also noted that the PVBP dianion was less rapidly protonated than the monomeric dianion. This is indicated by the higher ring current (i_r) in the region where the reoxidation of $PVBP^{=}$ is expected and reflects the decrease in chemical reactivity of the dianion when substituted on a vinyl polymer backbone (Section 2.3.3.).

FIGURE 33: PLOTS OF COLLECTION EFFICIENCY VS ROTATION RATE

● Benzophenone

△Poly(vinylbenzophenone)

in DMF/0.1M TEAP

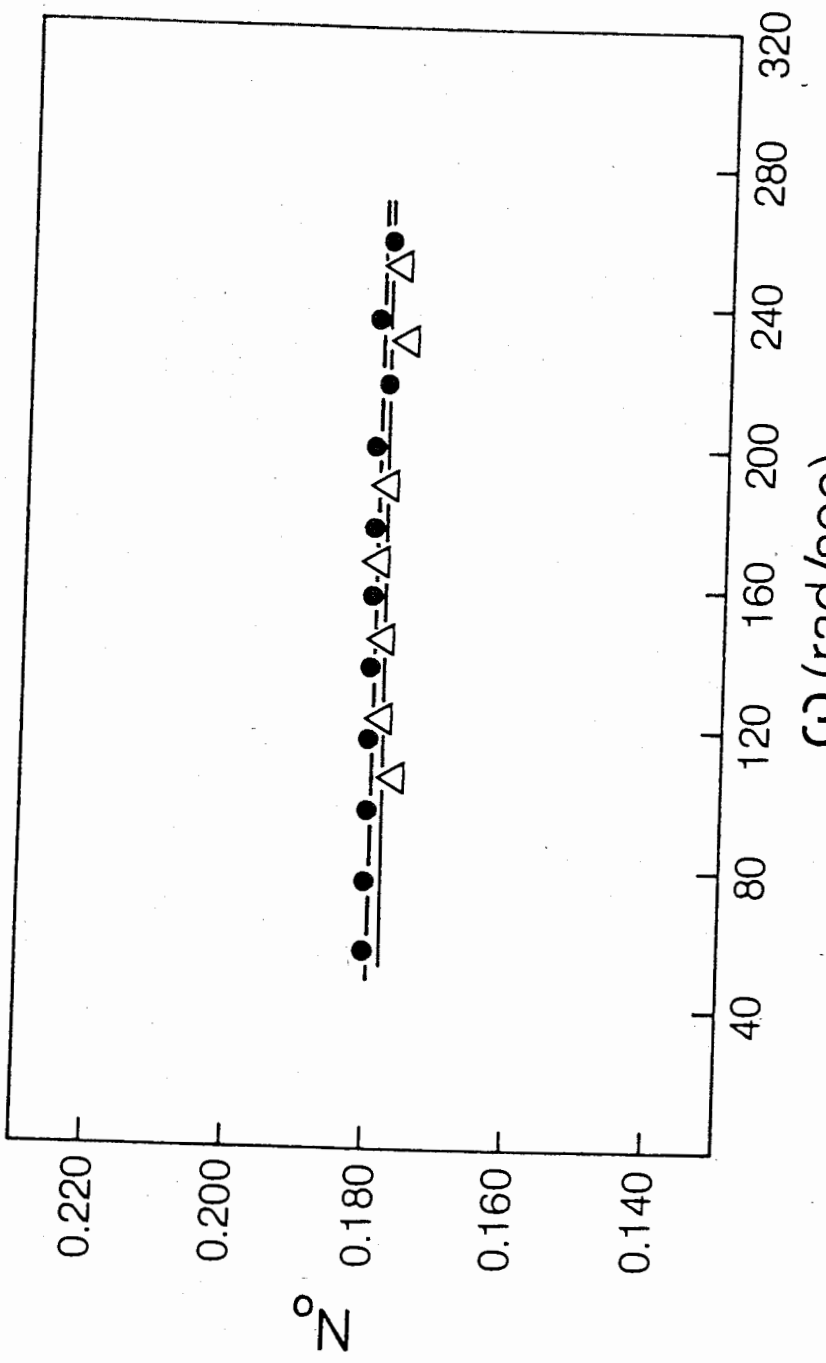
0.220
0.200
0.180
0.160
0.140
N_o
40
80
120
160
200
240
280
320
ω (rad/sec)

FIGURE 34: CYCLIC VOLTAMMOGRAMS OF BP AND PVBP-ST

(a) 3 mM PVBP-ST ($\bar{M}n$ = 6.5 X 10^4, % VBP = 52)

(b) 3 mM BP in 0.1 M TEAP/DMF

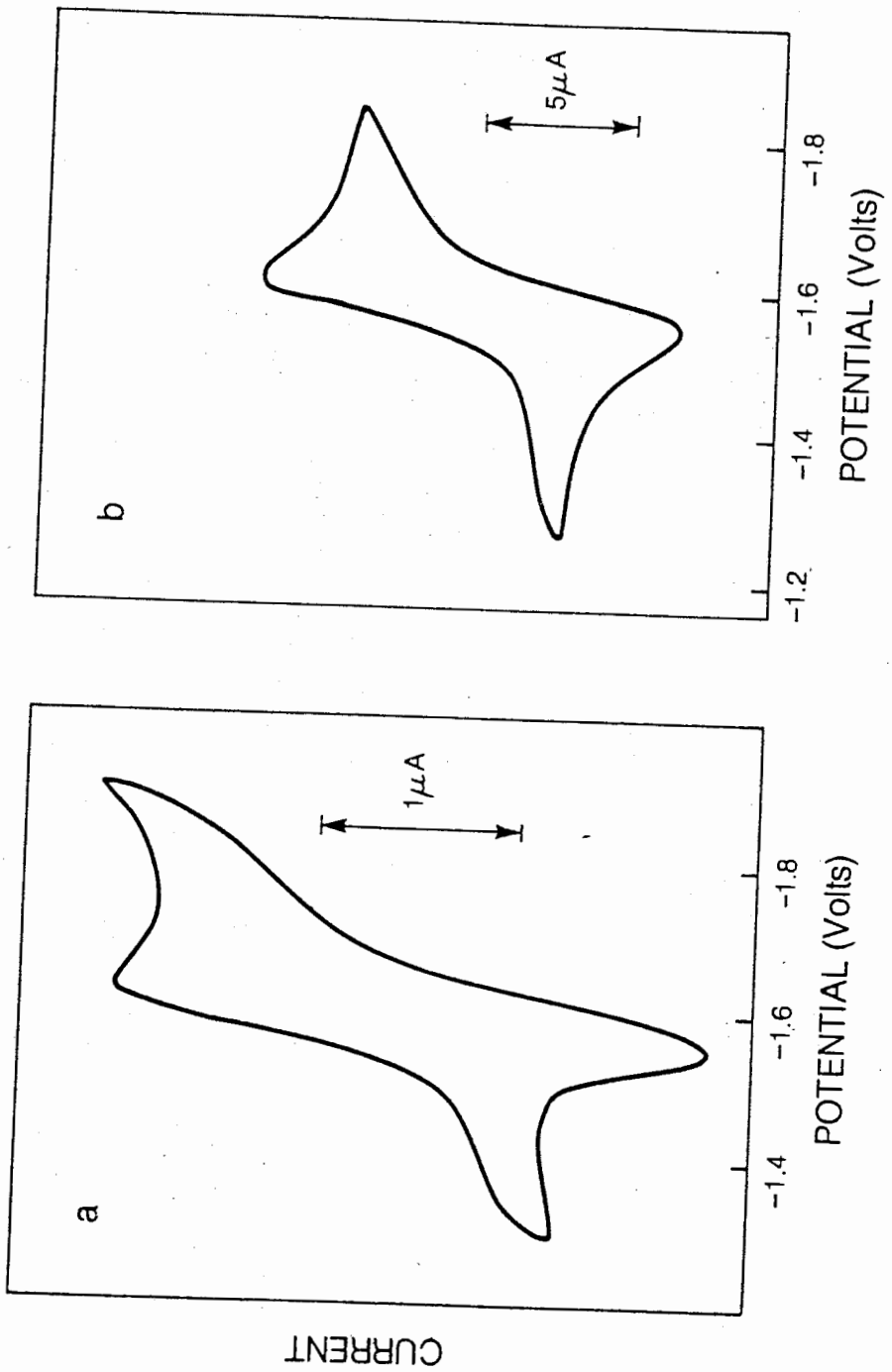
a
b
1μA
5μA
CURRENT
-1.4
-1.6
-1.8
-1.2
POTENTIAL (Volts)
POTENTIAL (Volts)

FIGURE 35: RRDE VOLTAMMOGRAM OF PVBP-ST

3 mM PVBP-ST ($\bar{M}n$ = 1.8 X 10^4, % VBP = 61)

in 0.1 M TEAP/DMF ω = 148 rad/sec

(a). disk current

(b). ring current

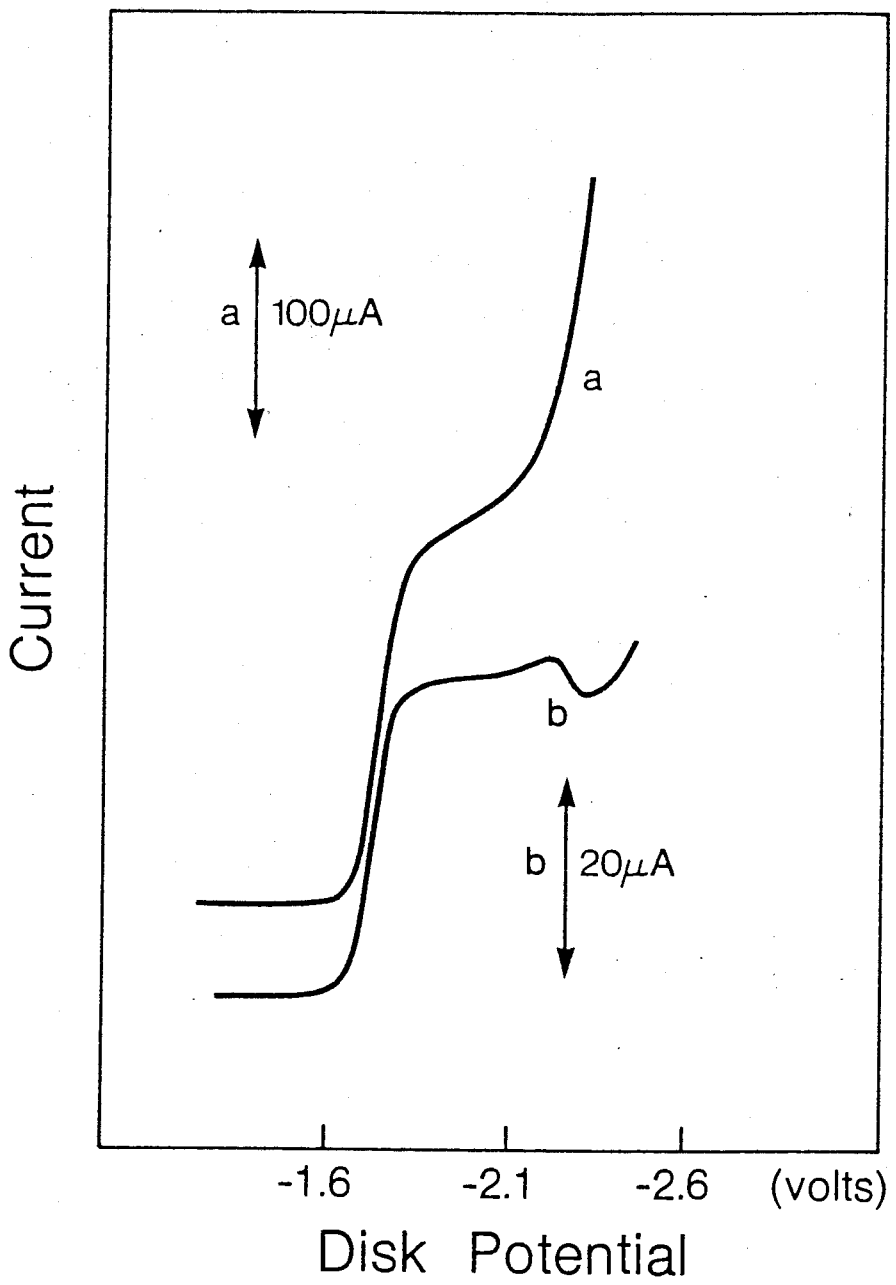
a
100μA
a
b
b
20μA
Current
-1.6
-2.1
-2.6
(volts)
Disk Potential

The collection efficiency for the PVBP was identical with that for BP (Fig. 33), and N_o = 0.178 was in good agreement with the theoretically predicted value. The ideal behavior of the substituted benzophenone group on a polymer at RRDE is thus evident.

Under the same experimental conditions, the limiting current values for polymers with molecular weights up to $\sim 3.0 \times 10^5$ were found to be very reproducible. No filming was observed as repetitive runs essentially gave superimposable voltammograms. In studies of polymers with higher VBP contents (ca. VBP>75%), however, a dip was observed after a limiting current plateau, corresponding to the reduction of VBP to $VBP^{\bullet -}$. The decrease in current is probably due to the intermolecular dimerization of $PVBP^{\bullet -}$. In turn this causes a sudden increase in the molecular weight of the electroactive species, thus lowering its diffusion rate. This postulate is supported by the experimental evidence that the dip intensified with decreasing scan rate (Fig. 36). At slower scan rates, higher concentrations of $VBP^{\bullet -}$ can be maintained, which facilitates the dimerization reaction. At moderate scan rate (Fig. 36), the dip disappeared, suggesting the dimerization is a relatively slow process. The observation is consistent with that found in the macro-electrolysis of PVBP (Section 2.3.3.) in which gel particles were obtained with polymers of high VBP contents.

A further comparison of the number of electrons transferred and the relevant half-wave potentials was made according to Eq. [101] :

$$E = E^\circ - (0.059/n) \log (i_L - i)/i \qquad [101]$$

where

$$E_{1/2} = E^\circ - \frac{RT}{nF} \ln \frac{K_2}{K_1}$$

FIGURE 36: EFFECT OF SCAN RATE ON REDUCTION OF POLYMER WITH HIGH VBP CONTENT

P8C ($\bar{M}_n$ = 1.42 X 10^4, VBP=89%)

3.0 mM VBP/0.1 M TEAP/DMF/25^{o}C

ω = 166 rad/sec

a : 30 mV/sec b : 15 mV/sec

c : 10 mV/sec d : 5 mV/sec

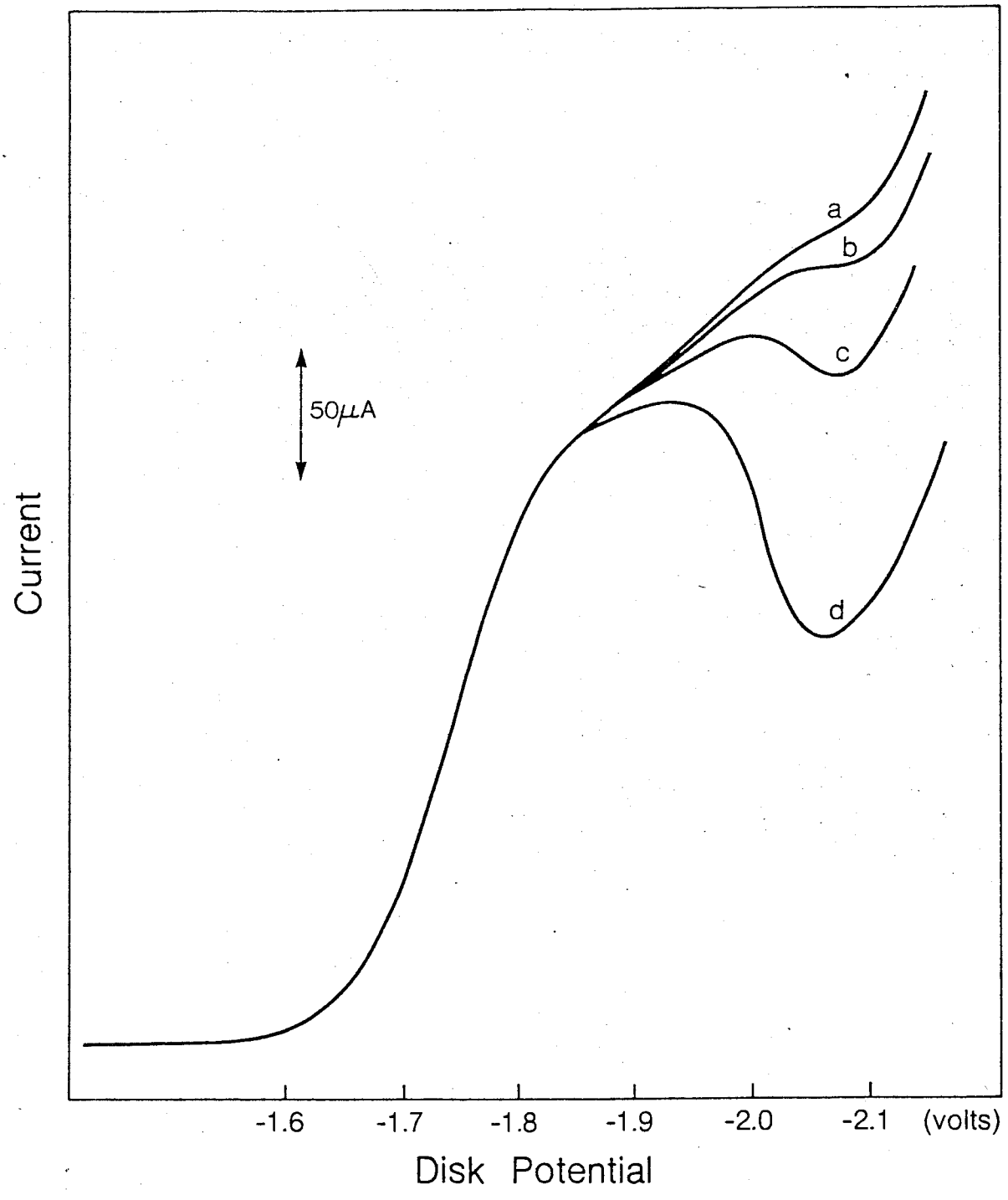
a
b
c
d
50μA
Current
-1.6
-1.7
-1.8
-1.9
-2.0
-2.1
(volts)
Disk Potential

where K_1 and K_2 are constants dependent on the mass transfer of the system (143). A plot of E vs log $(i_L - i)/i$ should be linear. Data for BP and PVBP in Fig. 37 indeed show the predicted linear behaviors. The theoretical slopes were 0.063 for BP and 0.071 for PVBP, indicating single electron transfer processes. The results indicate that BP and its macromolecular analogs are reduced at quite similar potentials and also confirm the theoretical model proposed by Flanagan et al (127) that, for molecules containing identical, non-interacting centers, the overall shape of the current-potential curve and the half-wave potential are identical to that of a molecule with one center.

3.3.2. Studies of Neighboring Group Interactions in Poly(vinylbenzophenone)

The reduction of an electroactive polymer involves the transfer of a large number of electrons to a single molecule. These electron transfer processes may occur sequentially at different potentials due to the inter- or intra-molecular interactions or independently at same potential. While the voltammogram of a polymer having a shape similar to that of the corresponding monomeric molecule indicates the gross absence of molecular reorganization and inductive effects, the magnitude of the current provides further quantitative information on the polymer behavior at an electrode. The limiting current is proportional to the concentration of electroactive groups at the surface of an electrode and, thus, provides a measure of the number of active centers that are "truly" electroactive. Any departure of the experimentally determined value from the theoretically predicted one is an indication of the inaccessibility of the active groups at the electrode and may be attributable to effects associated with the macromolecular environments.

FIGURE 37: LOGARITHMIC PLOTS OF BP AND PVBP-ST

● 2 mM BP, and △ 2 mM PVBP-ST

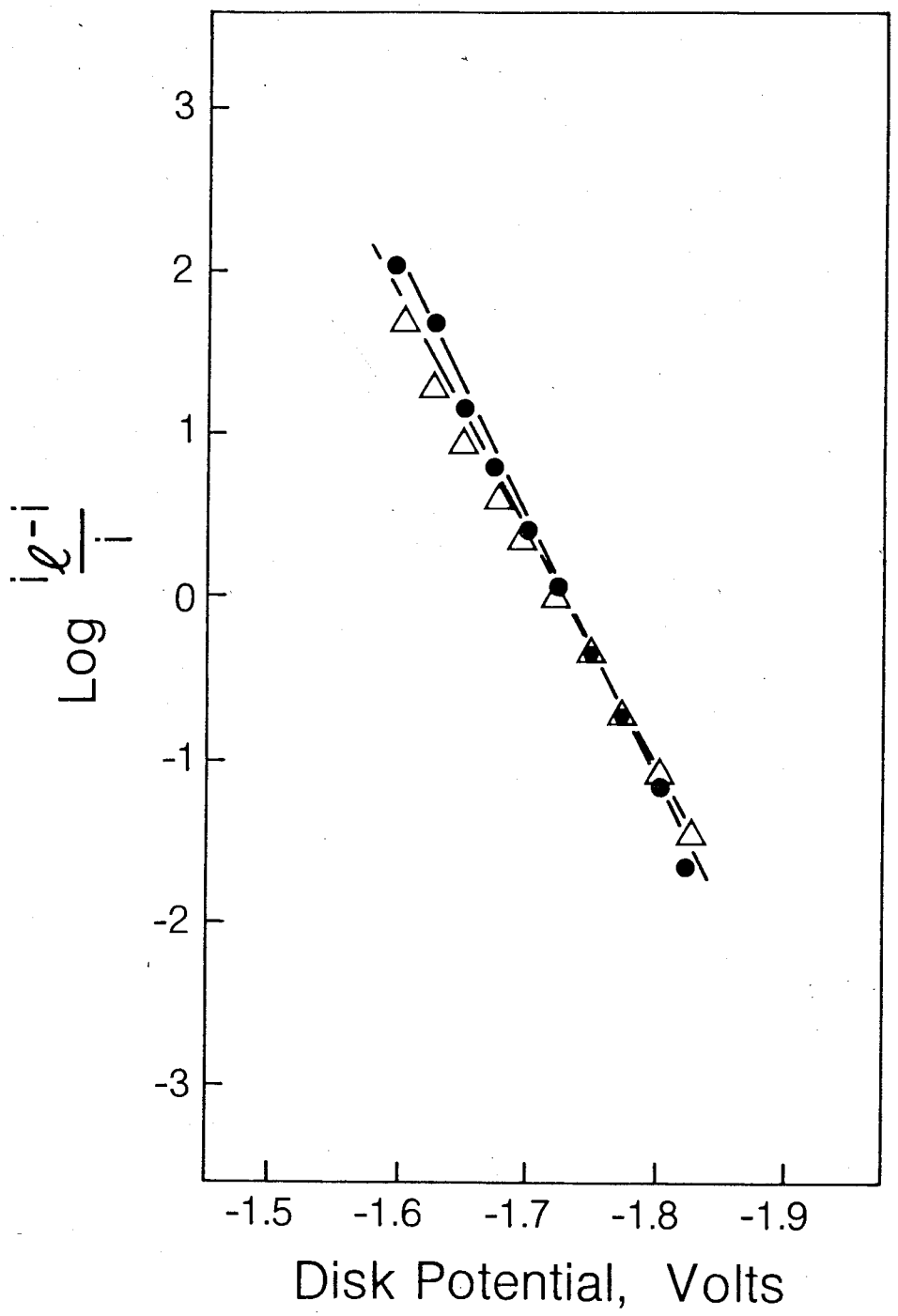
3
2
1
0
-1
-2
-3
Log $\frac{i_\ell - i}{i}$
-1.5
-1.6
-1.7
-1.8
-1.9
Disk Potential, Volts

An estimation of the theoretical limiting current is, however, not possible without a knowledge of the diffusion coefficient (D) of the electroactive species. Prevailing literature provides but little information on the electroactive polymers. The few available studies of the electron transfer processes of polymers employed various approximations to assess the diffusion coefficient of the polymers. Thus, Smith et al (126) deduced the extent of neighboring group interactions of a series of poly(vinylferrocene) from a comparison of the experimentally determined D values with those calculated from the Stokes-Einstein equation [85]. Based on this comparison, the authors suggested that there were some interactions between adjacent ferrocene groups which increased with increasing backbone chain lengths of the polymers and that not all ferrocene residues were oxidizable at the electrode. Although the overall shapes of current-potential curves were identical for ferrocene and poly(vinylferrocene), it was concluded that approximately one in four of the ferrocene groups were oxidized for polymers with molecular weights between 1.6×10^4 and 2.6×10^4; and one in three for 5.0×10^3 molecular weight; and one in 1.5 for 1.0×10^3 molecular weight. Flanagan (127) and Bard et al (128), on the other hand, estimated the diffusion coefficients of poly(vinylferrocene) and of poly(vinylnaphthalene) from Eq. [95], which were used to determine the number of electrons transferred per molecule.

In the present work, polymers of various constant chain lengths, but of differing spacings between electroactive centers (benzophenone) were prepared. The use of polymers with the same backbone chain length to which different amounts of electroactive centers are attached allows the effects of neighboring group interaction to be determined without the need of estimating values of D for the same series of polymers. The limiting currents were

measured with a rotating disk electrode system and the data were analysed on the basis of the Levich equation:

$$i_L = 0.62nFACD^{2/3}\nu^{-1/6}\omega^{1/2} \qquad [84]$$

Before examining the neighboring group interaction in the poly (vinylbenzophenone) system, the electrochemical behavior of isolated benzophenone molecules in the presence of an inert polymer was studied. Benzophenone was added to a solution of polystyrene in DMF with 0.1 M TEAP, and limiting currents were measured at several rotation rates. The results were compared with those obtained in the absence of the polymer. The essentially identical current (Fig. 38) observed for the two systems indicates that the presence of inert polymer neither interfered with the transport processes of the benzophenone molecules in solution nor had any effect on the accessibility of benzophenone to the electrode. The results also substantiates the fact that the much smaller magnitude of the limiting current observed in PVBP in comparison with that observed in BP is instrinsically related to the diffusion rate of electroactive entities.

Polymers of $\overline{DP}n = 23$ with 37% VBP ($\bar{M}n = 3.2 \times 10^3$) and with 100% VBP ($\bar{M}n = 4.7 \times 10^3$) were compared and the limiting currents are shown in Fig. 39. The total number of electroactive groups was maintained at equal values by adjusting the polymer concentration in the solution. Thus, the solution of 37% BP had a higher polymer concentration than the 100% BP. (The effect of the polymer concentrations on i_d was determined by measuring the kinematic viscosity of the solutions and was found to be negligible.) If the postulations of Smith et al (126) were generally applicable we would

FIGURE 38: LIMITING CURRENT VS ROTATION RATE FOR BP IN THE PRESENCE AND ABSENCE OF INERT POLYMER

□ 5 mM BP

⏱ 5 mM BP with equal weight of polystyrene

in 0.1 M TEAP/DMF

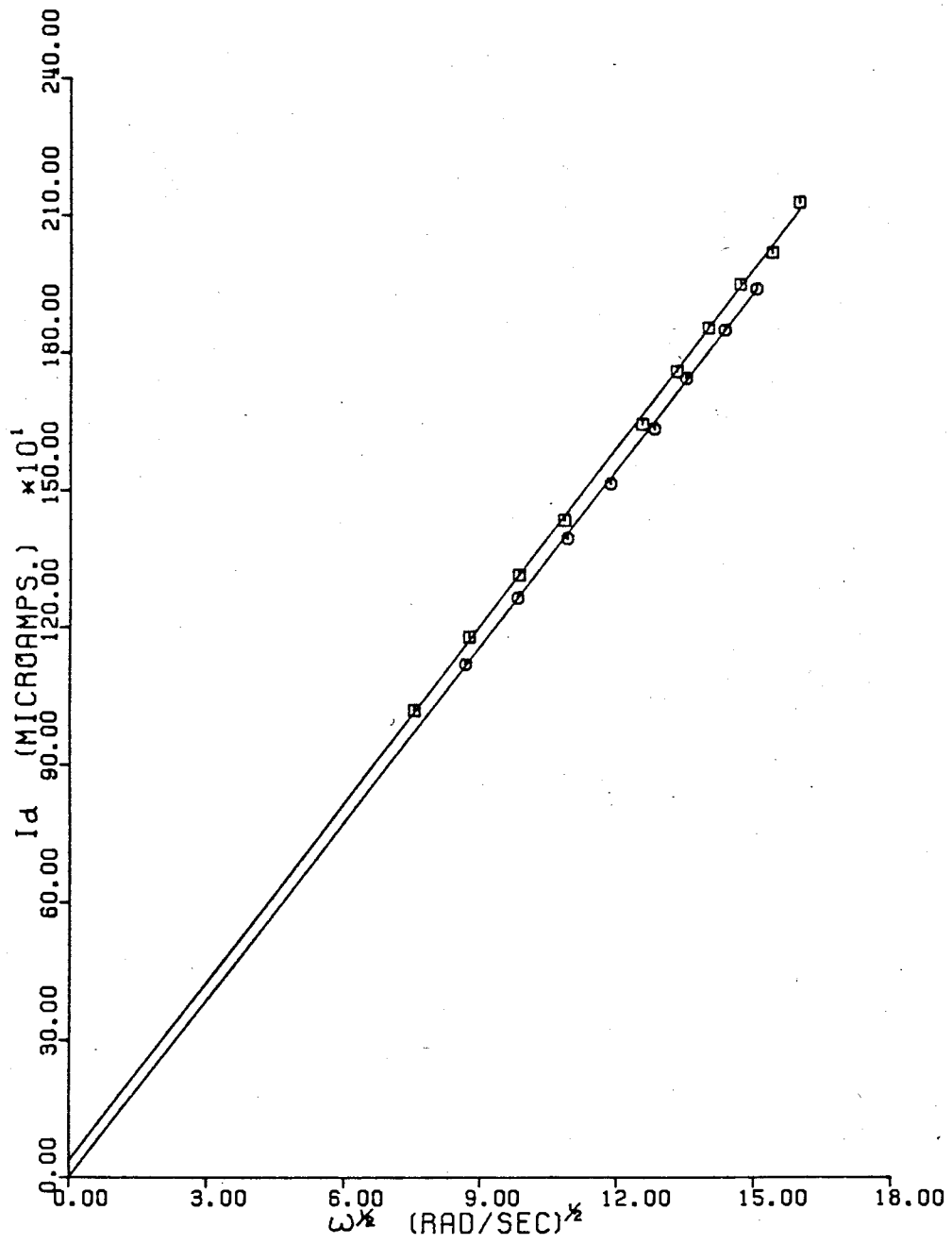
Id (MICROAMPS.) ×10¹
0.00
30.00
60.00
90.00
120.00
150.00
180.00
210.00
240.00
0.00
3.00
6.00
9.00
12.00
15.00
18.00
ω½ (RAD/SEC)½

FIGURE 39: EFFECT OF VARYING SPACING OF ELECTROACTIVE CENTERS FOR THREE VALUES OF $\overline{DP}n$ IN SOLUTION OF 2.8 mM VBP

$\overline{DP}n$ = 23, ⊡ % PVBP = 37, ⊙ % VBP = 100

$\overline{DP}n$ = 72, ⊠ % VBP = 31, ◇ % VBP = 77

△ VBP = 89

$\overline{DP}n$ = 108, × % VBP = 31, + % VBP = 61

⚠ VBP = 89

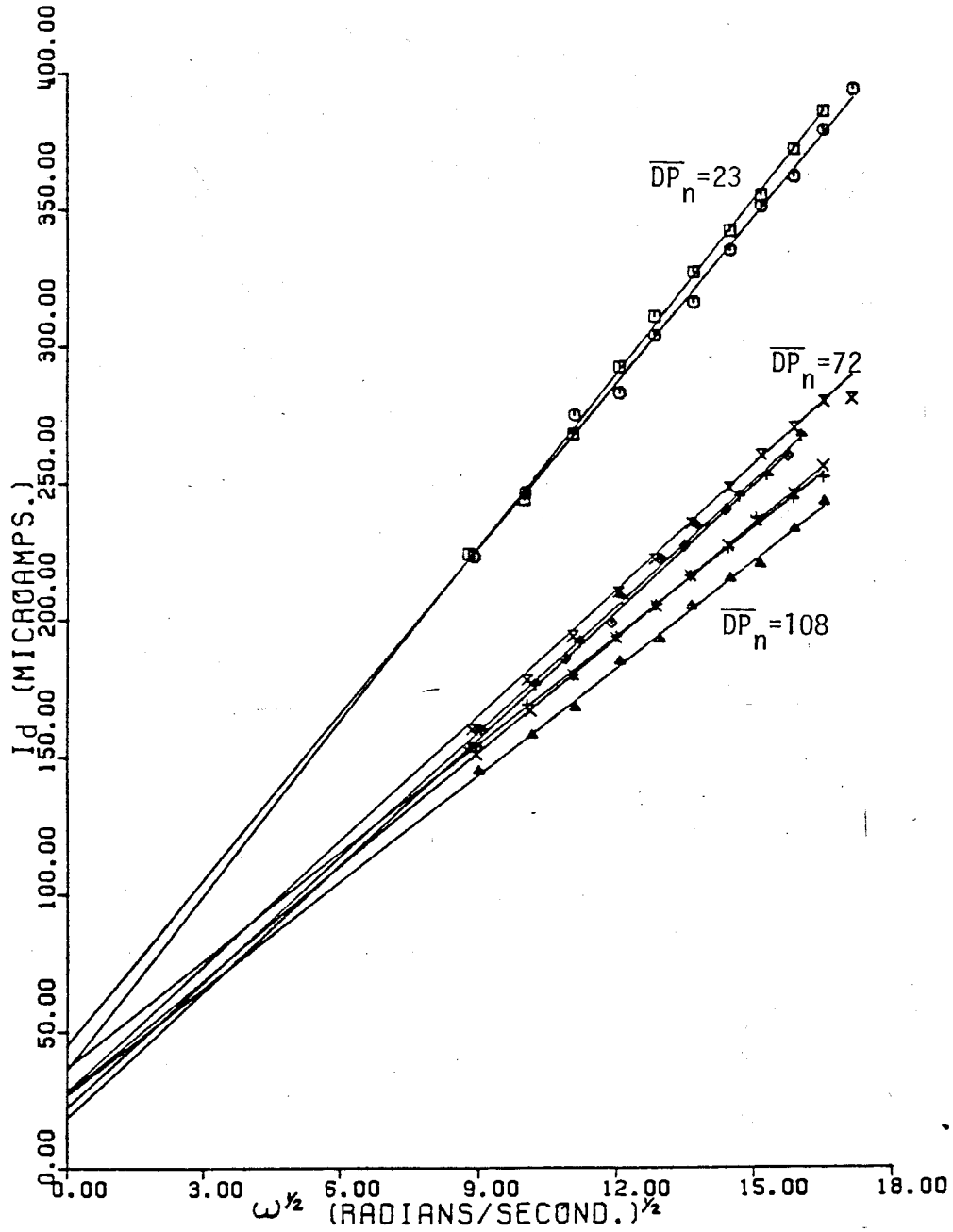
$\overline{DP}_n$=23
$\overline{DP}_n$=72
$\overline{DP}_n$=108
I_d (MICROAMPS.)
0.00
50.00
100.00
150.00
200.00
250.00
300.00
350.00
400.00
0.00
3.00
6.00
9.00
12.00
15.00
18.00
$\omega^{1/2}$ (RADIANS/SECOND.)$^{1/2}$

expect a three-fold variation in i_d. Instead, the data are almost identical for the two polymers. The absence of appreciable interaction is thus demonstrated quite clearly.

To further examine the effect of backbone chain length on the neighboring group interactions, experiments were extended to polymers of greater backbone chain lengths. Samples of $\overline{DP}_n$ = 72 and $\overline{DP}_n$ = 108 containing 30%, 60%, and 90% of the benzophenone moiety were studied. Plots of i_d vs $\omega^{1/2}$ are shown in Fig. 39 and again indicate no significant changes in i_d for equal amounts of BP per unit volume.

The constancy of the limiting currents for polymers of identical chain length but varying spacings between benzophenone groups thus indicates unequivocally the absence of neighboring group interaction in the present polymer system. The general results further elucidate that macromolecular environments do not interfere with the electroactivity of benzophenone moieties and point to the fact that every benzophenone group is reducible at the electrode. Attached benzophenone moieties appear to retain all the characteristics of molecular benzophenone, i.e. the reduction potential, the overall shape of the current-potential curve, the electrochemical reversibility, and the accessibility to the electrode. The ideal behavior of the poly-(vinylbenzophenone) system also provides definite experimental proof of the concepts of non-interacting centers proposed by Flanagan, Bard, and Anson (127)

3.3.3. Determination of Diffusion Coefficient

The results discussed in the previous section indicate that the electroactive groups are merely "passengers" on a slowly moving "train" - the benzophenone groups retain their individuality and characteristics, but their rate of transport is determined by the chain on which they are transported. The limiting current (i_L) measured at a RDE is proportional to the diffusion rate and the concentration of electroactive entities, the number of electrons transferred per molecule, the kinematic viscosity of the solution, and the area of the electrode. Thus, if the concentration of the electroactive species is known accurately, a precise determination of the diffusion coefficient (D) can be made by measuring i_L at several rotation rates according to the Levich equation [84] . A plot of i_L vs $\omega^{1/2}$ should yield a straight line with a slope of $0.62nFACD^{2/3}\ \nu^{-1/6}$ from which the value of D may be determined.

With the composition and molecular weights of the PVBP-ST determined experimentally (Table 9) and with the knowledge that the benzophenone moiety on the polymers undergoes a one-electron reduction to its radical anion, the number of electrons transferred per polymeric molecule and the concentration of polymer can be estimated unambiguously. Alternatively, one may utilize the concentration of benzophenone residue with the "n" designated as the number of electrons transferred per "active center" as, by either definition, the product of n X c is a constant. In this work the concentration of the polymers was expressed in moles of benzophenone residues per liter.

Fig. 40 shows the plots of i_L vs $\omega^{1/2}$ for PVBP-ST containing an average of 30% VBP but with increasing molecular weight. It can be seen that the i_L decreases steadily as the molecular weight of polymer increases. The slopes which measure the diffusion coefficient of the polymers also decrease with an increase in molecular weights. The diffusion coefficients calculated through least square analyses from the date in Fig. 40 along with the experimentally determined kinematic viscosities of the solutions are compiled in Table 12.

TABLE 12

DIFFUSION COEFFICIENTS FOR POLY(VINYLBENZOPHENONE-CO-STYRENE)

ELECTROACTIVE MATERIAL	NUMBER AVERAGE MOLECULAR WEIGHT ($\bar{M}n$)	D (cm^2/sec)	ν (cm^2/sec)
P2A	3.22×10^3	1.48×10^{-6}	9.92×10^{-3}
P5A	7.38×10^3	1.13×10^{-6}	9.96×10^{-3}
P8A	9.82×10^3	9.29×10^{-7}	1.00×10^{-2}
P8B	1.33×10^4	8.65×10^{-7}	1.00×10^{-2}
P12A	1.46×10^4	7.33×10^{-7}	1.01×10^{-2}
P40A	5.27×10^4	3.98×10^{-7}	1.02×10^{-2}
P200A	3.00×10^5	1.76×10^{-7}	1.06×10^{-3}

FIGURE 40: PLOTS OF LIMITING CURRENT VS ROTATION RATE FOR PVBP-ST WITH INCREASING CHAIN LENGTHS

◇ P2A : $\bar{M}_n = 3.22 \times 10^3$ %VBP = 37

\+ P5A : $\bar{M}_n = 7.38 \times 10^3$ %VBP = 37

□ P8A : $\bar{M}_n = 9.82 \times 10^3$ %VBP = 31

⊙ P12A : $\bar{M}_n = 1.46 \times 10^4$ %VBP = 31

▲ P40A : $\bar{M}_n = 5.27 \times 10^4$ %VBP = 23

× P200A : $\bar{M}_n = 3.00 \times 10^5$ %VBP = 33

All solutions containing 3 mM VBP/0.1 M TEAP/DMF

Temperature : $25^{o}C$

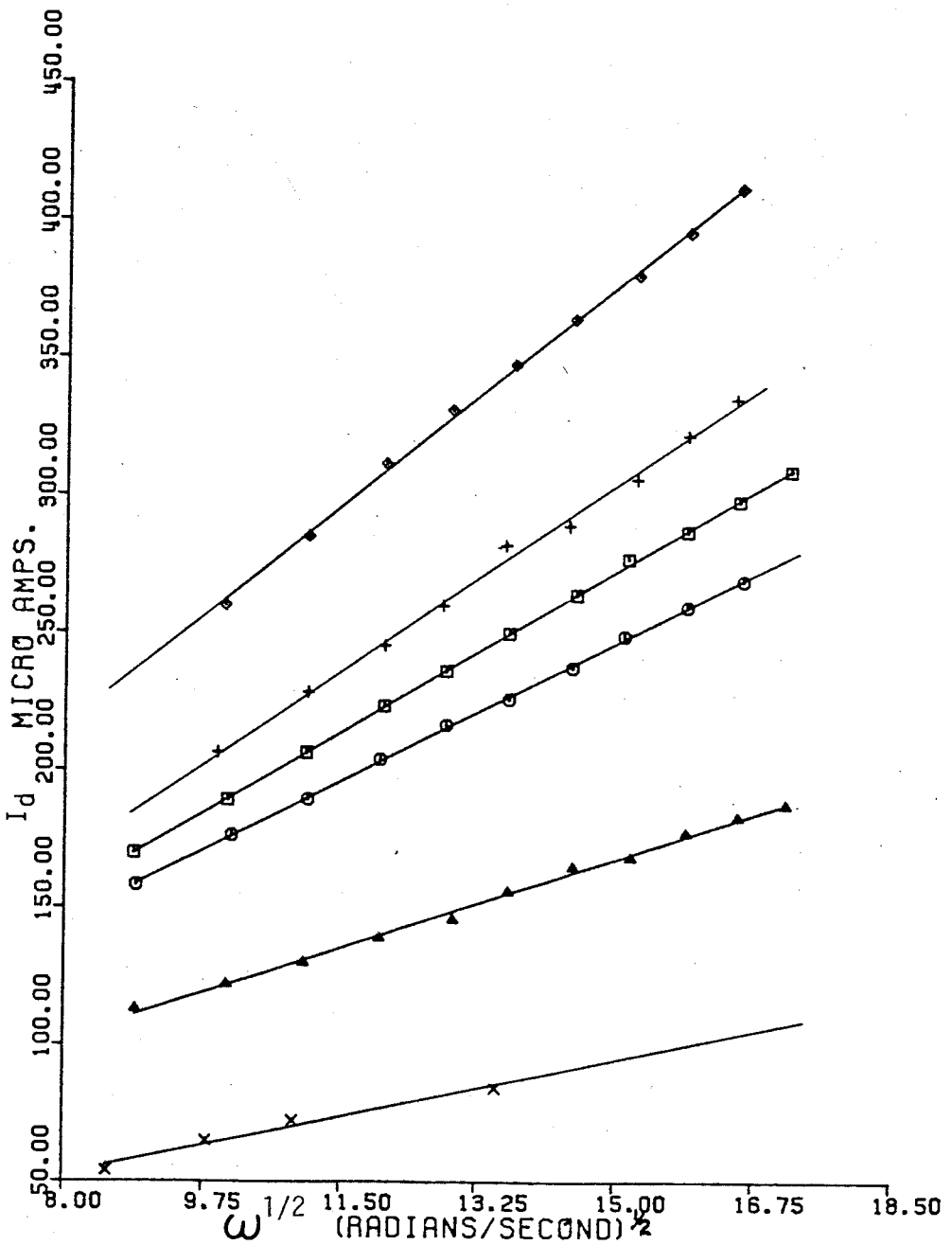
I_d MICRO AMPS.
50.00
100.00
150.00
200.00
250.00
300.00
350.00
400.00
450.00
8.00
9.75
11.50
13.25
15.00
16.75
18.50
$\omega^{1/2}$ (RADIANS/SECOND)$^{\frac{1}{2}}$

Similar plots for polymers with high VBP contents are shown in Fig. 41. The far greater i_L exhibited by benzophenone, in comparison with those exhibited by any of the polymers, is clearly illustrated in this figure. The corresponding values of D for this series of polymers are compiled in Table 13.

TABLE 13

DIFFUSION COEFFICIENTS FOR BENZOPHENONE AND POLYMERS WITH HIGH VBP CONTENTS

ELECTROACTIVE MATERIAL	NUMBER AVERAGE MOL. WT. ($\bar{M}n$)	D (cm^2/sec)
BP	182	8.96×10^{-6}
P2C	4.68×10^{3}	1.41×10^{-6}
P5B	9.33×10^{3}	1.07×10^{-6}
P8C	1.42×10^{4}	8.69×10^{-7}
P12C	2.11×10^{4}	6.46×10^{-7}

A comparison of data from Tables 12 and 13 also indicates that samples with an identical degree of polymerization but varying VBP contents have nearly identical diffusion coefficients.

FIGURE 41: PLOTS OF LIMITING CURRENT VS ROTATION RATE FOR PVBP-ST WITH HIGH VBP CONTENT


Benzophenone


P2C : 4.68×10^3 %VBP = 100


P5B : 9.33×10^3 %VBP = 73

P8C : 1.42×10^4 %VBP = 89

P12C : 2.11×10^4 %VBP = 89

All solutions containing 3 mM BP or VBP/ 0.1M TEAP/DMF

Temperature : $25^{o}C$

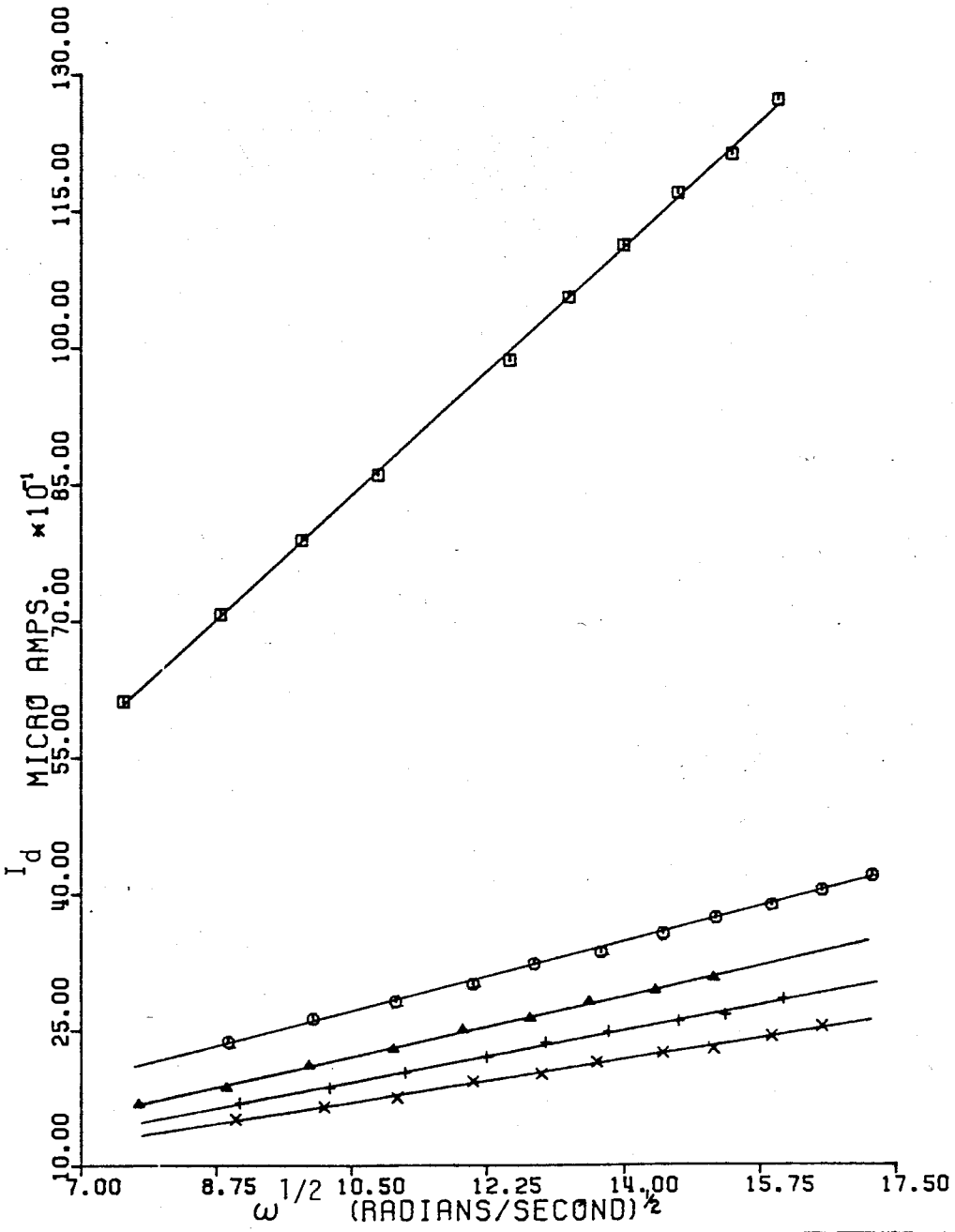
I_d MICRO AMPS. $\times 10^{-1}$
10.00
25.00
40.00
55.00
70.00
85.00
100.00
115.00
130.00
7.00
8.75
10.50
12.25
14.00
15.75
17.50
$\omega^{1/2}$ (RADIANS/SECOND)$^{\frac{1}{2}}$

3.3.4. Relation Between Diffusion Coefficient and Molecular Weight of Polymers

For flexible polymer molecules in dilute solution, the diffusion coefficient D is related to the molecular weight of polymer by the relation:

$$D = \frac{KT\, M_o^{1/2}}{6^{1/2}\pi\eta\alpha\beta\xi_f M^{1/2}} \qquad [95]$$

D should be proportional to $1/M^{0.5}$ in a poor solvent and $\backsim 1/M^{0.55}$ in an average good solvent as discussed in Section 3.1.5. The approximation

$$D = \frac{K}{M^{0.55}}$$

was utilized by Flanagan et al in their study of poly(vinylferrocene) in THF and by Bard et al (128) for poly(vinylnaphthalene) and poly(vinylanthracene) in THF to estimate the diffusion coefficient of the polymers. Consequently, THF was assumed to be a good solvent for the polymers they employed.

Eq. [95] is often expressed in the more general form of

$$D = K_T M^{-b} \qquad [102]$$

where K_T and b are constants for a given polymer-solvent system. A double logarithmic plot of D vs M should yield a straight line with an intercept K_T and a slope of b. This plot is shown in Fig. 42 for a series of differring molecular weight polymers containing an average of 30% VBP. b = 0.529 and K_T = 1.25 X 10^{-4} cm^2/sec were calculated from the plot through the least square analysis. The b value obtained falls in the range predicted by Eq. [95] and indicated that DMF is an intermediate solvent for the PVBP-ST copolymers.

FIGURE 42: MOLECULAR WEIGHT DEPENDENCE OF DIFFUSION COEFFICIENT OF PVBP-ST

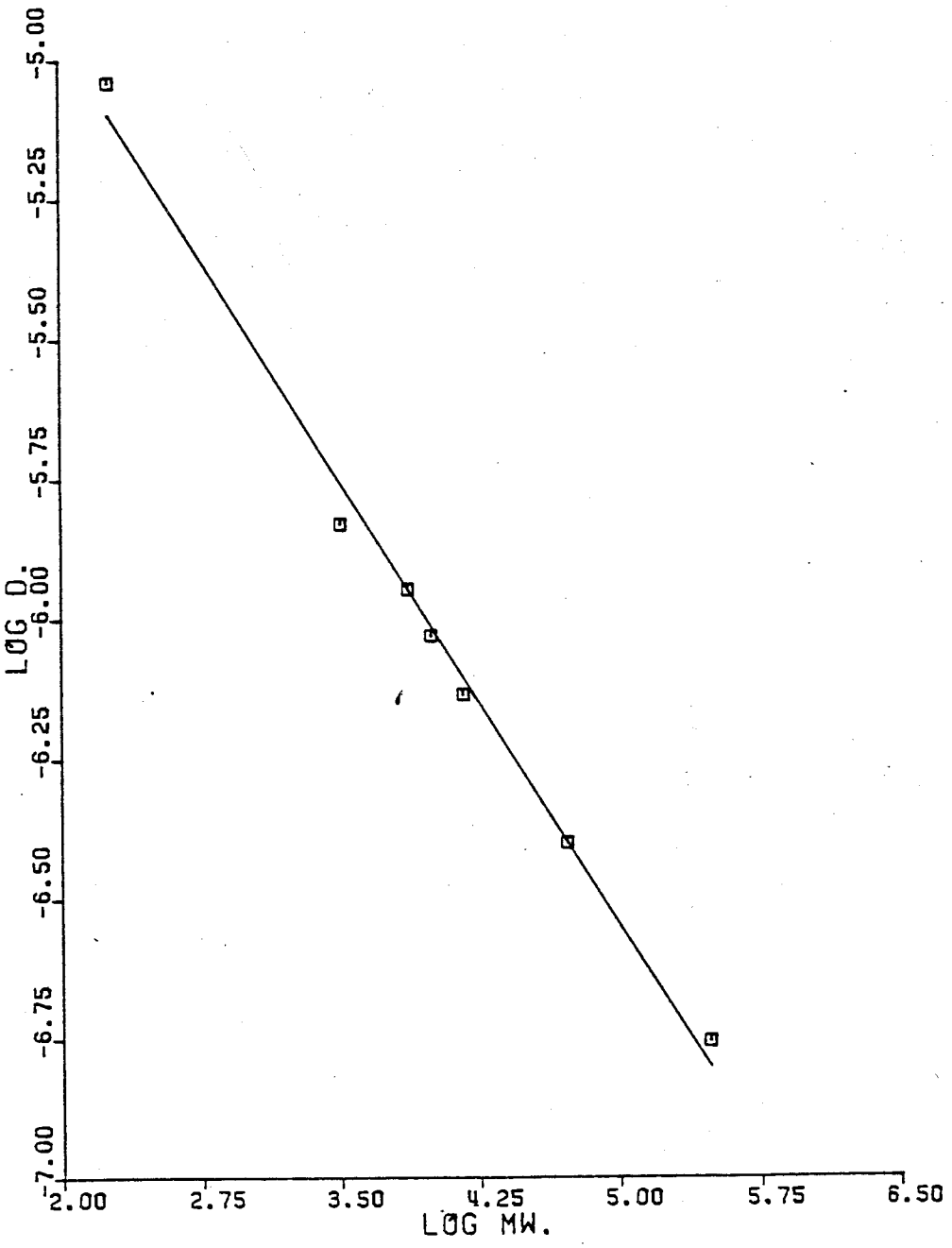
LOG D.
-5.00
-5.25
-5.50
-5.75
-6.00
-6.25
-6.50
-6.75
-7.00
2.00
2.75
3.50
4.25
5.00
5.75
6.50
LOG MW.

The parameter "b" in Eq. [102] is related to the exponent "a" of the Mark-Houwink relationship for the intrinsic viscosity, as

$$[\eta] = KM^{a} \qquad [97]$$

$$b = (1 + a)/3 \qquad [103]$$

A value of a = 0.587 was obtained from Eq. [103].

Since no literature values of Mark-Houwink constants are available for the PVBP-ST/DMF system, the K and a values were determined from viscometric measurements for the same series of PVBP-ST copolymers in the DMF/0.1M TEAP. Values of a = 0.583 and K = 3.39×10^{-4} were obtained from Fig. 43. The "a" value determined viscometrically is thus in good agreement with the value, 0.587, deduced voltammetrically and indicates the validity of estimating the diffusion coefficient in the manner described.

3.3.5 Relation Between Limiting Current and Molecular Weight

The quantitative comparison of the voltammetrically determined diffusion coefficient and related parameters with those obtained by conventional methods leads to the possibility of a determination of molecular weight by electrochemical methods. A simple relationship between limiting current and molecular weight may be obtained by combining Eq. [103] with the Levich equation [84] to give

$$i_L = k M^{-h} \qquad [104]$$

where $k = 0.62nFAC\nu^{-1/6}\omega^{1/2}K_T^{2/3}$

and $h = (2b)/3$

FIGURE 43: INTRINSIC VISCOSITY-MOLECULAR WEIGHT RELATIONSHIP FOR PVBP-ST IN DMF/0.1M TEAP

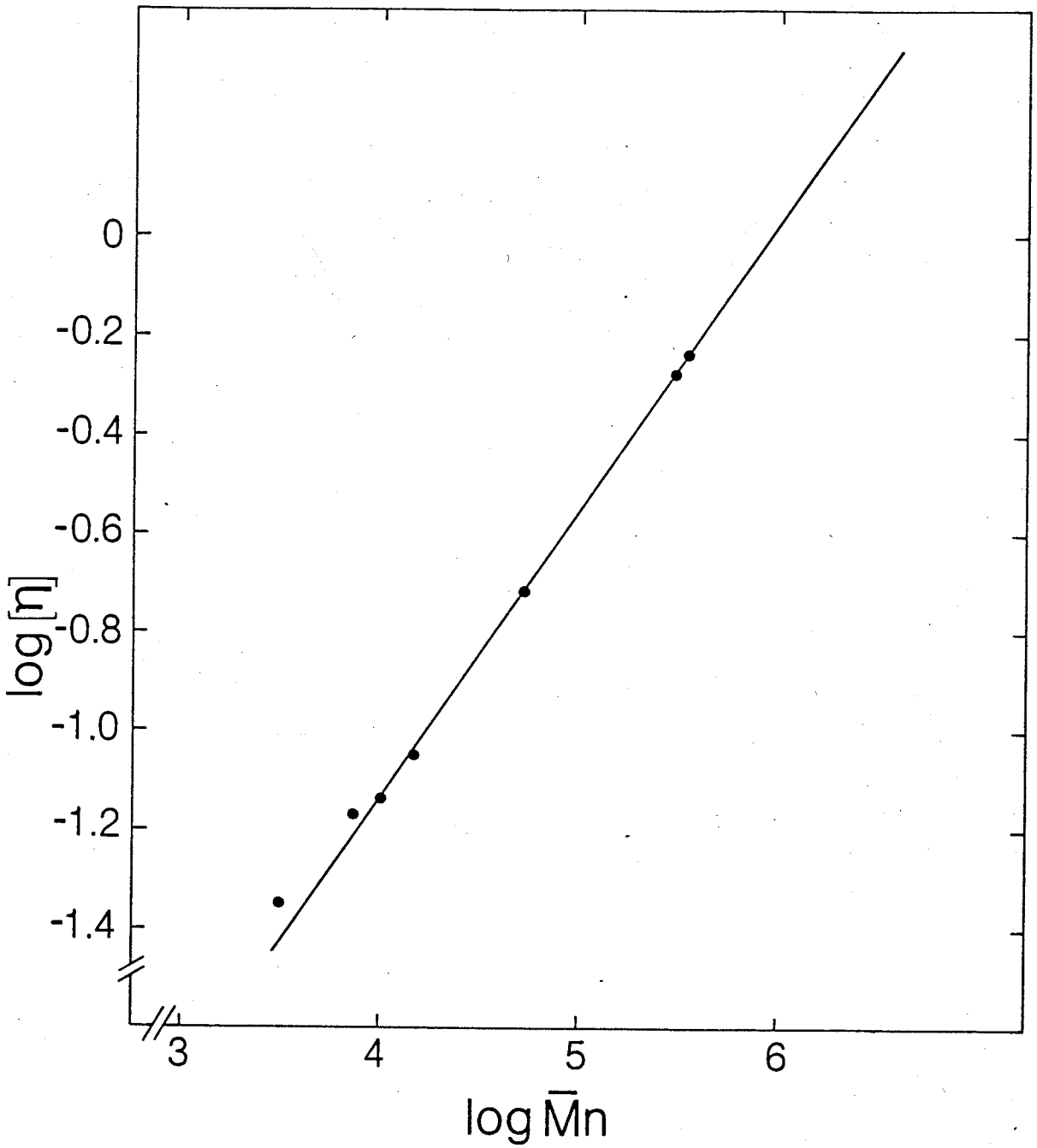
0
-0.2
-0.4
-0.6
-0.8
-1.0
-1.2
-1.4
log[η]
3
4
5
6
log M̄n

Thus, a single measurement of the limiting current should suffice to define the molecular weight of polymers. A test of Eq. [104] is shown in Fig. 44 where the predicted linearity of the double logarithmic plot is illustrated. For polymers containing electroactive groups, voltammetric methods may thus be conveniently employed to determine their molecular weights.

3.3.6. Effects of Concentration and Temperature on Diffusion Coefficient

The relation between diffusion coefficient and concentration is commonly written in a series expansion of the form

$$D = D_o(1 + k_oC + \cdots\cdots\cdots) \qquad [105]$$

where D_o = diffusion coefficient at infinite dilution, $k_o = 2A_2M - k_f$ with A_2, M, and k_f being the second virial coefficient, molecular weight of polymer, and a coefficient related to the concentration dependence of the friction coefficient respectively. This concentration dependence of D has been the subject of a large number of experimental and theoretical investigations. Nevertheless considerable discrepancies exist in results when only the first two terms are utilized. The approximation can be used only in a limited concentration range.

A preliminary study has been conducted to determin the D values at several concentrations of PVBP-ST ($\overline{M}_n$ = 1.33 X 10^4, VBP = 77%). Fig. 45 displays the plots of i_L vs $\omega^{1/2}$, whereas Table 14 shows the diffusion coefficient derived from the plots.

FIGURE 44: LIMITING CURRENT DEPENDENCE OF MOLECULAR WEIGHT OF PVBP-ST

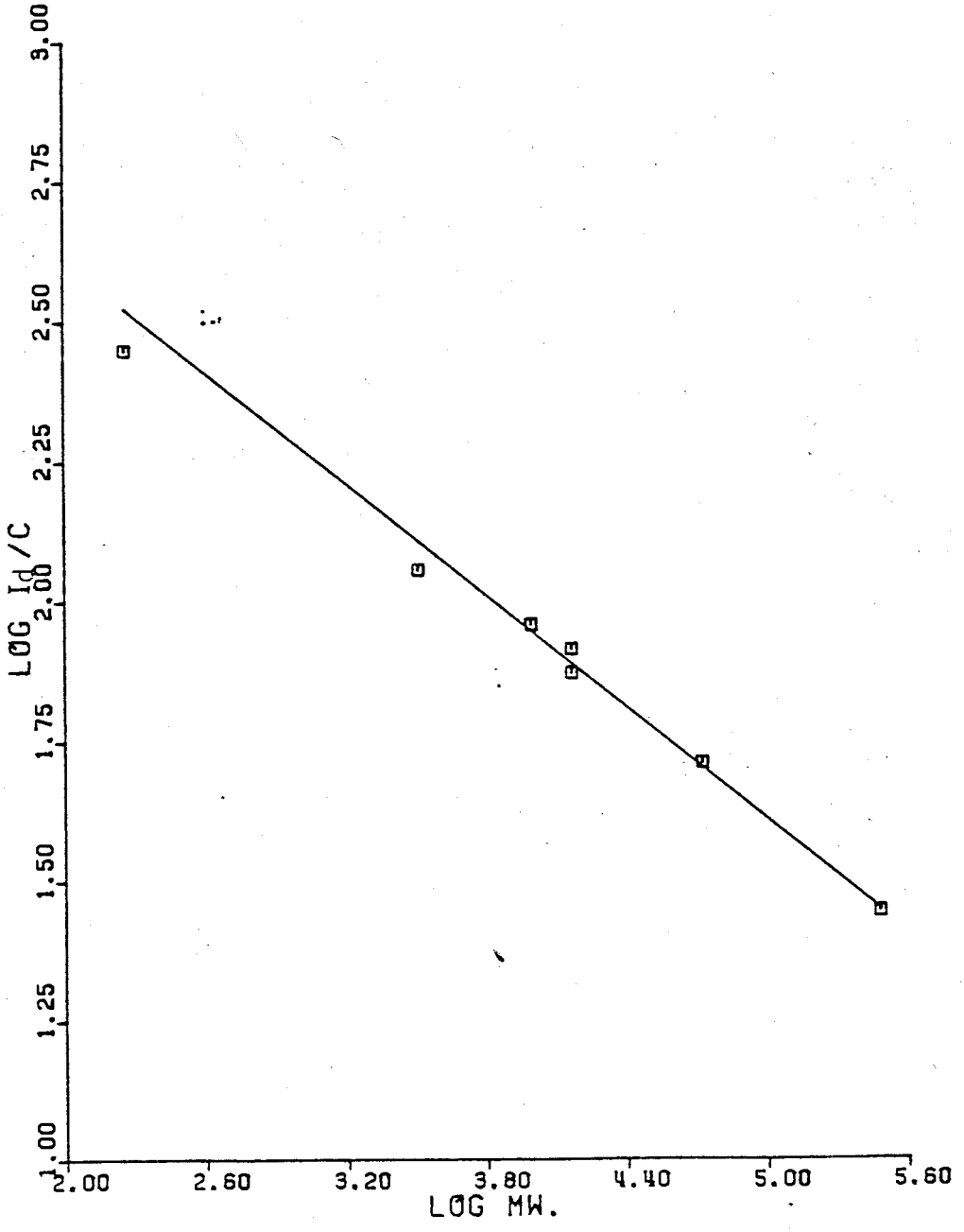
LOG Id/C
3.00
2.75
2.50
2.25
2.00
1.75
1.50
1.25
1.00
2.00
2.60
3.20
3.80
4.40
5.00
5.60
LOG MW.

FIGURE 45: EFFECT OF CONCENTRATION ON DIFFUSION COEFFICIENT FOR PVBP-ST IN DMF

P8B ($\bar{M}_n = 1.33 \times 10^4$, %VBP = 77)

+ 10 mM based on benzophenone residue

△ 5 mM

⏲ 4 mM

⊡ 3 mM

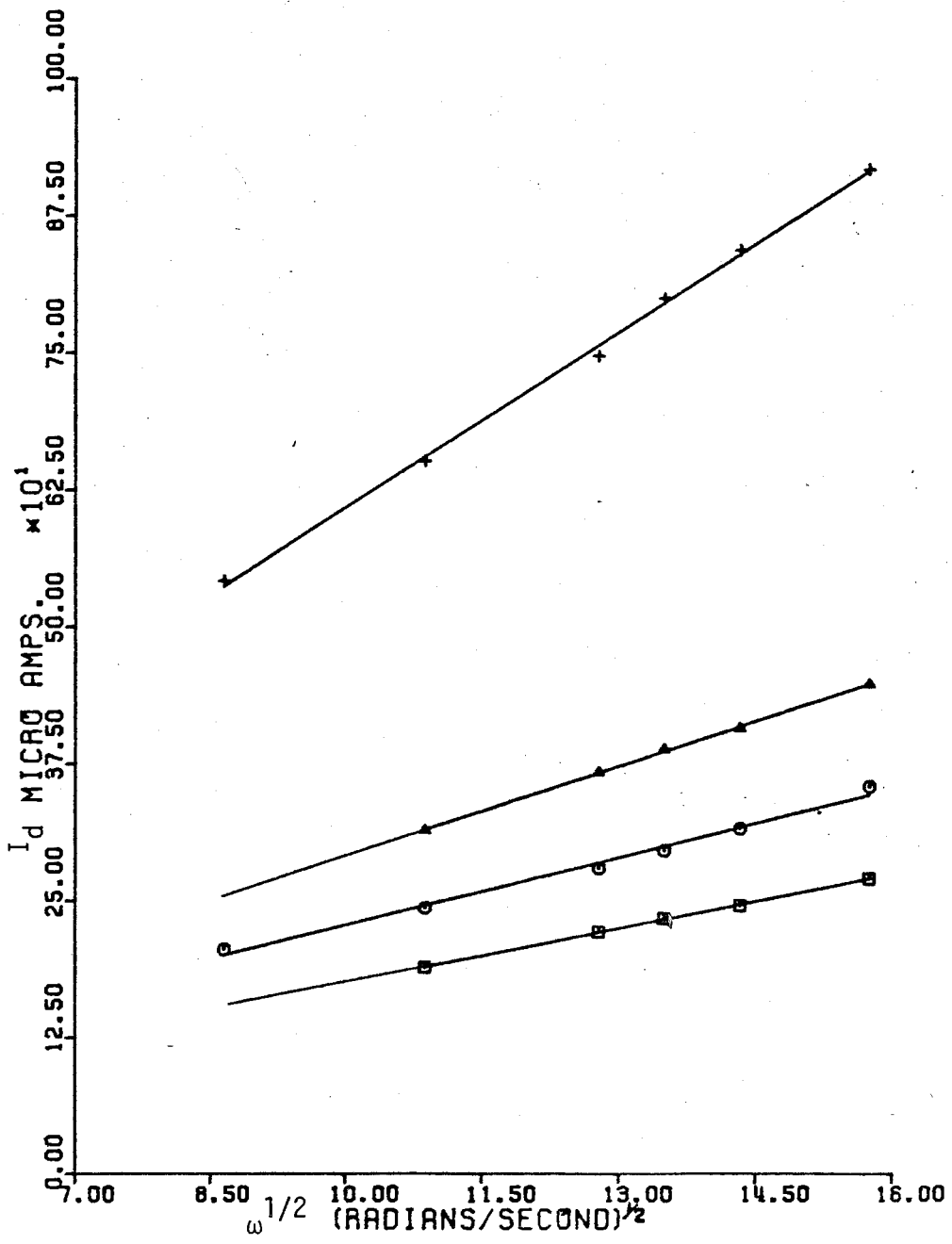
I_d MICRO AMPS. $\times 10^1$
0.00
12.50
25.00
37.50
50.00
62.50
75.00
87.50
100.00
7.00
8.50
10.00
11.50
13.00
14.50
16.00
$\omega^{1/2}$ (RADIANS/SECOND)$^{1/2}$

TABLE 14

DEPENDENCE OF DIFFUSION COEFFICIENT ON CONCENTRATION

PVBP-ST : $\overline{M}_n = 1.33 \times 10^4$, VBP = 77%

C(mM)	D (cm^2/sec)
3	8.6×10^{-7}
4	8.1×10^{-7}
5	8.7×10^{-7}
10	8.6×10^{-7}

It can be seen from Table 14 that the diffusion coefficient is independent of the concentration of the polymer.

In a study of the diffusion of poly(styrene) in tetrahydrofuran using a laser light scattering spectrometer, Mandema et al (142) observed a linear increase in D with C up to about 20g/l. On the other hand, Munk et al (139, 140) very recently studied the diffusion process of poly(styrene), using a ultracentrifuge, and found that in good solvents the value of D at higher concentrations was larger than D_0, as $2A_2M$ dominated over k_f. The effect increased with increasing molecular weight. For poor solvents, k_f terms prevailed; and D decreased with increasing concentration. For intermediate solvents, D was independent of the concentration. The constancy of the D

values shown in Table 14 implies that DMF is an intermediate solvent for the poly(vinylbenzophenone-co-styrene). This is consistent with the Mark-Houwink exponent, a = 0.583, as "a" value varies from 0.5 for a theta solvent to ~0.85 for a generally good solvent. This result also agrees the "b" value, 0.529, determined electrochemically.

The effect of temperature on the diffusion coefficient was ascertained for P8B ($\bar{M}_n$ = 1.33 X 10^4, VBP = 77%) and for P12A ($\bar{M}_n$ = 1.64X10^4, VBP = 31%). The diffusion coefficients calculated from the Levich equation are shown in Table 15.

TABLE 15

EFFECT OF TEMPERATURE ON DIFFUSION COEFFICIENT

P8B: $\bar{M}_n$ = 1.33 X 10^4, VBP = 77% , 5mM based on VBP

P12A: $\bar{M}_n$ = 1.46 X 10^4, VBP = 31% , 5mM based on VBP

Temp. °C	D X 10^7 cm²/sec (P8B)	D X 10^7 cm²/sec (P12C)
0	5.34	4.19
15	7.55	6.33
25	9.16	6.94
35	11.22	9.59
45	14.58	11.57

The Arrhenius plots of D against 1/T (Fig. 46) yield the activation energy of the diffusion rate for P8B and P12A as 3.8 and 3.9 Kcal/mole respectively.

FIGURE 46: EFFECT OF TEMPERATURE ON DIFFUSION COEFFICIENT

⏀ P8B (5 mM based on benzophenone residue)

⊡ $P12_A$ (5 mM based on benzophenone residue)

in DMF containing 0.10 M TEAP

P8B ($\bar{M}_n$ = 1.33 X 10^4, VBP = 77%)

P12A ($\bar{M}_n$ = 1.46 X 10^4, VBP = 31%)

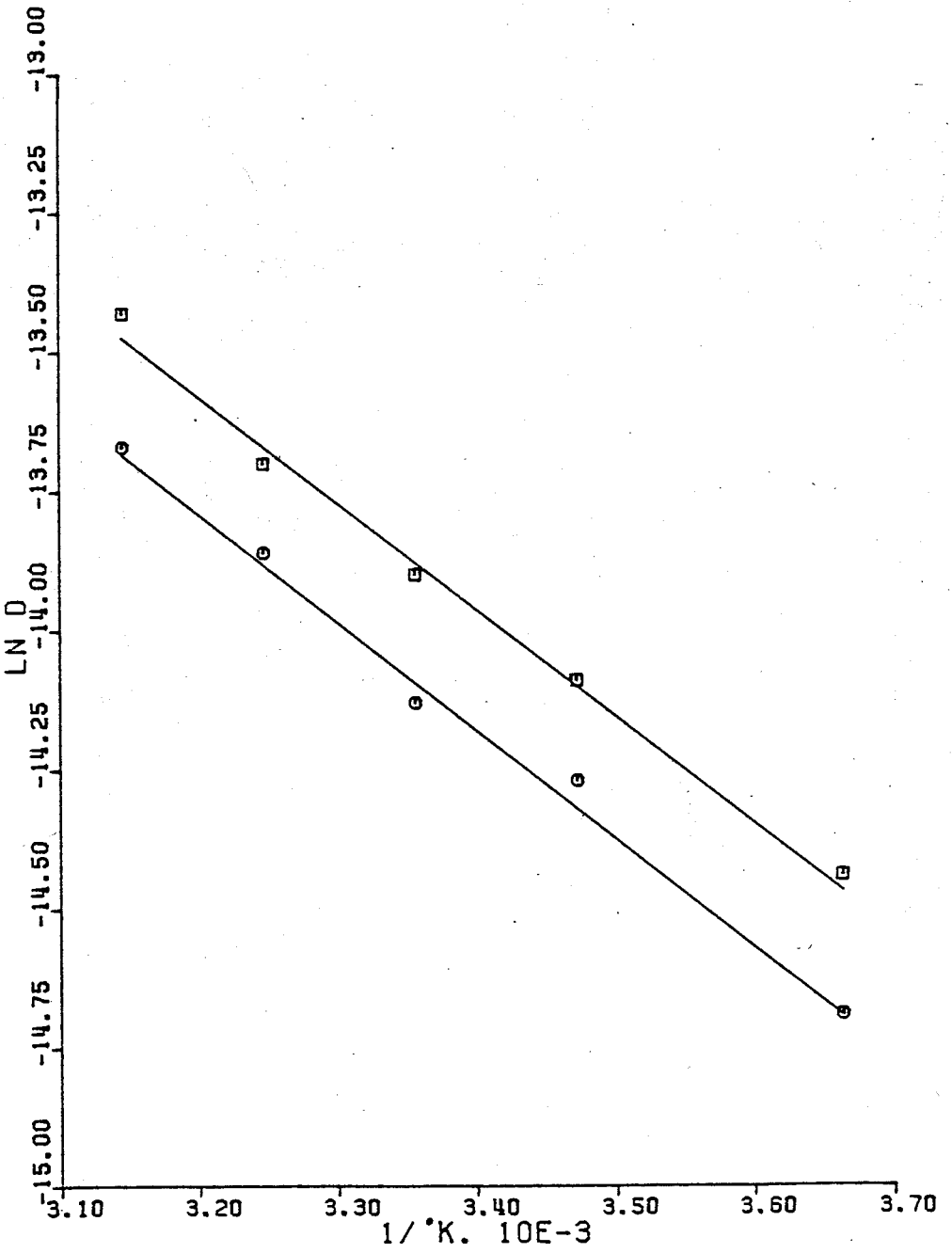
LN D
-13.00
-13.25
-13.50
-13.75
-14.00
-14.25
-14.50
-14.75
-15.00
3.10
3.20
3.30
3.40
3.50
3.60
3.70
1/°K. 10E-3

ORIGINAL CONTRIBUTIONS TO KNOWLEDGE

1. Definitive proof was provided that electroactive centers on macromolecules can be reduced independently.
2. Experimental verification of the theoretical model of non-interacting centers was obtained.
3. Quantitative evaluations were made of the diffusion coefficient of poly(vinylbenzophenone-co-styrene) in N,N'-dimethylformamide and of its dependence upon the molecular weight of the polymer.
4. The characterization of electroactive polymers by a voltammetric method was demonstrated.
5. The Mark-Houwink constants of poly(vinylbenzophenone-co-styrene) in N,N'-dimethylformamide determined by electrochemical methods and by viscometry were demonstrated to be identical.
6. The first electrochemical formation of graft copolymers was achieved by incorporating functional groups onto a macromolecular backbone from which grafting sites were created by electro-activation.
7. The reaction mechanism for the initiation of anionic polymerization by benzophenone radical anion was proposed and substantiated.
8. A direct method was developed, which utilized the rotating ring disk electrode in a free radical polymerization initiated by a redox reaction.
9. Rate constants of redox reactions including $Cu^{+}/S_2O_8^{=}$, $Fe^{+2}/S_2O_8^{=}$, Fe^{+2}/H_2O_2, and $Fe(C_2O_4)^{-4}/H_2O_2$ were determined by this electrochemical method.

10. The relative reactivities of a series of monomers to an initiating radical ion were determined for $SO_4^{-\bullet}$ which was generated and analyzed by the rotating ring disk electrode.

REFERENCES

1. B. L. Funt and J. Tanner, "Technique of Electroorganic Synthesis", vol. 2, Part II, N. Weinberg, Ed., Wiley - Interscience, New York, 1975.

2. N. Yamazaki, Adv. Polym. Sci., 6, 377 (1969).

3. B. L. Funt, Macromol. Rev., 1, 35 (1966).

4. G. Parravano, "Organic Electrochemistry", M. M. Baizer, Ed., Marcel Dekker, New York, 1973.

5. M. Szwarc, "Carbanions Living Polymers and Electron Transfer Processes", Chapter 4, John-Wiley, 1968.

6. R. W. Murry, Acc. Chem. Res., 13, 135 (1980).

7. M. Delamer, M. C. Pham, P. - C. Lacaze, and J. - E. Dubois, J. Electroanal. Chem. 108, 1 (1980).

8. G. Mengoli and G. Vidotto, Makromol. Chem., 150, 277 (1971).

9. G. Mengoli, G. Vidotto, and F. Furlanetto, Makromol. Chem., 137, 203 (1970).

10. G. Mengoli and G. Vidotto, Makromol. Chem., 129, 73 (1969).

11. B. L. Funt and V. Verigin, Can. J. Chem., 52, 1643 (1974).

12. A. Glasel, K. Murry, and B. L. Funt, Makromol. Chem., 177, 3345 (1976).

13. B. L. Funt, W. Severs, and A. Glasel, J. Polm. Sci., Polym. Chem. Ed., 14, 2763 (1976).

14. W. J. Albery and M. L. Hitchman, "Rotating Ring - Disc Electrodes", Oxford University Press, London, 1971.

15. F. Rauwel and D. Thevenot, J. Electroanal. Chem., 75, 579 (1977).

16. F. S. Dainton and D. H. Deaman, J. Polym. Sci., 39, 279 (1959).

17. M. Watanabe and H. Kiuchi, J. Polym. Sci., 58, 103 (1962).

18. J. H. Baxendale, M. G. Evans, and G. S. Park, Trans. Faraday Soc., 42, 155 (1946).

19. C. F. Wells and M. A. Salam, Trans. Faraday Soc., 63, 620 (1967).

20. C. Walling and S. Kato, J. Am. Chem. Soc., 93, 4275 (1971).

21. D. A. House, Chem. Rev., 62, 185 (1962).

22. I. M. Kolthoff, A. I. Medalla, and H. P. Raaen, J. Am. Chem. Soc., 73, 1733 (1951).

23. A. Prakash, R. N. Mehrotra, and R. C. Kapoor, J. Chem. Soc., Dalton, 1578 (1976).

24. T. R. Mohanty and B. C. Sigh, J. Polym. Sci., Polym. Chem. Ed., 13, 2075 (1975).

25. I. Pecht and M. Anbar, J. Chem. Soc., (A), 1902 (1968).

26. I. M. Kolthoff and E. P. Parry, J. Am. Chem. Soc., 73, 3718 (1951).

27. Von D. Haberland and R. Landsberg, Ber. Bunsenges. Phys. Chem., 70, 724 (1966).

28. F. Opekar and P. Beran, J. Electroanal. Chem., 32, 49 (1971).

29. K. B. Prater and A. J. Bard, J. Electrochem. Soc., 117, 1517 (1970).

30. V. G. Levich, Acta Physicochim URSS, 17, 257 (1942).

31. L. Meites "Polarographic Techniques", Chapter 8, Interscience, New York, N.Y., (1965).

32. L. N. Nekrasov and N. P. Berezina, Dokl. Akad. Nauk SSSR, 142, 855 (1962).

33. G. A. Feldman and S. Brunkenstein, J. Electroanal. Chem., 9, 395 (1965).

34. S. Brunkenstein and B. Miller, Acc. Chem. Res., 10, 54 (1977).

35. N. B. Ivanov and V. G. Levich, Dokl Akad. Nauk. SSSR, 126, 1029 (1959).

36. W. J. Albery, Trans. Faraday Soc., 62, 1915 (1966).

37. W. J. Albery and S. Brunkenstein, Trans. Faraday Soc., 62, 1920, 1946, 2584, 2596 (1966).

38. V. G. Levich, "Physicochemical Hydrodynamics", Prentice-Hall, Englewood Cliffs, N.J., 1962.

39. V. Yu. Pleskov and V. Yu. Filinovskii, "The Rotating Disk Electrodes", Consultant Bureau, N.Y., 1976.

40. A. C. Riddiford, "Advan. Electrochem. and Electrochem. Eng"., P. Delahay, Ed., vol. 4, pp 47, Interscience, N.Y. 1966.

41. B. L. Bircumshaw and A. C. Riddiford, Quart. Rev., 6, 157 (1952).

42. D. P. Gregory and A. C. Riddiford, J. Chem. Soc., 3756 (1956).

43. J. Newman, J. Electrochem. Soc., 113, 501 (1966).

44. J. Newman, J. Electrochem. Soc., 113, 1235 (1966).

45. Z. Galus and R. N. Adam, J. Phys. Chem., 67, 65 (1963).

46. A. M. Frumkin and L. N. Nekrasov, Dokl. Akad. Nauk SSSR, 126, 115 (1959).

47. S. Brunkenstein and G. A. Feldman, J. Electroanal. Chem., 9. 395 (1965).

48. S. W. Feldberg and C. Auerbach, Anal. Chem., 36, 505 (1964).

49. A. J. Bard and K. B. Prater, J. Electrochem. Soc., 117, 207 (1970).

50. A. J. Bard and K. B. Prater, J. Electrochem. Soc., 117, 335, 1517 (1970).

51. V. J. Puglisi and A. J. Bard, J. Electrochem. Soc., 119, 833 (1972).

52. L. - S.R. Yeh and A. J. Bard, J. Electrochem. Soc., 124, 189 (1977).

53. L. - S.R. Yeh, A. Electroanal. Chem., 84, 159 (1977).

54. J. - M. Nigretto and A. J. Bard, J. Electrochem. Soc., 123, 1303 (1976).

55. D. T. Napp, D. C. Johnson, and S. Brunkenstein, Anal. Chem., 39, 481 (1967).

56. M. Anbar and P. Neta, Int. J. Appl. Radiat. Isot., 18, 493 (1967).

57. L. Dogliotti and E. Hayton, J. Phys. Chem., 71, 3802 (1967).

58. I. M. Kolthoff and R. Woods, J. Am. Chem. Soc., 88, 137 (1966).

59. K. B. Prater, Private Communication.

60. W. J. Barb, J. H. Baxendale, P. George and K. R. Hargrave, Trans. Faraday Soc., 47, 462 (1951).

61. T. J. Conocchioli, E. J. Hamilton, Jr., and N. Sutin, J. Am. Chem. Soc., 87, 926 (1965).

62. H. N. Po and N. Sutin, Inorg. Chem., 7, 621 (1968).

63. P. Dalahay and G. L. Stiehl, J. Am. Chem. Soc., 74, 3500 (1952).

64. P. Beran and S. Brunkenstein, J. Phys. Chem., 72, 3630 (1968).

65. C. V. King and O. F. Steinbach, J. Am. Chem. Soc., 52, 4793 (1930).

66. J. W. L. Fordham and H. L. Williams, J. Am. Chem. Soc., 73, 4855 (1951).

67. R. J. Orr and H. L. Williams, J. Am. Chem. Soc., 77, 3715 (1955).

68. E. C. Szarvasy, J. Chem. Soc., 77, 207 (1900).

69. E. A. Rembold, Ph. D. Thesis, Ohio State University (1947).

70. L. C. Wilson, E. Dineen, and T. C. Schwann, Trans. Electrochem. Soc., 96, 226 (1949).

71. P. Giusti, J. Polym. Sci. Symp., 50, 133 (1975).

72. G. Pistoia and O. Bagnarelli, J. Polym. Sci., Polym. Chem. Ed., 17, 1001 (1979).

73. B. L. Funt and S. N. Bhadani, J. Polym. Sci., C, 23, 1, (1968).

74. B. L. Funt and D. Richardson, J. Polym. Sci., A-1, 8, 3339 (1971).

75. N. Yamazaki, S. Nakahama, and S. Kambara, Polym. Lett., 3, 57 (1965).

76. B. L. Funt, U.S. Patent 3,448,020 (1970).

77. B. L. Funt and V. Hornof, J. Polym. Sci., A-1, 9, 2429 (1971).

78. B. L. Funt and V. Hornof, J. Polym. Sci., A-1, 9, 217 (1971).

79. J. A. Epstein and A. Bar-Nun, Polym. Lett., 2, 27 (1964).

80. C. Simionescu and C. Ungureanu, Cell. Chem. Technol. (Jassy), 1, 33 (1967).

81. G. Smets, X. Van der Borght, and G. Van Haeren, J. Polym. Sci., A, 2, 5187 (1964).

82. D. A. Holden and J. E. Guillet, J. Polym. Sci., Polym. Chem. Ed., 18, 565 (1980).

83. J. P. Kennedy, J. Appl. Polym. Sci. Appl. Polym. Symp., 30, 1 (1977).

84. J. P. Kennedy, "Recent Advances in Polymer Blends, Grafts and Blocks", L. H. Sperling, Ed., Plenum, 1974.

85. V. Stannet, J. Macromol. Sci., Chem., A4, 1177 (1970).

86. A. Noshay and J. E. McGrath "Block Copolymers", Academic Press, N.Y. 1977

87. H. A. Battaerd and G. W. Tregear, "Graft Copolymers", Polymer Review, 16, Interscience, 1967.

88. M. Szwarc, Nature, 178, 1168 (1956).

89. A. Rembaum and J. Moacanin, J. Polym. Sci., Polym. Lett., 1, 41 (1963).

90. G. Goutiere and J. Gole, Compt. Rend., 257, 674 (1963).

91. G. Greber and G. Egle, Makromol. Chem., 54, 136 (1962).

92. G. Greber, J. Tolle, and W. Burchard, Makromol. Chem., 71, 47 (1964).

93. Y. Minoura and H. Harada, J. Polym. Sci., A-1, 7, 3 (1969).

94. J. C. Falk, R. J. Schott, and D. F. Hoeg, J. Macromol. Sci., (Chem.), A7, 1647 (1973).

95. J. C. Falk and R. J. Schott, J. Macromol. Sci. (Chem.), A7, 1663 (1973).

96. D. Rahlives, J. Roover, and S. Bywater, Macromolecules, 10, 604 (1977).

97. N. Hadjichristidis and J. Roover, Polymer Priprint, 19, 201 (1978).

98. J. G. Van Dusen and J. J. O'Malley, Polymer Priprint, 20, 110 (1979).

99. M. Morton, A. A. Rembaum, and J. L. Hall, J. Polym. Sci., A-1, 1, 461 (1963).

100. H. O. House, E. Feng, and N. P. Peet, J. Org. Chem., 38, 2371 (1971).

101. A. J. Bard, Pure Appl. Chem., 25, 379 (1971).

102. O. Hammerich and V. D. Parker, Electrochimica Acta, 18, 537 (1973).

103. S. H. Merril, C. C. Unruh, and E. M. Robertson, U.S. Patent 2,871,768 (1958).

104. N. Yamazaki, I. Tanaka, and S. Nakahama, J. Macromol. Sci. (Chem.), 6, 1121 (1968).

105. G. L. Collins and N. W. Thomas, J. Polym. Sci., Polym. Lett. Ed., 13, 73 (1975).

106. Y. Avny and A. Moshonov, Eur. Polym. J., 13, 99 (1977).

107. D. Braun, W. Neumann, and G. Arcache, Makromol. Chem., 112, 97 (1968).

108. S. Inoue, T. Tsuruta, and J. Furukawa, Makromol. Chem., 42, 12 (1962).

109. S. Smith, J. Polym. Sci., 38, 259 (1959).

110. A. Zilkha, P. Neta, and M. Frankel, J. Chem. Soc., 184, 3357 (1960).

111. M. Ogasawara, H. Yoshida, and K. Hayashi, Polym. J., 7, 86 (1975).

112. I. M. Panayotov, C. B. Tsvetanov, and A. C. Alexandrov, Eur. Polym. J., 11, 875 (1975).

113. A. N. Frumkin and E. A. Aikazyan, Dokl. Akad. Nauk SSSR, 100, 315 (1955).

114. Y. Iwakura, F. Toda, H. Katsuki, and H. Watanabe, J. Polym. Sci., B, 5, 1013 (1967).

115. C. K. Mann and K. K. Barnes, "Electrochemical Reactions in Nonaqueous System", Chapter 6, Marcel Dekker Inc., N.Y. 1970.

116. H. G. Cassidy, Macromol. Rev., 6, 1 (1972).

117. H. G. Cassidy and K. A. Kun, "Oxidation - Reduction Polymers", Interscience N.Y. 1965.

118. A. S. Lindsey, M. E. Peover, and N. G. Savill, J. Chem. Soc., 193, 4558 (1962).

119. S. E. Hunt, A. S. Lindsey, and N. G. Savill, J. Chem. Soc., 791 (1967).

120. A. S. Lindsey, J. Appl. Chem., 15, 161 (1965).

121. R. E. Moser and H. G. Cassidy, J. Org. Chem., 30, 2062 (1965).

122. G. Wegner, T. F. Keyes III, N. Nakabayashi, and H. G. Cassidy, J. Org. Chem., 34, 2822 (1969).

123. G.M. Brown, T. J. Meyer, D. O. Cowan, C. LeVanda, K. Kaufman, P.V. Roling, and M.D. Rausch, Inorg. Chem., 14, 506 (1975).

124. C. LeVanda, K. Beckgaard, D. C. Cowan, and M. D. Rausch, J. Amer. Chem. Soc., 99, 2964 (1977).

125. W. H. Morrison, Jr., S. Krogsrud, and D. N. Hendrickson, Inorg. Chem., 12, 1998 (1973).

126. T. W. Smith, J. E. Kuder, and D. Wychick, J. Polym. Sci., Polym. Chem. Ed., 14, 2433 (1976).

127. J. B. Flanagan, S. Margel, A. J. Bard, and F. C. Anson, J. Am. Chem. Soc., 100, 4248 (1978).

128. T. Saji, N. F. Pasch, S. E. Webber, and A. J. Bard, J. Phys. Chem., 82, 1101 (1978).

129. M. R. Van De Mark and L. L. Miller, J. Am. Chem. Soc., 100, 3223 (1978).

130. A. Merz and A. J. Bard, J. Am. Chem. Soc., 100, 3223 (1978).

131. K. Doblhofer and W. Durr, J. Electrochem. Soc., 127, 1041 (1980).

132. Z. Glaus, C. Olson, H. Y. Lee, and R. N. Adams, Anal. Chem., 34, 162 (1962).

133. Von B. Gostisa-Mihelcic, W. Vielstich, and A. Heindrichs, Ber. Bunsenges, Phys. Chem., 76, 19 (1972).

134. J. T. Edward, J. Chem. Ed., 47, 261 (1970).

135. P. J. Flory and T. G. Fox, Jr., J. Am. Chem. Soc., 73, 1904 (1951).

136. C. Tanford, "Physical Chemistry of Macromolecules" Chapter 6, John Wiley, N.Y. (1961).

137. G. Meyerhoff and G. V. Schutz, Makromol. Chem., 7, 294 (1952).

138. V. N. Tsvetkov, S. I. Klenin, J. Polym. Sci., 30, 187 (1958).

139. T. M. Aminabhavi and P. Munk, Macromolecules, 12, 607 (1979).

140. T. M. Aminabhavi and P. Munk, Macromolecules, 12, 1194 (1979).

141. A. J. Rowe, Biopolymers, 16, 2595 (1977).

142. W. Mandema and H. Zeldenrust, Polymer, 18, 835 (1977).

143. B. Chu and E. Gulari, Macromolecules, 12, 445 (1979).

144. M. B. Weismann, R. C. Pan, and B. R. Ware, J. Chem. Phys., 70, 2897 (1979).

145. H. V. Drushel and J. F. Miller, Anal. Chem., 29, 1456 (1957).

146. T. Tsukamoto, T. Kambara, and I. Tachi, Proc. 1st Intern. Polarog. Congr., Prague, pp 524 - 541 (1951).

147. B. S. Jensen and V. D. Parker, J. Chem. Soc., Chem. Commun., 367 (1974).

148. P. H. Given and M. E. Peover, J. Chem. Soc., 385 (1960).